AD A124 324 INTEGRATED METHODOLOGY FOR ADHESIVE BONDED JOINT LIFE PREDICTIONS(U) GENERAL DYNAMICS FORT WORTH TX FORT WORTH DIV J ROMANKO ET AL. NOV 82 AFWAL-TR-82-4139 1/2

UNCLASSIFIED F33615-79-C-5088 F/G 13/5 NL

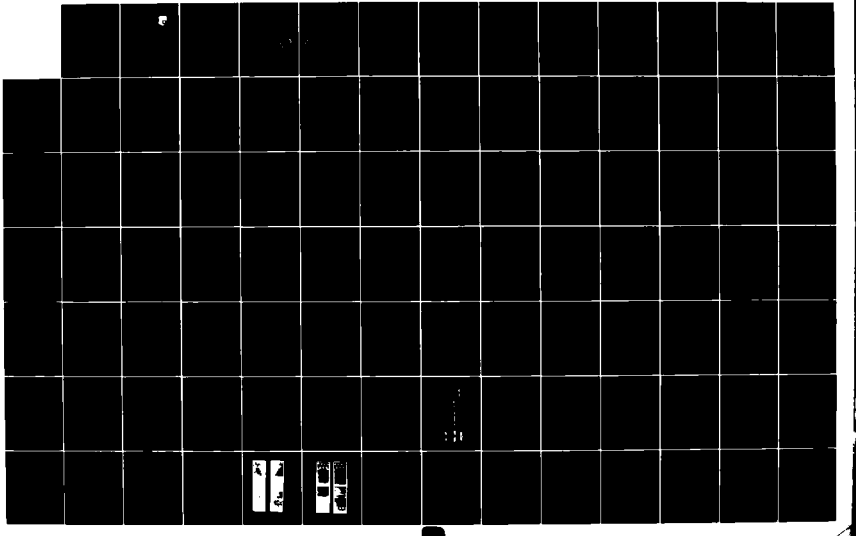

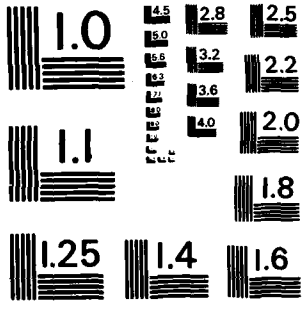

12

AFWAL - TR - 82 - 4139

INTEGRATED METHODOLOGY FOR ADHESIVE BONDED JOINT LIFE PREDICTIONS

JOHN ROMANKO, K.M. LIECHTI, W.G. KNAUSS*
GENERAL DYNAMICS FORT WORTH DIVISION
FORT WORTH, TX 76101
*PASADENA, CA 91125

NOVEMBER 1982

FINAL REPORT FOR PERIOD JULY 1979 – JULY 1982

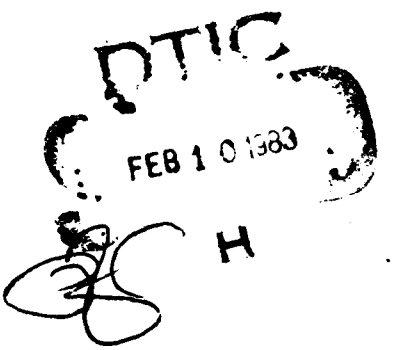

APPROVED FOR PUBLIC RELEASE; DISTRIBUTION UNLIMITED

MATERIALS LABORATORY
AIR FORCE WRIGHT AERONAUTICAL LABORATORIES
AIR FORCE SYSTEMS COMMAND
WRIGHT - PATTERSON AIR FORCE BASE, OHIO 45433

NOTICE

When Government drawings, specifications, or other data are used for any purpose other than in connection with a definitely related Government procurement operation, the United States Government thereby incurs no responsibility nor any obligation whatsoever; and the fact that the government may have formulated, furnished, or in any way supplied the said drawings, specifications, or other data, is not to be regarded by implication or otherwise as in any manner licensing the holder or any other person or corporation, or conveying any rights or permission to manufacture use, or sell any patented invention that may in any way be related thereto.

This report has been reviewed by the Office of Public Affairs (ASD/PA) and is releasable to the National Technical Information Service (NTIS). At NTIS, it will be available to the general public, including foreign nations.

This technical report has been reviewed and is approved for publication.

William B. Jones Jr

WILLIAM B. JONES, JR., Proj Engr
Composites, Adhesives & Fibr Matls Br
Nonmetallic Materials Division

Robert L. Rapson

ROBERT L. RAPSON, Chief
Composites, Adhesives & Fibr Matls Br
Nonmetallic Materials Division

FOR THE COMMANDER

F. D. Cherry

FRANKLIN D. CHERRY, Chief
Nonmetallic Materials Division

"If your address has changed, if you wish to be removed from our mailing list, or if the addressee is no longer employed by your organization please notify AFWAL/MLBC *W-PAFB, OH 45433 to help us maintain a current mailing list".*

Copies of this report should not be returned unless return is required by security considerations, contractual obligations, or notice on a specific document.

Unclassified

SECURITY CLASSIFICATION OF THIS PAGE (When Data Entered)

REPORT DOCUMENTATION PAGE		READ INSTRUCTIONS BEFORE COMPLETING FORM
1. REPORT NUMBER AFWAL-TR-82-4139	2. GOVT ACCESSION NO. AD-A124 324	3. RECIPIENT'S CATALOG NUMBER
4. TITLE (and Subtitle) INTEGRATED METHODOLOGY FOR ADHESIVE BONDED JOINT LIFE PREDICTIONS.		5. TYPE OF REPORT & PERIOD COVERED Technical-Final July 1979 - July 1982, 6. PERFORMING ORG. REPORT NUMBER
7. AUTHOR(s) John Romanko K. M. Liechti W. G. Knauss*		8. CONTRACT OR GRANT NUMBER(s) F33615-79-C-5088
9. PERFORMING ORGANIZATION NAME AND ADDRESS General Dynamics Fort Worth Division P. O. Box 748, Fort Worth, TX 76101 *Pasadena, CA 91125		10. PROGRAM ELEMENT, PROJECT, TASK AREA & WORK UNIT NUMBERS P.E. 62102F 2418 01 24180114
11. CONTROLLING OFFICE NAME AND ADDRESS Materials Laboratory (AFWAL/MLBC) Air Force Wright Aeronautical Laboratories AFSC WPAFB, OH 45433		12. REPORT DATE November 1982 13. NUMBER OF PAGES
14. MONITORING AGENCY NAME & ADDRESS(if different from Controlling Office)		15. SECURITY CLASS. (of this report) Unclassified 15a. DECLASSIFICATION/DOWNGRADING SCHEDULE

16. DISTRIBUTION STATEMENT (of this Report)

Approved for public release; distribution unlimited.

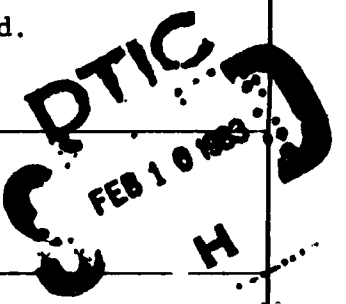

17. DISTRIBUTION STATEMENT (of the abstract entered in Block 20, if different from Report)

18. SUPPLEMENTARY NOTES

19. KEY WORDS (Continue on reverse side if necessary and identify by block number)

20. ABSTRACT (Continue on reverse side if necessary and identify by block number)

A comprehensive integrated methodology for adhesive bonded joint life predictions is outlined. While poorly made joints can fail at the adherend interface, properly made joints are far stronger, tending to fail by failure in the adhesive interlayer. The approach taken herein is that the useful life of bonded joints is determined by failure in the adhesive inter-
(Continued)

DD FORM 1 JAN 73 1473 EDITION OF 1 NOV 65 IS OBSOLETE

Unclassified

SECURITY CLASSIFICATION OF THIS PAGE (When Data Entered)

20. Abstract (Continued)

layer, and this is the basis for a systematic analysis of information and the techniques required to provide valid predictions. Emphasis is placed on time-dependent fracture mechanics procedures, including detailed through-the-adhesive thickness viscoelastic finite element calculations of the stress-strain distributions, and on analytical methods involving the constitutive relations of the adhesive interlayer. Use is made of instrumented bonded joint data obtained from structural overtest methods under a number of U.S. Air Force-sponsored programs. A logical program rationale is outlined which has sufficient generality to apply to any adhesive bonded joint structure including metal and composite adherends, various loading/environmental conditions, which apply to high-performance aircraft. The five main modules of the integrated methodology are: (Definition of) Loads/Environments; (Adhesive) Material Properties; Stress Analysis; Fatigue Mechanisms and Failure Critiera; and Structural Failure Analysis (Life Predictions). The necessary contents of each module, including input and output data, are specified and a system approach is taken interconnecting the modules into a logical sequence suitable for making service life predictions for bonded structures. Finally, a life prediction is made on a structural lap joint geometry approximating the circumferential bonded splice of the PABST full-scale demonstration component. Influence coefficients (i.e., sensitivity factors) outlining the variation limits of the lifetime with temperature, moisture and stress level are discussed.

FOREWORD

This technical report describes the research conducted for the Air Force Wright Aeronautical Laboratory, Air Force Systems Command, Wright-Patterson Air Force Base, OH 45433, under Contract F33615-79-C-5088, with Dr. W. B. Jones, Jr., MLBC, as Project Engineer.

Dr. John Romanko, GD/FWD Program Manager, acknowledges the interest and guidance of Dr. Jones and consultant Dr. W. G. Knauss of California Institute of Technology in this program. Many scientists of Materials and Structures Technology, General Dynamics' Fort Worth Division, contributed to the efforts reported herein: Dr. K. M. Liechti was responsible for the task on damage accumulation and failure criteria. Mr. M. E. Tohlen conducted the task on Loads/Environments Definition. Messrs. F. C. Nordquist and C. P. Fisher were responsible for the cyclic fatigue testing. Mr. B. O. McCauley was involved in the bonded joint specimen fabrication task, with the metal surface preparation and priming conducted at Vought Corp., Dallas, TX. Mr. L. R. Collins of the Stress Analysis Group conducted the finite element calculations.

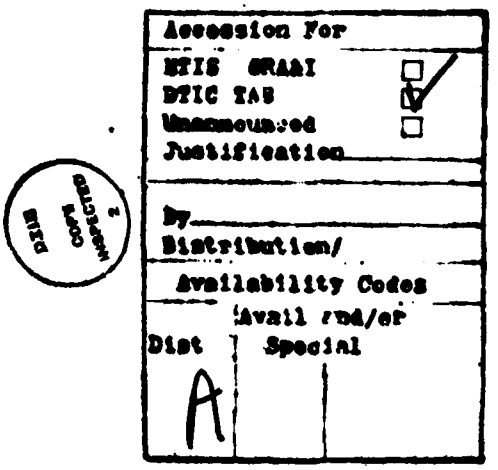

TABLE OF CONTENTS

TABLE OF CONTENTS (Continued)

TABLE OF CONTENTS (Concluded)

LIST OF ILLUSTRATIONS

LIST OF ILLUSTRATIONS (Continued)

LIST OF ILLUSTRATIONS (Concluded)

LIST OF TABLES

LIST OF TABLES (Concluded)

I. INTRODUCTION

1.1 General Remarks

The use of polymeric adhesives to structurally join metal and join or repair composite aircraft structural components offers significant cost and weight savings. Initial costs are reduced through design simplicity and reduced part count as proven recently in at least two advanced technology programs (References 1 and 2). Operational costs are potentially reduced through longer service lives, and maintenance costs are reduced through demonstrated damage tolerance and fatigue endurance far superior to that of riveted joints. Fuel savings result from reduced weight. In an effort to properly evaluate the cost savings through improved service life of the bonded structures, and to be able to more accurately estimate the total cost of ownership prior to commitment to hardware, several programs have been sequentially initiated. They are highly productive of fundamental understandings of bonded joint fatigue endurance and damage tolerance. The backbone program of one such series of closely coordinated programs conducted in concert is the "Integrated Methodology" program described herein.

1.2 Report Structure

The program described in this report is rather wide ranging and covers many different aspects. Its basic interest is to summarize the methodology of failure prediction of adhesively bonded joints for design as well as repair purposes. Underlying these developments is the strong belief that the integration of mechanics concepts with those of surface chemistry or physics is a necessary prerequisite to effective use of bonded joints in aircraft construction.

The development of these methods draws on several disciplines not normally addressed together in science curricula and it is this interdisciplinary character of the design effort that makes the presentation of this work difficult and possibly appear disjointed. In order to clarify the presentation, and following some introductory comments, we divide this report into severl parts, each one being identified with a specific program task; these (technical) tasks are:

(II) Review of Structural Analysis Requirements, the major five subtasks of which (viz., 2.3, 2.4, 2.5, 2.6 and 2.7 of the Table of Contents) developed into the program modules of various disciplines discussed in the task on

(III) Module Definition and Integration. Here we discuss the analytical background in terms of methodical application. The use of these test and computation methods are then illustrated in the task outlined under IV entitled

(IV) Demonstration of the Integration Method. Here we discuss the development of the necessary data for evaluating the failure prediction for a test article as a demonstration of the overall method. Finally, we follow with a brief critical review of

(V) (Identification of) Expanded Requirements.

We conclude with a summary and recommendations for further work.

1.3 Program Objectives

The intent of the "Integrated Methodology" program is to identify the structural mechanics procedures necessary to design durable adhesively bonded aircraft structural joints and to integrate these procedures into a logical and internally consistent method for predicting their service life. The approach includes characterization of the mechanical behavior of adhesives and calculation of stress/strain distribution in bonded joints subjected to loads/environments typical of modern, high performance aircraft in service; failure criteria are then determined and compared to the duress levels. Changes of either the duress or the failure criteria with service/load/environment/time is quantitatively considered. The emphasis is placed on developing analytical predictive capabilities.

One of the underlying features under consideration in the Integrated Methodology program is the recognition of the viscoelastic nature (time dependence) of the interlayer of an adhesively bonded metal-to-metal joint. Epoxy resins are polymers and as such exhibit viscoelasticity (time dependent creep) which means that their mechanical properties can change with time, and also with temperature and moisture content. This viscoelasticity may or may not be a desirable property in an engineering application depending on the situation, but nevertheless it must be addressed if only to

set a limit under which the adhesive can be employed as a load transferring medium in a structural application. The USAF's practice of restricting the use of an adhesive to applications below its glass transition (temperature) certainly lessens the structural problems associated with the polymer's creep behavior, but it does not eliminate them, especially in cases of long term applications (up to 20 years) and under moisture and high load conditions. Moisture can lower the glass transition temperature of a polymeric adhesive by as much as 40°F and high loads may introduce nonlinearities in the material response and fracture properties which also accelerate the creep behavior.

In addition to this, noncrystallizable polymers, such as epoxies, when cooled from the liquid state into the glassy state become non-equilibrium materials. Changes in these materials toward a more nearly equilibrium state is termed physical aging and is manifested by spontaneous changes in their thermodynamic properties (e.g., specific volume and entropy) and hence, in their mechanical properties which can be important considerations in technological applications. Physical aging introduces changes in the free volume and consequently corresponding response property changes below Tg. The time-temperature shift procedures using the normal Boltzmann superposition principle is strictly applicable only to equilibrium material behavior (i.e., above Tg) and to unaged material, and as such may not correctly describe the behavior of the non-equilibrium state of the material below Tg.

Other aging processes that can change polymer material mechanical properties with time include chemical aging and structural aging.

Chemical aging results from reactions as a function of time of unreacted species in the material, including continuation of cure reactions in the resin after the autoclaving procedure during piece part formulation; from new chemical reactions that can occur due to thermal oxidation and/or moisture interactions with the resin matrix with time and temperature due to the introduction of oxygen (from the air) and moisture from a variety of sources.

Structural aging or damage results from the growth of cracks, microcracks, and/or crazes in the material with mechanical fatigue cycling which will change the effective stiffness and/or load carrying capacity of the structural members under consideration.

Again, exposition of the above phenomena occurring in epoxy resins is not meant as an indictment of the use of polymers in engineering applications. On the contrary, it is intended to bring to the user's attention possible problem areas and to set the limits of use of viscoelastic materials recognizing the aforementioned time, temperature, moisture environmental effects which will change the mechanical properties of interest in structural design applications.

1.4 Background

Adhesive bonding offers many advantages for aircraft structural applications. These advantages are primarily economic in nature, with initial fabrication costs being reduced by design simplicity and reduced part count. Bonded structures are also potentially more economical to maintain than riveted structures since the continuous bond lines more uniformly distribute the skin stresses and are therefore more fatigue resistant. Until only a few years ago, these potential advantages were not fully realized due to intermittent corrosion and delamination problems and correspondingly low confidence levels on the part of the designer.

In recent years, rapid and substantial improvements in materials and processing and in bonded joint structural analysis have been made that contribute directly to improved reliability of bonded joints. Aluminum surface preparations have been developed that are durable in service environments, and polymeric adhesive materials with improved processability and durability have become available. These improvements have facilitated the transition of adhesive bonding into aircraft primary structural applications. Advanced development efforts applying adhesives to primary structures were demonstrated in the PABST program (Air Force Contract F33615-75-C-3016). For the specific PABST application, the static, fatigue and damage tolerance (including effects of bondline defects) evaluation of the bonded structure (i.e., the longeron to skin joints, the circumferential shear tee-to-skin joints, and the longitudinal skin splices) was accomplished through extensive accelerated and long-term coupon and component testing. In addition, from five to ten years of sophisticated expensive testing is required in order to fully qualify the structure on a purely empirical basis. And finally, while this approach addresses the adequacy of bonded joints in an after-the-fact manner, the results do

not provide for the prediction of joint life in either the longer term or any significantly different service condition. Thus, the empirical approach is presently, and will continue to be, expensive. The time and expense cannot be afforded in the course of an aircraft engineering development program. The expanded use of adhesive bonding in primary structure is therefore dependent on fully developed analytical methods.

Translation of material-mechanical characteristics and short-term, intensified fatigue endurance behavior to other structural configurations, to other loads / environmental conditions and to extended durations of service are facilitated through the concepts of structural mechanics. Recognizing this, the Air Force has funded programs exploring adhesive bonded joints as structural elements, with their own internal stress distribution arising from component material properties, configuration, and applied loadings. Instrumentation for measuring joint compliance was developed under Contract F33615-76-C-5205 (Ref. 3). Inquiries into the mechanisms of fatigue damage accumulation were conducted in Contract F33615-75-C-5220 (Ref. 4). Methods for dealing with the advancement of debonding and fracture criteria for bonded joints were developed during Contract F33615-75-C-5224 (Ref. 5) and are documented in AFML-TR-77-163, Parts I and II.

These developments, in conjunction with the finite element and closed-form stress analyses contributed by other investigators, are rapidly advancing the state-of-the-art of joint analysis. It now appears feasible to integrate these procedures into a logical and internally consistent method for predicting the service life of bonded joints. This method would provide for improved capability for design, for estimating appropriate inspection intervals, and for estimating the maintenance portion of the bonded aircraft structures in consideration of cost of ownership (life-cycle costs).

II. REVIEW OF STRUCTURAL ANALYSIS REQUIREMENTS

2.1 Introduction

A detailed review was conducted of existing analytical and experimental structural mechanics procedures to determine the type and accuracy of the methods required for the rigorous structural analysis of bonded joints. This review included consideration of the adhesive material mechanical (response) properties in the environmental conditions experienced in service needed to perform a stress analysis, the numerical (finite element) or analytical (closed form) stress analysis methods available, a study of the adhesive material fatigue mechanisms and damage accumulation and material failure (fracture) properties required for a structural integrity evaluation or strength analysis. Also included in the review was a definition of the load/environment envelop experienced by modern high-performance aircraft, in detail, on the sensitivity of the adhesive material mechanical response and failure characteristics to these environments.

Before discussing the results of this review, a survey is made of the four main philosophies used in bond design. This sets the stage for the approach used in subsequent analyses used in this program.

2.2 Review of Philosophies in Bond Design

In this section we argue that a proper application of Fracture Mechanics (not to be confused with the later described Thickness-Averaged Fracture Mechanics) provides the vehicle to organize and rationalize problems of bond performance; Fracture Mechanics provides thus also the proper viewpoint for developing techniques that lead to a better understanding and improved predictability of bond performance.

Commercial development of bonding in the various industries has developed essentially by trial and error. That process is expensive if several different bonding systems and applications are required. As a consequence, a technologically - based methodology becomes desirable to define and document the basic building blocks of such a technology; in this fashion the understanding, interaction and trade-offs between contributing disciplines allow for a more economical development process. The recognition of

this need has spawned several analytic concepts for bond strength analysis. Here we are concerned only with four of these, which represent essentially different degrees of sophistication in bond strength evaluation. We call these analytic concepts,

1) P-over-A analysis
2) Strength of materials approach
3) Thickness-averaged fracture mechanics
4) Fracture mechanics.

We acknowledge here that we start off the discussion of bond strength analysis with the mechanics aspects of the overall problems, rather than with the important problem of the nature of the bond between adhesive and adherend. We do this deliberately, for it is clear that most of the time a bond serves the purpose of transmitting mechanical forces. The safe design of a bond must, therefore, be concerned with the details of how those forces are transmitted. In fact the evaluation of the strength of an interfacial bond, however carefully prepared or characterized in terms of surface chemistry or physics, has ultimately meaning only in terms of its ability to transmit loads. In fact, from a viewpoint of applications, the quality of an interfacial bond is defined in mechanical terms, and its numerical evaluation and comparison with other bonds must be effected through mechanical testing and the pertinent test analysis.

It is clear then that the degree of refinement in the (test) analysis is a very fundamental consideration in the characterization of the bond interface (interphase). To expand on this point, it makes little sense to devote great resources to a careful microscopic characterization of the bond chemistry and not to match that care in the analysis of how mechanical forces are transmitted across it. (The proposition is similar to that for a hi-fi system in which an excellent system would sound poor were it not complemented by an excellent set of speakers.)

To be sure, a simplistic mechanics analysis is not useless for evaluating the strength of different bond forming systems. Such a simple approach allows the relative comparison of bond forming systems and has thus been the main vehicle for developments in surface chemistry and surface preparation related to bond formation. The simplest such approach is represented by the

P-over-A analysis: this form of bond strength description derives from the joining of two pieces by an adhesive (in lap or butt joint form) and from subjecting

that arrangement to a transmitted load P: The load at failure in relation to the bond area gives an average (failure) stress as the measure of bond strength provided the same geometry (adherend thickness in overlap in a lap joint) and same adherend materials are always used. Elementary examinations of this proposition as a valid bond strength characterization show that the non-uniform aspects of stress distribution play an important, or even dominant role in joint strength. This observation prompted the more detailed description of load transfer through a bonded joint which we wish to categorize for these present purposes as a

Strength of Materials analysis: In this method one treates the adhesive layer as experiencing strains averaged over the bondline thickness, but allows for variations of this average strain along the bond line, as well as for elastic deformations of the (usually thin) adherends parallel to the bond. Basically the analysis by Goland and Reissner (Ref. 6) is of this type; a variant thereof, allowing for "nonlinear" adhesive behavior, formed the basis of the bonding design in the PABST program by Dr. L. John Hart-Smith (Ref. 7).

This "Primary Adhesively Bonded Structures Technology" (PABST) program carried out at the McDonnell Douglas Company (Long Beach, California) (Ref. 8) was devoted to examining the manufacturing problems for large bonded structures (fuselage) and to subject the latter to life-like fatigue loading. On the whole, that program was successful in demonstrating that a bonded structure could withstand life simulating loads for a period in excess of four times the anticipated life of the service hardware. Much has been learned in terms of manufacturing bonds on a large structure and our confidence in the capabilities of bonded structures has increased significantly beyond the demonstrations by the Fokker Aircraft Company's successful experience in this area (Ref. 9). However, one cannot argue equivocally that our understanding of how to design bonding systems has increased to the point where bonding is a totally reliable joining method for future aircraft systems.

After all, the strength-of-materials analysis underlying most bond engineering assumes that the bond interface remains intact and the polymer adhesive is the weak link in the systems. The method is thus unable to inquire into the stresses near or at the interfaces. An understanding of the stress distributions then serves to better organize results from interface studies. The study of the characteristics of the interface playsan important role in our attempt to

advance the reliability of bond usage in critical applications.

We find the strength of materials method too limited a tool on which to base a fundamental study of bond performance. It also leads to conservative estimates. Similarly, the approach which we call here

Thickness-Averaged Fracture Mechanics is beset by similar kinds of shortcomings. Upon recognizing that properly-made bonded structures fail (mostly) by propagation of cracks through the bond line, one resorts in this method to identifying the whole bond line as the weak link in the bond system. By arguing that the bond line is ("infinitesimally") thin compared to other dimensions of the bond system, the strength determination is reduced to the equivalent problem of a continuous body with a weak (bond line) plane in which a crack propagates. The problem is thus reduced to a standard fracture problem in which the polymeric bond line is, hopefully, characterized by an energy parameter. In fact, this energy parameter must be a function of bond line thickness - which is often a statistical variable - as well as a function of whether fracture occurs near one adherend interface or through the center of the bond. Neither is usually enforced controllably. The neglect of the details of the fracture process within the adhesive region is a major shortcoming of Thickness-Averaged Fracture Mechanics. There are a host of phenomena that occur within the polymer layer at or near its boundary with an adherend, which are important in the process of bond failure. The question of why failure occurs "at" or near the interface or through the middle of the bond can never be answered by Thickness-Averaged Fracture Mechanics.

We turn now to the analysis method which has the greatest (only) promise of complementing the developments within surface chemistry and physics, viz.,

Fracture Mechanics: This discipline is concerned with the growth or stability of cracks in solids or at interfaces. In principle there is no restriction on the shape and size of cracks, nor on the size of the structure containing the crack. In principle this growth can be in any direction with respect to an existing crack and is determined by energy principles. Fracture Mechanics presupposes that cracks exist and is concerned with their growth. Under such a condition, the bond strength of an interface can be characterized by an energy of adhesion, measured in energy consumed per unit of disbond area. (For

the present we assume that rate effects or viscoelasticity do not play a major role.) As we shall see in greater detail later on, Fracture Mechanics offers the unifying link between mechanical loads on a bond, the geometry of the bond, the material properties involved and the interface conditions, and provides thus the tool for interrelating the disciplines that contribute to the complexities of the bonding problems.

2.3 Adhesive Material Characterization

The local stress distribution developed in a bonded joint will be greatly influenced by the material properties which define the response and fracture deformation characteristics of the joint. The physical and mechanical properties of the adhesive interlayer of a bonded joint or structure can be divided into two categories for the convenience of the purposes of this program: these are the "response" properties on the one hand, dealing with deformational characteristics (up to material failure) and the "fracture" or "failure properties" on the other hand, dealing with fracture properties or crack growth.

Response properties, such as the creep compliance, thermal coefficient of linear expansion and moisture coefficient of absorption (and desorption), among others, are measured over a wide temperature range, regardless of what the end use environmental conditions may be. The reason for this is the use of time-temperature equivalence (superposition) principles which are commonly employed in viscoelastic stress analysis. For example, the creep compliance at -65°F might be equivalent to the compliance characteristics of the adhesive interlayer at room temperature over a shorter time period. Similarly, calculations of the effects occurring at room temperature over a long period of time would employ the compliance determined at an elevated temperature. Factors such as temperature or moisture content, which affect the response properties of a material, have also been found to affect the fracture properties of the material (Refs. 10-16).

The importance of obtaining the response and fracture properties of FM-73M adhesive at periodic intervals and various environmental conditions has been recognized and acted upon throughout the course of the Integrated Methodology and related programs. The relevance and applicability of this data base to this program is discussed in Sections 2.3.1 and 2.3.2 which deal with the response and fracture properties, respectively. The possibility of

conducting additional time-dependent fracture properties is discussed in Reference 17, although it is recognized that this is not the main thrust of the current program.

2.3.1 Time-Dependent Response Properties of FM-73M Adhesive

The two main material properties of the FM-73M adhesive selected in the Fatigue Behavior program are the tensile creep compliance, D(t), and Poisson's ratio, $\nu(t)$. As indicated by the "t" in parentheses after the appropriate defining symbol, these are time (t)-dependent material properties, in general. Measurements made in the Fatigue Behavior program (Ref. 19) indicate that Poisson's ratio of dry FM-73M adhesive displays no measureable time dependence, at least over a period of 30 days (Ref. 18). However, the tensile creep compliance, D(t), is a strong function of time, especially around and above the glass trasition temperature, T_g, of the material (Ref. 19). The fact that T_g is a constant over the stated time interval simplifies the constitutive relation involving D(t) and ν for the dry (neat) material since this ν-value can be treated as a material constant and can be removed from under the integration sign of the corresponding constitutive equation, thus simplifying the material description, e.g., in the stress analyses thereof.

Other important material properties for adhesives that affect the stress state in a bonded joint include the temperature coefficient of expansion, α_T, for the dry and wet adhesives, and the moisture coefficient of expansion (for absorption) and contraction (for desorption), α_p, thereof. These have also been measured under the Fatigue Behavior program at General Dynamics (Ref. 19). Of particular significance is the fact that, not only are the two curves different over the temperature range of interest for the corresponding dry and wet adhesives, but the glass transition temperature, T_g, is lowered by approximately 40°F for the wet material, and hence in the resultant corresponding stress states (analysis) of the bonded joint.

The commercially-available adhesive FM-73M is supplied by the manufacturer in 8 to 10 mil thick tape containing a matte carrier. Moreover, FM-73M is a rubber-modified epoxy so that the material is, strictly speaking, neither homogeneous nor isotropic. However because the carrier is a random matte, it can be assumed specimens laminated from these films to form adhesive test coupons are sufficiently isotropic in the bondline specimen plane so that

characterization techniques developed for isotropic solids are sufficiently accurate. Results on the time dependence (or independence) of the adhesive system are not markedly violated by this assumption. Another consideration which will affect the stress/strain distribution in the adhesive interlayer is the scrim cloth per se, which in this case is a matte Dacron. Its existence is recognized, and it may participate in the failure process, but it will be ignored as a separate phase, for the sake of simplicity.

The entire procedure for adhesively bonded joint design analysis may be extended for purposes of service life prediction if a valid means is made available for accelerating the deterioration of the adhesive system. Since the adhesive is the most significant age-sensitive component in the bonded structure and since catastrophic failures occur due to cracks or debonds, it is particularly appropriate that accelerated aging techniques be established for each specific formulation. Relationships between results of accelerated aging tests and results from actual long-term tests are being established in the Basis for Accelerated Testing program (Ref. 20).

Another important consideration with regard to the response properties is their linearity. Two different representations of nonlinear viscoelastic material behavior are being incorporated in the Viscoelastic Stress Analysis (VISTA) finite element code which is being considered in Reference 21. The first representation is due to Knauss (Ref. 22) and is known as the intrinsically nonlinear viscoelastic model of material behavior. The model, which has linear viscoelastic behavior as a special case, accounts for the effects of temperature, moisture and high stresses in a unified, and therefore efficient manner. The nonlinear behavior thus modeled arises from the molecular network response (changes in free volume) in the absence of micro damage and temporally precedes the appearance of damage-induced nonlinear behavior. The second model of nonlinear viscoelastic material behavior being considered by VISTA has been proposed by Schapery (Ref. 23). The model is derivable from thermodynamics principles and accounts for nonlinear creep with a strong stress dependence. A single integral, which is very similar to the Boltzmann form in linear theory, arises as a result of assuming special forms for Gibbs free energy and other thermodynamic concepts. The applicability of the model to FM-73U was demonstrated in the Residual Stress program (Ref. 24). Another study in this area includes the work of Findley (Ref. 25).

The time-dependent response properties that are required for input to VISTA are the shear and bulk relaxation moduli. These are expressed analytically in the form of a Prony Series representation as

$$\mu(t) = \mu_o + \sum_{i=1}^{N} \mu_i e^{-t/\tau_i} \quad \text{(shear relaxation)} \qquad (1)$$

$$\text{and} \quad K(t) = K_o + \sum_{i=1}^{N} K_i e^{-t/\tau_i} \quad \text{(bulk relaxation)} \; . \qquad (2)$$

For the intrinsically non-linear viscoelastic material description , the temperature-, moisture- and stress - time shift factor, a, is expressed analytically as

$$\log a(T,C,\theta) = - \frac{B}{2.303 f_o} \frac{[\alpha\Delta T + \gamma C + \delta\theta]}{[f_o + \alpha\Delta T + \gamma C + \delta\theta]} \qquad (3)$$

and the reduced time t' governing the relaxation behavior is given by

$$dt' = \frac{dt}{a(T,C,\theta)} \quad , \qquad (4)$$

where α is the thermal coefficient of volume expansion,

γ is the moisture coefficient of volume expansion,

δ is the mechanical coefficient of volume expansion,

f is the free volume fraction,

f_o is the free volume fraction at some reference, condition, and

B is a constant.

The stress-strain law for viscoelastic, isotropic media involves no more than two mechanical property functions. The two mechanical property functions that were measured in the Fatigue Behavior program were the tensile creep compliance and Poisson's ratio. Shear creep compliance data for FM-73U was obtained by Knauss (Ref. 26) and is being obtained at the same laboratory for both FM-73U and FM-73M under the auspices of the Viscoelastic Stress Analysis program (Ref. 21). As earlier indicated, the Poisson's ratio was found to be constant over a period of 30 days at

room temperature but the creep compliances were found to be time dependent.

It will be necessary to convert the creep compliance and Poisson ratio data to shear and bulk relaxation moduli representations for input to VISTA. The constancy of Poisson's ratio provides some simplification and means that the shear and bulk relaxations have the same time dependence as is shown in Equation (5) below :

$$\frac{K(t)}{\mu(t)} = \frac{2(1+\nu)}{3(1-2\nu)} = \text{constant} . \qquad (5)$$

Equation (5) also implies that, once the shear relaxation is known, the bulk relaxation can be quickly calculated because the Poisson's ratio is known. The shear relaxation can be determined from either the tensile or shear compliance data. However, the use of the shear compliance data is attractive from two points of view. There are less steps involved in the conversion to shear relaxation and the shear creep compliance data was obtained at very low stress levels, whereas the tensile creep data could be complicated by the fact that the tensile creep tests were conducted at relatively high stress levels. The method of inverting the shear relaxation from creep compliance data is now discussed.

If the field equations and stress-strain laws of linear viscoelasticity are subject to a Laplace transform in time, then they have an identical form to those of linear elasticity if the transform of the viscoelastic variables are associated with the corresponding elastic variables and if the quantities made up of the transform variable-multiplied-transformed shear and bulk relaxation functions are associated with the elastic shear and bulk moduli (i.e., $s\bar{\mu}(s)$ and $s\bar{K}(s)$ replaces μ and K). Thus any solution governed by the elastic field equation is also a solution to the Laplace-transformed viscoelastic field equations with μ and K replaced by $s\bar{\mu}(s)$ and $s\bar{K}(s)$. The final solution to the viscoelastic field equations is then obtained by inverting the transformed solution.

In linear elasticity the shear modulus μ and the shear compliance J are related by:

$$\mu = 1/J. \qquad (6)$$

Thus in linear viscoelasticity we have

$$s\bar{\mu}(s) = \frac{1}{s\bar{J}(s)} , \qquad (7)$$

where $\bar{\mu}(s)$ and $\bar{J}(s)$ are the Laplace transforms of the shear relaxation, $\mu(t)$, and shear creep compliance, $J(t)$. Equation (7) implies that, in the time domain, the shear relaxation and creep compliance are related by

$$\int_0^t \mu(t-\tau)\, J(\tau)\, d\tau = t. \tag{8}$$

Equations (7) and (8) form the basis of schemes that are used to determine relaxation moduli from creep compliances and vice versa. Hopkins and Hammings (Ref. 27) proposed and demonstrated a technique based on Equation (8) for the inversion of relaxation data to creep compliance. Heymans (Ref. 28) attempted to use the same technique to obtain the relaxation modulus <u>from</u> creep compliance data and found the method to be ill-conditioned. The problems of ill-conditioning were alleviated by taking very small time steps.

In order to avoid the penalties involved in checking for ill-conditioning and in refining the time steps, equation (7) has been chosen as the basis for inverting the creep compliance data. The technique, which is currently being developed in the Viscoelastic Stress Analysis program (Ref. 21), consists of representing the creep compliance by a Prony Series, substituting that representation in Equation (7) and then using a standard numerical Laplace inversion routine to obtain the shear relaxation, $\mu(t)$.

That is, if the creep compliance has the form

$$J(t) = J_o + \sum_{i=1}^{N} (1-J_i e^{-t/\tau_i}), \tag{9}$$

then equation (7) becomes

$$\bar{\mu}(s) = \frac{1}{s^2\left[J_o/s + \sum_{i=1}^{N}\left[1 - \frac{J_i}{(s + 1/\tau_i)}\right]\right]} \tag{10}$$

$$\text{and } \mu(t) = L^{-1}\left\{\bar{\mu}(s)\right\}. \tag{11}$$

The bulk modulus, $K(t)$, is obtained using equation (5):

$$K(t) = \frac{2}{3}\frac{(1+\nu)}{(1-2\nu)}\ \mu(t)\ . \tag{12}$$

2.3.2 Time-Dependent Fracture Characteristics of FM-73M Adhesive

The failure of adhesively bonded joints is generally due to the growth of cracks. It is therefore appropriate to use the concepts of Fracture Mechanics which can be used to relate the rate of crack growth in a material to the geometry, load and environment to inherent qualities of the material. These qualities are referred to as the fracture properties of the material. One such property is the ability to resist final, catastrophic failure. It is referred to as the fracture toughness of the material. It is well recognized that, under conditions of fatigue loading, cracks can propagate in an uncatastrophic manner. The property that is used to describe this crack growth rate is da/dN, the crack growth occurring for a single cycle of fatigue loading. The crack growth rate is not solely a property of the material but is also dependent on the loading, environment and geometry (which involves the crack length itself). The latter are accounted for through fracture parameters such as, for the sake of discussion, the stress intensity factor K. Crack growth rates are then presented in the form of plots of da/dN vs. ΔK where ΔK is the applied stress intensity factor range. Other fracture parameters that are used in this representation are the strain energy release rate and J-integral.

Fatigue crack growth occurring within the adhesive layer is controlled by the fracture properties of the neat material. In a bonded joint there must also be an adhesive/adherend interface. Fatigue crack growth occurring along the interface depends on the adherend, the surface preparation and the properties of the adhesive itself. Thus "interface" fracture properties may be thought to exist which reflect the resistance to crack propagation along the interface. Such interface cracks were shown to occur in the Fatigue Behavior Program (Ref. 19). Thus interfacial fracture properties may also be required.

In order to predict the life of a joint, comparison must be made of the impact of the loading with the resistance to crack growth or fracture properties. Since the response properties of FM-73M were found to be time dependent, it is to be expected that the fracture properties will also be time dependent. For a life prediction to be made with any generality, fracture properties must be determined for the range of times, temperatures and moisture contents that are consistent with those conditions typical of the service life of the joint (e.g., a joint within a modern transport aircraft). In connection with time-dependence, it should be

noted here that crack growth rates must also be measured at different frequencies, including very low frequencies, to allow for the occurrence of time-dependent crack growth at peak load. Brinson et al. (Ref. 29) have also considered the effects of environment and related these to changes in moduli and strengths and creep rupture changes in composites.

The selection of a fracture parameter that is descriptive of the material properties must be linked to the fracture parameter that is calculated from a stress analysis in order to assess the severity of a condition being analyzed. For linear elasticity, this task is relatively simple because of easily established relationships between the parameters. Such relationships are not as easily determined in less specialized cases, such as nonlinear viscoelasticity.

Calculations of fracture parameters, for use in determining fracture properties or the impact of a particular service condition, are routinely made using finite element stress analysis codes. Stress intensity factors are calculated from the crack flank displacements, strain energy release rates from the change in energy due to an extension of the crack and J-integrals from contour integrations of the stress and displacement fields surrounding the crack. The finite element code VISTA, to be used in this program, will include a representation, due to Schapery, for the J-integral which accounts for the nonlinear viscoelastic conditions (Ref. 30).

Fracture Properties for FM-73M have already been determined in a number of programs (Refs. 19, 31, and 32) under various configurations of loading, temperature and moisture. This data base is currently being confirmed and extended under the Time-Dependent Fracture Properties program (Ref. 33).

2.4 Definition of Loads/Environment

Loads/Environments contribute to stress in bonded joints and are vital for determining the life of a structure. For an adhesively bonded joint, it is necessary to define mechanical structural (loading) forces, thermal, hydral (moisture), and cure shrinkage effects. The effects will generally vary with time; that is, the loads may be monotonic or cyclic with time, and in general will be "statistical" in application as in an actual aircraft flight mission. Any meaningful definition of loads must consider

the sensitivity of the adhesive material mechanical response and failure characteristics to the varying environmental conditions.

2.4.1 Mechanical Loads

The complete description of any load to be used in a viscoelastic analysis requires information about the magnitude, duration, and sequence of the load. The importance of these parameters can be seen when one considers that even under relatively small loads, a crack in a viscoelastic material could grow to failure as a result of the large strains created by creep of the adhesive.

Loads typical of aircraft have a very broad range of frequencies. The low frequency would correspond to simple maneuvers such as those required by navigation. The high frequency would involve effects, such as windshear, turbulence, or landings where the dynamic response of the plane becomes important. The importance of frequency on the response of a viscoelastic material is very dependent on the temperature and moisture concentration of the adhesive. The adhesive behaves nearly elastically under high frequency loads when dry and cold. At the other extremes, when the adhesive is hot and wet, low frequency loads could cause large amounts of creep.

Frequency of loading is a very important factor in an analysis since some tradeoff must be made between this and the total time period of the analysis. If one wishes to consider the effects of high frequency loads (turbulence, as an example), on the response of the joint, then he must be willing to reduce the total time period examined so that the analysis is performed at a reasonable cost. On the other hand, if one is satisfied with looking only at very low frequency loads, i.e., on the order of hours, it is then possible to consider response of the joint for several years.

As an example, consider the mechanical loads involved in the flight of a modern transport aircraft (See, for example, the PABST Full Scale Test report, Ref. 34). If one ignores frequencies greater than about 1 hertz, the joint would see fairly uniform loads for its whole life. The primary changes would result from cargo loading and unloading, refueling, takeoff, and simple navigational maneuvers that might double the load. This type of analysis where the load is considered to vary only occasionally could be analyzed for time spans of a year or more. Admittedly, one cannot

ignore the effects of high frequencies and suddenly applied loads on joint life. However, even with an efficient finite element program, the computational power is not currently widely available to analyze the whole range of load frequencies involved in aircraft for typical aircraft life spans. Thus, one must accept, for the time being, the tradeoffs required between load frequency and analysis time span or develop a summary method for calculating damage accumulation through crack growth.

Mechanical loads at frequencies of 0.1, 1.0, and 10.0 cycles per second, and constant loads should be considered. These frequencies span the range of cyclic loads typical of modern transport aircraft. Time spans to be analyzed will correspond to roughly 10 to 20 cycles based on 10 to 15 increments per cycle. Thus, the largest time span will occur for the lowest frequency. The time span considered for the constant load is expected to be 10 to 20 years. This can be accomplished due to the logarithmic nature of creep. For example, by taking 10 increments of 1 second, then 10 increments of 10 seconds, etc., until we reach increments of 10^8 seconds, a time span of 20 years can be covered in less than 100 increments. This, of course, assumes that the material representation is accurate to 20 years at the given temperature.

Mechanical loads for a simplified mission would have to remain fairly constant, perhaps two or three changes per flight, in order to span a reasonable time period. This may not be a severe penalty since a joint in a transport would in fact spend a large portion of its life at a fairly constant load level.

2.4.2 Temperature Variations

Temperature has a significant influence on the creep of an adhesive. As temperature increases, the adhesive creeps more rapidly. Temperature variations, like mechanical loads, are cyclical in nature. Diurnal cycles, as well as cycles associated with missions should be considered. The temperature of the adhesive in a joint depends on its location. It will seldom equal the ambient temperature particularly when on the ground in direct sunlight. This radiation heating can be minimized by using a light color, preferably white, for exposed metallic or composite surfaces. However, other effects such as hot air from a jet engine or heat convection from a hot runway could cause the adhesive to become unacceptably hot.

In addition to the effect of temperature on creep of the adhesive, one must also include the strains created by expansion or contraction of the adhesive. This in itself could be sufficient to cause bond failure. One simple elastic finite element study (Ref. 19) indicates that the stresses created in a joint by expansion could approach the strength of the adhesive.

A third important factor to consider is shrinkage created by cure and cool down from cure to room temperature. Weitsman (Ref. 38) deals with the cool down problem by determining the optional temperature path to minimize residual stresses. Here too, bond failure is the possibility to be designed against if the cooldown proceeds too rapidly.

Temperature variations can be defined as an assembly of typical daily variations and seasonal variations and then combined into the desired time span similar to mechanical loads. In constructing the daily variations, one would have to consider the two extremes of service; hot/wet and cold/dry. An airplane could face these extremes daily or monthly or yearly. This would have to be accounted for since the heating/cooling can have a pronounced effect on life of the joint.

Temperatures of -65°F, RT, and 140°F are the primary temperatures for analysis in this program. The high temperature represents a practical limit for dry FM-73 as it is desirable to restrict the maximum temperature to below the glass transition temperature which is 140°F for the dry condition. For the wet condition, the practical limit is 120°F. The low temperature (-65°F) represents a reasonable minimum that a transport would see during its lifetime.

The temperature profile for a typical mission will consider the diurnal change in temperature plus the flight temperature. Thus, one includes in the profile a step increase in temperatue in the morning and a step decrease in late afternoon. On flight days, a temperature increase or decrease would have to be considered upon takeoff depending on the location of the joint. This temperature change arises from cooling that could take place at cruising altitude or heating that could occur due to heat generated by a jet engine.

2.4.3 Moisture Variations

Moisture affects the adhesive through plasticization (i.e., lowering of the glass transition temperature, Tg) and the swelling created by moisture ingression. A number of papers in the literature discuss the stresses created by the absorption/desorption of moisture by the adhesive layer. Weitsman has investigated the effects of moisture diffusion with both an elastic adhesive (Ref. 39) and a viscoelastic adhesive (Ref. 40) using a variational formulation. The results show that for exposure to steady ambient humidity, the viscoelastic stresses are smaller than their elastic counterparts. However, under functuating ambient humidity, the viscoelastic response caused stress reversals and thus possible failure modes that were not predicted by elasticity theory.

Jen (Ref. 41) using an approach similar to Weitsman analyzed a symmetric double lap joint. His results indicate that the most detrimental stresses arise during moisture desorption.

These analyses indicate that the most severe effects of moisture are created when distribution in the adhesive fluctuates. The rate at which moisture diffuses into the joint depends on the ambient humidity (and the adhesive diffusivity). Although a thin portion of the adhesive layer near an exposed surface reacts fairly rapidly to changes in humidity, the inner portion of a joint could take years to saturate. Thus, one is faced with a frequency problem similar to that encountered with mechanical loads. One can consider monthly or quarterly changes in the adhesive where a significant portion of the overlap experiences moisture absorption/desorption and evaluate its effect over a long period of time. Alternately, daily humidity changes could be considered where only a thin portion of adhesive is affected by moisture absorption/desorption. It is not difficult to see how this could cause a detrimental effect if the alternate swelling/shrinking caused sufficiently large stresses.

Moisture levels in the adhesive layer to be analyzed are dry, 50% saturated, and saturated. Transient moisture conditions will also be examined based on Fickian diffusion. These moisture levels cover the range of possibilities.

For a mission profile, the moisture concentration will be determined by the changes in ambient humidity. This would in turn depend on the location where the airplane is stationed. It is expected that the most severe effects would result from a profile that stationed the plane in an

area of very high humidity for several months and then stationed the plane in an area of very low humidity. This would produce significant moisture absorption/desorption in the adhesive layer if the time span is long enough.

2.5 Stress Analysis Methods

2.5.1 Introduction

Stress analysis is an important module of an integrated methodology for bonded joint life predictions. It relates the time-dependent response properties of the adhesive, such as the creep compliance, D(t), to the corresponding time-varying stress-strain distribution at any point in the adhesive interlayer, and shows how this distribution is modified as a result of volume changes resulting from temperature changes, from moisture absorption and desorption effects and from cure shrinkage effects. The accuracy and degree of "fineness" to which this time-varying stress-strain distribution can be calculated at any point in the volume of the interlayer is only a function of the resources at hand.

It has been established in the Fatigue Behavior program that great resources need not be expended on computing the distribution in bonded joints to arbitrary refinement. Some experimentation with gridding has been performed and an understanding has been achieved of how fine grids need to be made for various purposes.

It was clear from the beginning of that earlier work, as well as it is now, that the greatest uncertainty exists in connection with the singularities arising from corners. No amount of refinement that is economically tractable will provide sufficient detail to resolve the character of the singularity. What needs to be established yet is how much such singularities need to be resolved. This question is to be answered in two possible ways: One way would simply use more or less existing finite element codes and accept the highest stresses computed by standard elements available in the vicinity of the singularity points. The alternate way would be to use computer codes which have built into them singularity elements which capture at least the proper strength of the singularity. The only reason that this may have to be done is that the singularity may be relatable to the initiation of failure in a bonded joint. Such a failure criterion might be constructed in parallel to a standard

fracture mechanics principle which is concerned with comparing energy states of pre- and post-fracture situations. It appears clear to us now that when problems of this nature need to be dealt with, it becomes essential to employ a finite element code which encompasses special elements that can represent the corner singularities adequately.

In the following sections, we review stress analysis procedures that have been brought to bear on bonding problems in the past. It will become clear in this development that the earlier methods consisting essentially of energy approximations and similar closed-form exact solutions are inadequate to deal with the present complex design methodology. A necessary tool for the integrated methodology program is a suitably-designed finite element code. The minimum requirements of such a code are: a) Unlimited geometry adaptation. This capability is combined in virtually every user-oriented code today. b) Arbitrary material description. The list includes not only linearly elastic behavior; and possibly nonlinear material behavior of the elastic-plastic type. c) The code must contain or be adaptable to incorporate special elements admitting crack geometries and corner geometries that accurately reproduce stress intensity factors and/or singularity behavior in corners.

2.5.2 Stress Analysis

A detailed stress analysis of the adhesive interlayer is essential to the understanding and prediction of the response of an adhesively-bonded aircraft structural joint. This analysis must account for the detailed changes in the stress distribution in the adhesive interlayer arising from the effective volume changes induced in the adhesive material from various environmental effects which include temperature, moisture absorption and desorption, cure shrinkage and other phenomena, that will be seen in practical applications. An important set of parameters for the prediction of joint failure are crack tip stress intensity factor and energy release rates or J-integrals which must be supplied by the stress analysis.

2.5.3 Analytical (Closed Form) Methods

A review of the analytical or closed form stress analysis methods used to calculate the stress/strain distributions in bonded joints should include the following:

1) Exact expansions, 2) Approximations, and 3) Energy methods. In these discussions is a listing of reference papers dealing with the present subject matter amplified by a listing of the abstracts usually provided by the author (Refs. 42 to 52). While this listing and synoptic treatment of these references should give a fairly comprehensive overview of the field of analytical methods of stress analysis, we choose to mention here a few salient treatments that are crucial in any development of a stress analysis that is geared to the failure of bonded joints.

In 1952, Williams (Ref. 42) established the singularity treatment for discontinuous line defects in materials. He subsequently also dealt with a line discontinuity between two materials and pointed out the unnatural occurring state of deformation and stress in the vicinity of that point. This problem has been further studied by England. The satisfactory nature of that stress field results in a wrinkling of the supposedly stress-free flanks of the discontinuity in the vicinity of the termination point. The wrinkling is such that material would have to interpenetrate, a situation which is physically impossible. This means of eliminating or explaining this oscillatory singular behavior has been offered. It seems to have been pointed out first by Sternberg and Knowles that this is a direct consequence of the linearization of the problem and that it does not occur when large deformations are admitted. However, within the framework of linearly elastic analysis, Comninou, Dundurs, Achenback, Keer, Khetan, and Chen have developed failure models which allow for zones of bounded cohesive and shear stresses near the termination point of the discontinuity. Under those conditions, the oscillatory abnormal behavior can also be eliminated.

Bond terminations form re-entrant corners. It is often the case that cracks begin to propagate from such a re-entrant corner. This is a problem to which Westmann has paid special attention. The important point to be made in this context is that even when no crack is present in a re-entrant corner, the stresses are high. If a small crack is now introduced, it becomes embedded in an already high tensile field. The consequence of this superimposition or combination of stress fields is that a surprisingly high stress intensity factor occurs even though the crack itself may be very small. This has severe significance in the initiation of bond failure from improperly formed terminations. In a more approximate vein, Goland and Reissner analyzed the distribution of stress in a single lap joint. they determined the stresses for both a relatively stiff bond layer in which the adhesive layer is ignored per

se, and for a soft layer that includes the properties of the adhesive. It was assumed that the joint acted as a cylindrically bent plate of variable cross section. Their results gave good estimates of the peaking which occurs in the adhesive shear and peel stresses.

Energy methods, such as the application of potential or complementary energy theory, are applicable to the problem of bond fracture, since in many instances fracture criteria are based on energy criteria. Although the detailed distributions of stresses in the bonded joint are not reproduced with the energy only forced to a relative minimum, it may be that the energy release rate or other such quantities are quite accurate.

Sometimes the approximations are not made in a mathematical sense but rather through geometric means. Thus Knauss (Ref. 51) has, for example, dealt with a layer structure in which a central crack is embedded, the length of which is large compared to the thickness of the layer which does simulate a flawed bond line. Erdogan (Ref. 89) has considered problems of a similar nature except that the cracks of arbitrary length were located parallel to the boundary of the interlayer except at different distances from one of the two interfaces. Although these types of analyses would also lend themselves readily to parallel investigation for the elastic or other stress experimental methods, such experimental methods have not been done. These types of problems would seem natural condidates for investigation by the more recently developed method of caustics related to crack tip stresses.

2.5.4 Numerical Methods

In contrast to the analytical (closed form) approaches, there are available numberical methods of analysis: Finite difference codes such as PISCES solve the fundamental partial differential equations of continuum mechanics expressed in the explicit finite difference form. This allows the analysis of static and dynamic problems to calculate in great generality nonlinear, large-amplitude responses of structures, fluid bodies, and solid media. However, because of this generality, the cost of running such models is often staggering. In recent times, the finite difference approach has virtually been abandoned in favor of finite element methods. Some computer codes such as STAGS use a combination of finite element and finite difference methods for solutions.

The finite element method is an idealization which represents a continuous physical structure by a mathematical model made up of discrete elements whose element properties are known from the theory of elasticity. There are a vast number of computer codes in existence which use finite element principles. Many of these are special purpose programs with small element libraries and a limited problem-solving capability. Although these types of programs can be very useful and economical for solving certain problems, much more sophisticated methods are available. It is necessary then to concentrate on numerical codes which allow diversification and detailing of the special problems encountered in determining the stress distribution in a bonded joint. There are several such codes available, among which MARC, VISCEL, ANSYS, TEXGAP, and NONSAP are possible choices. Table 1 contains a comparison of some of the more important program features. All of the programs listed have common capabilities in material properties, mechanical loadings, and linear elastic analyses. In addition, each has one or more areas of specialization.

TEXGAP is useful in evaluating the stress intensity factor for Mode I and II, viz., K_I and K_{II}, respectively, for fracture analysis. It contains a two-dimensional crack tip element for analyzing plane of axisymmetric bodies. The most recent TEXGAP version, at least the one available at the University of Texas at Austin, is also able to deal with an interface crack which calls for both Mode I and Mode II deformations.

VISCEL incorporates a linear viscoelastic anlaysis, and as such allows a detailed time-dependent material characterization to be specified. VISCEL does not, however, provide any capability related to crack problems per se.

Nonlinear capabilities are found in MARC, ANSYS, and NONSAP. All three programs allow geometric nonlinearities (large deformations) and elastic-plastic material definitions, but NONSAP is more restrictive in applied loading and has no capability for heat transfer analysis. MARC and ANSYS are very similar in capabilities, but differ in at least two areas: crack tip elements and linear viscoelastic analyses. ANSYS has no linear viscoelastic potential. ANSYS has, however, a crack tip element, but it is strictly a 3-D solid element. Although MARC has no special crack element, it does have features that can be extremely valuable in fracture analysis. By positioning the mid-side nodes of the linear strain quadrilateral elements at the quarter point, an $r^{-\frac{1}{2}}$ strain variation, as found at the tip of a crack, can be modeled. This can be very useful

Table 1 Comparison of Selected Finite Element Programs

	CRACK TIP ELEMENT	MATERIAL PROPERTIES		ANALYSIS			GEOMETRIC NONLINEARITY	LOADING			HEAT TRANSFER	
		ISOTROPIC	ANISOTROPIC	LINEAR ELASTIC	LINEAR VISCOELASTIC	ELASTIC PLASTIC		MECHANICAL	THERMAL	TIME FUNCTION	LINEAR	NONLINEAR
MARC		X	X	X	X	X	X	X	X	X	X	X
VISCEL		X	X	X	X			X	X	X		
ANSYS	3-D Only	X	X	X		X	X	X	X	X	X	X
TEXGAP	2-D	X	X	X				X	X			
NONSAP		X	X	X		X	X	X				

in properly analyzing the stress-strain state in the vicinity of a crack. The MARC program also allows the evaluation of the J-integral. For linear elastic analysis, this is identically equal to the strain energy relase rate, G. A Prony series version of MARC is also available (Ref. 53).

General Dynamics has successfully used the MARC finite element program to analyze the model joint in the Fatigue Behavior Program. MARC was selected because it offers the greatest overall flexibility in application to adhesively bonded joints. The linear viscoelastic capability for the standard linear solid has been checked out and used in an analysis of the joint subjected to one sinusoidal cycle of loading and unloading.

The MARC program contains several other features that can be applied to the analysis of a bonded joint. Because bonded joints can undergo relatively large dormations, including rotations which can affect the stress distribution significantly, the large-deflection analysis will be needed. Since the program can solve the basic thermal expansion problem, it can also be used to calculate the stress introduction due to moisture diffusion. In addition, the stress analysis procedure is coupled with a diffusion problem solver that can be used to evaluate the moisture problem.

General Dynamics has obtained a wide range of experience in applying the MARC finite element program to the analysis of the model joint studies in the Fatigue Behavior program over a period of three years. The results of a simple elastic analysis were found to successfully predict the displacement measured at the saw cut, as shown in Reference 19. A viscoelastic model has also been prepared and used to calculate the stress distribution in the adhesive layer through one sinusoidal cycle of loading and unloading. Because of our past experience with the MARC code and because of its recent amplification in the viscoelastic domain, we shall choose to continue with that code until a more efficient code becomes available.

One of the major problems involved in the use of finite element procedures is the selection of a model which is both economical and provides the necessary degree of solution accuracy. In analyzing a bonded joint that consists of thick adherends and a very thin adhesive layer, it is very difficult to obtain a well-constructed grid without creating elements having very large aspect ratios. Depending on the degree of refinement, we find it advantageous to perform the analysis in two stages. With the first set of boundary

conditions that can then be applied to a second model of the particular region of interest. Since it is then not necessary to model the entire structure, a high degree of refinement can be made in a much smaller domain. This technique coupled with the use of higher-order finite elements provides very accurate stress distributions.

Applying the finite element method forces the user to deal with the tedious task of preparing the necessary input data for the analysis. If many models are to be created or if the models are very large, this can require a substantial amount of time. About 60% of the cost involved in completing a finite element analysis is tied up in the definition and verification of the model. Recently, General Dynamics' Fort Worth Division improved the efficiency of the modeling process by installing the GIFTS 4 model generation and static solution procedure on the VG-11 system (Fig.1).

The GIFTS (Graphics-Oriented Interaction Finite Element System for Time Sharing) System was developed by Dr. H. G. Kamel at the University of Arizona. It is an integrated system of programs that generates, solves, and interprets finite element structural analyses. Each individual specialized program contributes to the model UDB (Unified Data Base). The UDB contains nodal definitions, element connectivities, material properties, and boundary conditions for the pre-processing task of model verification, and element stresses and nodal displacements for plotting stress contours and deflected shapes in post-processing. By generating and preparing models with GIFTS on the VG-11 system, input errors can be virtually eliminated. All model generation, plotting, editing, and even the solution of small problems is performmed off line from the host computer with no charge for computer time. It is then a simple matter to access the data base and write a magnetic tape with the information extracted and formatted for the appropriate program input. The tape is then loaded into the host computer for analysis by the desired finite element program.

2.5.5 Environmental Effects

Problems dealing with transient stresses induced by the environment have been dealt with by several investigators. Amongst these, Weitsman's work is to be mentioned. This work is of an approximate nature in a closed form solution which provides a useful background problem against which numerical codes can be evaluated. A program recently completed at Texas A & M University (Ref. 24) dealt with a

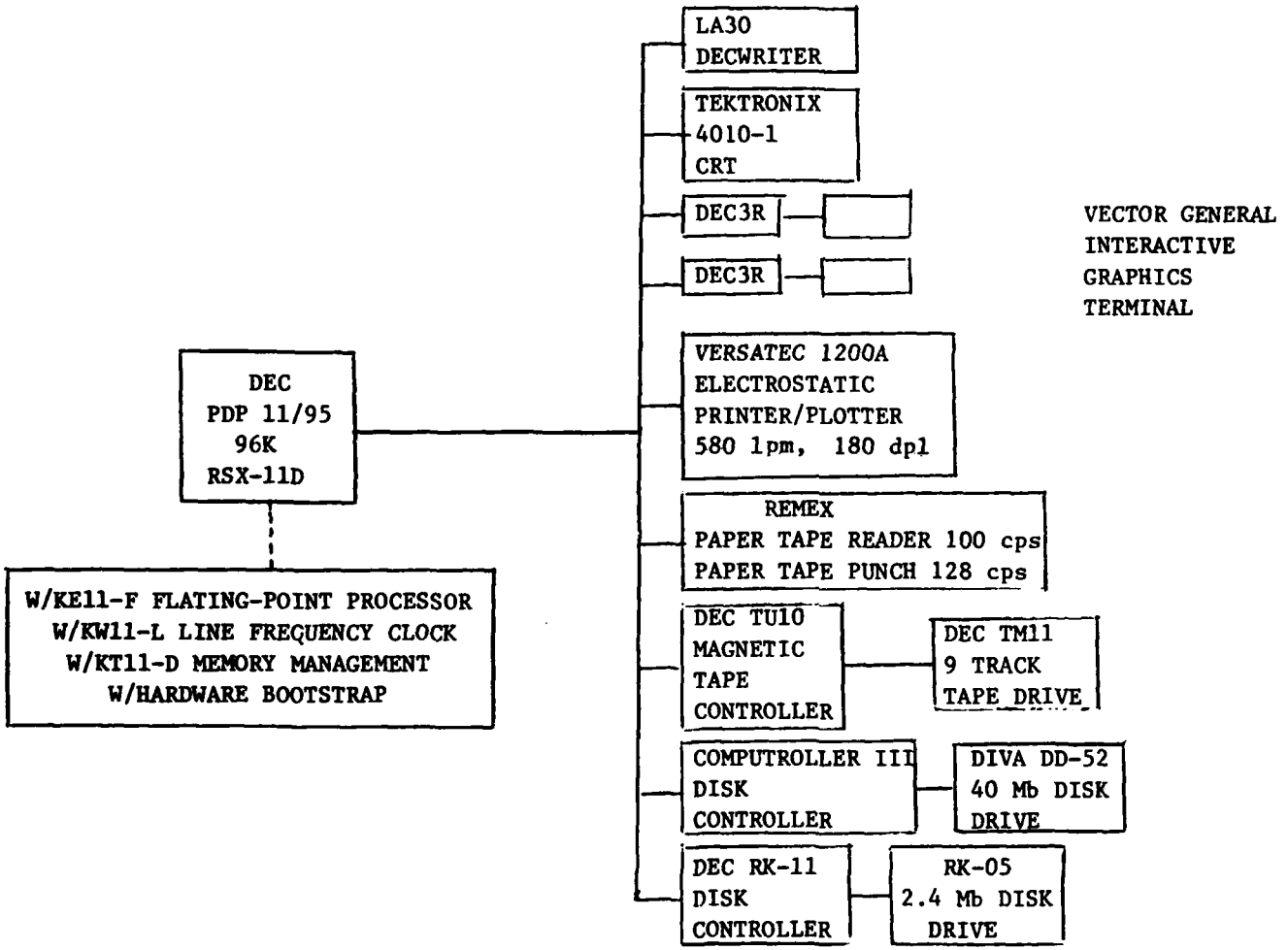

Figure 1 VG-11 Computer System

continuation of several programs. In general applications closed form solutions tend to be too time consuming and cumbersome although they are certainly of greater parametric value when they have been obtained. For this reason, we deal with environmental problems also in terms of finite element computer codes. A recent problem along this line has been resolved in our laboratory in connection with the Fatigue Behavior program. The problem posed was simply that of determining the stresses induced in a bonded joint after the joint had been submerged into an environment of different humidity. A MARC elastic analysis was used and a coarse grid finite model was developed for the bonded joint. The bonded joint was held analytically at 60°C while it was submerged in an atmosphere of 100% relative humidity. Moisture distributions for times of 3 days, 7, 29, 100, and 350 days were determined using Fickean diffusion theory and the stress distributions corresponding to those times were then determined. The computer analysis showed clearly how the maximum tensile stress in the bond area depends on the time as a result of the water diffusion process. The tensile stresses appear to achieve a maximum value somewhere around 30 days. By attaining 350 days exposure, the transient stresses had decayed again to nearly 0 value.

2.5.6 Stress Intensity Factors

To date, most of the information written on fracture mechanics is associated with linearly elastic materials, although some work has also been done with plastic deformations. In both cases, time independence is virtually essential. Although adhesives possess time-dependent properties,, under many circumstances they appear as if they were relatively rigid. It takes special conditions, namely long time, high temperature, or high moisture to bring out the more strongly viscoelastic properties. Since these conditions are involved in any practical structure, these phenomena must be considered.

To evaluate the crack growth properties of a specimen or joint subjected to a cyclic load, it will be necessary to make use of a quasi-elastic or viscoelastic stress intensity factor, or if the environmental conditions permit, an elastic energy release rate or stress intensity factor. As has been mentioned, the MARC program does not have a crack tip element per se for evaluating stress intensity factors. There are, however, other program capabilities that can be brought to bear on this problem. The fundamental problem in the analysis of the crack tip domain is the singularity in the strain field at the crack tip. For an elastic analysis,

the singularity is of the order of $r^{-\frac{1}{2}}$, where r measures the distance outward from the crack tip. The second-order linear strain isoparametric elements available in the MARC program can reproduce this type of singularity when the side nodes are placed at the 1/4-points instead of at the mid-sides. However, these elements have bounded stiffness only as triangles. A second feature of importance is the J-integral. The MARC program is set up to evaluate this quantity. It outputs a strain energy difference for a particular differential crack advance. This must then be normalized by the crack opening area to obtain the appropriate value of J. For linear elastic analysis, the J-integral is identical to the strain energy release rate, G. This can be related to the Mode I stress intensity factor, K_I, by the elastic relation:

$$K_I = \left[\frac{EJ}{1 - \nu^2}\right]^{\frac{1}{2}} \quad \text{(Plane Strain)} \quad , \qquad (13)$$

where E is Young's modulus, and ν is Poisson's ratio of the adhesive.

The strain energy release rate is not a defined quantity in viscoelastic terms, although the K-integral is. The viscoelastic stress intensities will, therefore, have to be evaluated by use of an extrapolation technique to determine the crack tip stress/strain. Knowing this, the stress intensity factors can then be obtained through use of closed-form analytical methods.

2.5.7 Selection of VISTA in Fracture Analysis

Compared, say, to elastic structural analysis or to elastic-plastic analysis, the area of viscoelastic analysis has received very little attention from the developers of finite element programs. The reasons for this situation are economic - the industrial need to analyze polymeric materials is miniscule in comparison with the need to analyze metal structures.

The large "general purpose" finite element codes, such as MARC, ABAQUS, ANSYS, ADINA and NASTRAN treat true viscoelasticity as an afterthought, if at all. These codes, intended primarily for the market of metal structures in elastic analysis, all contain capabilities for treating high temperature creep in conjunction with plasticity, but the

constitutive relations are not appropriate for the behavior of polymeric materials.

The second implication of the nature of general purpose codes is that they tend to be unwieldy both from the point of view of modification and use. These codes handle much larger amounts of data and numbers of operations than are required by a special application. The time and cost of modification and use of these codes rule them out as candidate vehicles for the present purpose of achieving an accurate and cost effective analysis of adhesively bonded joints.

To be truly useful as a research and/or design tool, a finite element code must possess the following attributes:

1. It must be capable of utilizing sufficient modeling detail, both geometric and with respect to material properties, to achieve the accuracy required. More importantly, it must be reliable - that is, thoroughly debugged and tested.

2. It must be user oriented in the sense that the analyst can easily define the problem at hand. Grid generation, loading and material property description should be both flexible and highly automated. The analyst should not have to describe in detail the sequence of operations to be performed by the code. For example, in the solution of transient problems, time steps should be calculated automatically by the code based on an appropriate accuracy criterion. Of course, the user must be able to over-ride such automatic features when he wants to.

3. The code must be efficient. The simplest way to judge efficiency is by the computer cost incurred for an analysis. Other factors, often of at least as great significance include cost of learning to use the code, cost of data preparation and cost of modification of the code.

4. The code must be well documented and supported. Documentation includes concise statement of the theory and algorithms on which the code is based, user's guide to input and output (including modeling criteria) and programmer's manual which describes the data management scheme, identifies important variables and describes all subroutines.

The general purpose codes are typically user oriented and capable of quite general geometric modeling. They are

also well documented. As noted above, they do not, in general, possess the material modeling capability requisite for this program nor are they readily modified by the user (in many cases modifications can be made only by the proprietary owner of the code). The major factor that rules out the use of such codes for the present purpose is the lack of computational efficiency that is a result of the data management requirements associated with general purpose coding. Problems of adhesively bonded joints are special enough in their character so that a code designed specifically for them is far more efficient and easy to use than any general purpose code.

The viscoelastic codes VISCEL, THERMVISC and THERMVINC are neither user oriented nor well documented. They are not supported, nor are they endowed with the modeling capabilities required.

In order to meet the criteria given above, the team of General Dynamics and Dr. Eric B. Becker of University of Texas (Austin) is currently developing a new code specifically designed to be accurate, reliable and efficient in the viscoelastic stress analysis of adhesively bonded joints (Ref. 21).

This new finite element code, termed VISTA (VIsco-elastic STress Analysis) and currently being developed under AFWAL funding (C-5167), is being designed specifically for the analysis of adhesively bonded joints. The code will provide adequate modeling capabilities to produce accurate solutions to two dimensional problems in adhesively bonded joints of general geometry and loading conditions. Advantage will be taken of the special nature of such problems to reduce the size of time-dependent calculations to a minimum, thus achieving a high degree of computational efficiency. The following discusses the special provisions that will be available to VISTA in this respect.

In time-dependent viscoelastic stress analysis, the stiffness equations must be recalculated and resolved at each time step. Sufficient history of the stress/strain fields to evaluate the constitutive equation must be available at each integration point in the viscoelastic material. For problems with many elements, the history must be saved external to the central memory. Unless special provisions are made, these factors imply that the cost of computing solutions will be very expensive. In general purpose codes, such as MARC, for example, this data management task causes large overhead in the computation cost. Even in the case of codes written specifically for

viscoelastic analysis such as THERMVINC, the history is read and rewritten to tape for each element at each time step.

By taking advantage of the special character of adhesively bonded joint problems, VISTA will eliminate the need to use low-speed storage for saving the history and reduce to a small fraction the size of the stiffness matrix that must be reformed and eliminated at each time step. This scheme should reduce the total computational cost of viscoelastic analysis by an order of magnitude.

Since in the modeling of a bonded joint problem only a small number of the elements in a problem (usually something like one-fourth) are actually used to model the adhesive layer, there is no need to provide history storage for the total element capacity of the program. Using Prony series representation of material properties of up to ten terms, VISTA will store in core the history for up to 100 adhesive elements. The storage will be dynamically allocated so that problems demanding smaller history storage will run with reduced core requirements. Fewer terms in the Prony series will allow more elements with the trade-off made automatically by the code.

Since the finite element model of the adherends are considered time independent, the adherend model will be automatically formed as substructures at the beginning of a run and the substructure stiffness and loads saved for reuse at each time step. This reduces the size of the matrix problem to be solved at each time step to only that of the adhesive layer itself.

By taking advantage of the special character of the adhesively bonded joint problem, VISTA will provide an efficient tool capable of accurate modeling at modest computational cost.

2.6 Failure Mechanisms and Damage Accumulation

The primary activity which guides the analytical and experimental procedures and which leads to economy of effort is establishment of fatigue degradation mechanisms, failure modes and failure criteria. A comprehensive study of failure modes in environmentally conditioned neat FM-73U and FM-73M adhesively bonded joints, and in particular in the model joint, the thick-adherend single-lap shear model joint design, was conducted in the Fatigue Behavior program. Development of a model of the failure modes in the model

joint is well documented in the final report to the Fatigue Behavior program (Ref. 19). The failure modes of the CLS and SLJ geometries have been determined in the Integrated Methodology program (Refs. 31 and 32).

Crack growth in the adhesive layer due to cyclic loading must be considered in an assessment of the lifetime of adhesively bonded joints. This required identification of the fatigue mechanisms and phenomenological description, baseline crack propagation data, and detailed fatigue crack growth models. Both interface (adhesive) crack growth and cohesive crack growth may have to be considered in the general case, although adhesive crack growth may be absent for certain geometries as noted in the Integrated Methodology program. Specifically both the CLS and SLJ geometries seem to display only cohesive initiation and failure modes.

A second element necessary for life predictions is baseline fatigue data. For cohesive failure, neat adhesive coupons may be used to obtain crack growth rate data. When the dominant failure mode is interface fatigue crack growth, baseline fatigue data must be obtained from bonded joint specimens. Data obtained is probably specific to each particular combination of adherend, primer and adhesive. For either case, temperature and moisture content are important parameters.

The above description assumes that the analytical crack growth model can be expressed in terms of crack growth per cycle. That is, it is assumed that crack growth per cycle and applied loads are related by the model. This relation may be through a convenient intermediate parameter, such as strain energy release. It is certain that the crack growth for a given load excursion will be strain-rate, and therefore frequency dependent. In addition, hold time at the higher loads can cause crack growth. Crack growth is the damage parameter in both cases and, of course, crack extensions are additive. Whether or not analytical predictions of the two types of crack growth can be superposed accurately is not as certain.

As mentioned above, the limiting condition for fatigue crack growth in the model joint is final fracture, which occurs as a cohesive failure near the adhesive midplane. The transition from fatigue crack growth at the interface to fracture at the midplane in the model joint necessitates crack "branching". The point at which this transition occurs must be defined in order to be able to predict model joint life. There is, therefore, a dual failure criterion

to consider within the failure analysis for the model joint. In performing the stress analysis, it will be necessary to periodically interrogate whether the interface fatigue crack or the midplane fracture crack is the dominant mode of failure. A condition will have to be found indicating when a critical state is reached causing a transition from one to the other. For example, an examination of energy may indicate when the fracture energy of the adhesive is less than the energy of debonding at the interface.

Fatigue crack growth and transition to final failure must both be understood for various relative proportions of Mode I and Mode II. A successful bonded joint prediction methodology must rely on baseline data from which this information can be derived. Accordingly, the test program includes testing for two different mixes of Mode I and Mode II.

An in-depth review has been conducted of the fatigue and fracture mechanisms of polymeric adhesives and bonded joints. Factors considered included the damage mechanisms possible over the range of the service environmental condition, the rate of damage accumulations during exposure to each environment, and possible synergistic effects. The kinetic chemical and physical aging effects were also considered.

In order to be able to predict the lifetimes of adhesive joints, one must first determine the possible failure modes so as to provide a basis for subsequent modeling. The second quarterly progress report of the Integrated Methodology program (Ref. 35) outlined failure through crack growth and excessive deformation as possible failure modes and provided the rationale for a more detailed consideration of the former failure mode. Fatigue testing of model lap shear joints (MJ) under the Fatigue Behavior program (Ref. 19) uncovered two crack propagation modes; namely, slow initial interfacial debonding branching to catastrophic cohesive cracking. The extent of interfacial crack growth prior to branching was found to depend on load level and frequency as well as the environmental conditions and was also summarized in Ref. 19. Since the cohesive crack growth in the model joint is catastrophic, the lifetime of the joint is essentially governed by the time for branching from the interfacial debond to occur. Thus, life prediction is "reduced" to determining when conditions are favorable for branching to occur. The method of analysis and several possible fracture criteria to be used to determine the onset of branching are discussed in the following section. The

results of the analysis to date are presented in Reference 37.

As already mentioned, the CLS and SLJ geometries display only cohesive crack initiation, growth and failure modes.

The MARC finite element code has been used to provide stress analysis of MJ, CLS and SLJ geometries having different lengths of interfacial debonds and cohesive cracks. In addition to computing the stress, strain and displacement fields in the joint, MARC calculates the value of the J-integral for a given crack length. Two fracture criteria are therefore available for determining the lcoation of the crack path; namely, the vectorial crack opening displacement (VCOD) and the J-integral.

Both criteria have the advantage that they can be used in cases where material nonlinearities occur. Although only linear elastic analyses have been made to date, these features will be useful in later analyses which do consider non-linear effects. In an experimental investigation of interfacial unbonding of adhesive joints (Ref. 54), it was found that VCOD (obtained by the vectorial addition of the crack flank displacements normal to and tangential to the bondline) provides the most unified fracture criterion under the different combinations of applied displacements normal to and tangential to the bondline experienced by an adhesive joint. It is of interest to compare the VCOD criterion with a critical stress intensity factor criterion for a crack at a bimaterial interface under the constraints of linear elasticity. In Ref. 55, Smelser found that the complex crack opening, $\underline{u}$ (or VCOD) was related to the complex stress intensity factor, k, as follows:

$$\Delta\underline{u} = \frac{1}{4\sqrt{2}} (\Lambda_1 + \Lambda_2) \frac{k}{\lambda} r^{\lambda} e^{-i\pi/2} \quad , \tag{14}$$

where $k = k_I + i\, k_{II} = k_o\, e^{i\beta}$,

$\lambda = \lambda_o e^{i\delta}$, $\lambda_o = \sqrt{\frac{1}{4} + \varepsilon^2}$ and $\delta = \tan^{-1} 2\varepsilon$,

$\varepsilon = \frac{1}{2\pi} \ln \gamma$, is the bimaterial constant

and $\Lambda_\alpha = \frac{4(1-\nu_\alpha)}{\mu_\alpha}$ plane strain

$= 4/\mu_\alpha\,(1 + \nu_\alpha)$ plane stress .

The magnitude of $\Delta\underline{u}$ is thus

$$|\Delta\underline{u}| = s = \frac{1}{4\sqrt{2}} (\Lambda_1 + \Lambda_2) \frac{k_o}{\lambda_o} \sqrt{r}. \tag{15}$$

Thus, at a given distance, say r_o, from the crack tip, the VCOD is equivalent to the square root of the sum of the squares of the local Mode I and Mode II stress intensity factors.

Furthermore, Smelser and Gurtin (Ref. 56) found that the J integral for a bimaterial is equal to the energy release rate of a crack extending along the interface and related J to the stress intensity factors k_I and k_{II} by

$$J = \frac{\pi}{16} (\Lambda_1 + \Lambda_2)(k_I^2 + k_{II}^2) \quad . \tag{16}$$

Combining equations (15) and (16), we find

$$s = \frac{2\sqrt{2}}{\pi} \frac{J}{\lambda_o} \sqrt{r} \quad , \tag{17}$$

thus establishing the equivalence of the VCOD and J integral.

However, in this inherently mixed-mode interfacial fracture problem, it should be noted that the J integral alone does not provide adequate information for determining the individual values of k_I and k_{II}. In contrast, the components of the VCOD give a direct measure of the relative mix of the local Mode I and Mode II deformations (or the angle of the VCOD). The VCOD can be used to determine the Mode I and Mode II stress intensity factors (Ref. 55).

In a cracked, uniform, isotropic material, loaded in shear, a crack does not propagate as a Mode II crack. Instead it naturally will branch at an angle to its original direction, tending to become a Mode I crack. Since the MJ is loaded in shear, there must be a tendency for an interfacial crack to branch toward or away from the adhesive midplane. This is apparently prevented for a time because the interfaces provide an easier path for crack propagation than either the adherend or adhesive. The length of the debond, in addition to the bond design, affects the proportion of Mode I to Mode II in the joint. In addition to presenting results on the VCOD and J integral for various lengths of interfacial debonds and cohesive cracks in Reference 57 information on the ratio of Mode I to Mode II is also given.

2.7 Structural Integrity Evaluation (Strength Analysis)

The strength of a structural joint is usually defined in terms of its load-carrying capability. It depends, in turn, on the geometry of the joint and the local stresses induced in the bondline as a result of the applied loads, whatever their origins may be, be they mechanical, thermal, or hygral.

For the purpose of discussing the importance of structural geometry in the framework of life prediction methodology, a large structure, say a PABST-like or F-16 fuselage is used in the discussion. Aircraft flight loads applied thereto generate joint stresses over the entire structure. A simplification in the analysis by breaking out the various joint geometries into smaller "bondline" geometries can be broken down for detailed bond analysis, although this cannot, in general, be done quite independently of the selected stress analysis method.

At this point, these smaller "bondline" geometries can be further reduced into the proposed program test geometries, or at least test geometries which can in some way be related to the latter such as the cracked lap shear (CLS), the structural single lap shear joint (SLJ), and the thick-adherend single lap shear or model joint (MJ). These were the geometries which were used in the various phases of the experimental test program in the current program, in either the baseline property measurement phase, or in the verification test phase.

The classical structural integrity procedure of comparing calculated stress/strain levels to the ultimate material properties to determine a margin of safety has been considered by General Dynamics (see, for example, Ref. 57). The applicability of this procedure to both the design phase and subsequently for in-service evaluations, was also investigated. How well the classical strength analysis method, usually used for metallic airframes, applies to bonded joints and a definition of those areas where improvements are necessary in the formulation of a life prediction methodology for adhesive bonded joints was conducted and summarized in Reference 57.

The structural integrity of adhesive bonded joints is assumed to include both strength and life considerations. This interpretation is based on the philosophy of U.S. Air Force specification MIL-STD-1530A for metallic airframes.

III. MODULE DEFINITION AND INTEGRATION

3.1 Module Logic Development

Figure 2 shows the major elements or modules of the predictive method as developed in this program and their inter-relationships as applied to adhesively bonded structures. It parallels the systems approach for solid rocket service life prediction first proposed by Kelley and Trout in 1972 (Ref. 58). Extension of Kelley's ideas from solid rocket propellants to adhesively bonded structures is possible in view of the time/temperature (and moisture) dependence of the constituent material (polymer) properties and similar failure modes (crack propagation) in both cases.

The Integrated Methodology (IM) program was viewed from its inception as the backbone program , which when augmented by a series of feeder sub-programs (see Figure 3) would produce the desired results, namely, the best estimate of life prediction on a structural bonded joint of arbitrary geometry, obtained from a combination of available analysis techniques based on proven fundamental scientific principles, i.e., using the deterministic approach and suitable experimental fatigue tests. This would then be followed later by a calculation reflecting the probabilistics of the measurements used to give a statistical result with "probable error bars."

The IM program was thus viewed as an organizing program, or a demonstration program to highlight the (best) methods to be used in making a structural bonded joint life prediction based on the findings in the feeder sub-programs, labelled ② through ⑧ in Figures 2 and 3 and the consequences of using them. The IM program was designed to take a large step into the unknown, but hopefully would reduce risks by observing well-established and understood scientific principles. It would develop the analytical tools and methods, with projections into the unknown environments (e.g., temperature, humidity, mechanical loads) with lowest element of risk possible based on the scientific method. Program ② would in the main develop equation(s) for the stress-strain law of the adhesive interlayer, including effects of moisture diffusion and cure shrinkage; program ③ would develop the method(s) for assessing the consequences of speeding up and/or slowing down the tests, and by how much with the different environments, including temperature, moisture, mechanical load, cyclic frequency, etc.; program ④ would design a practical, easy-to-use

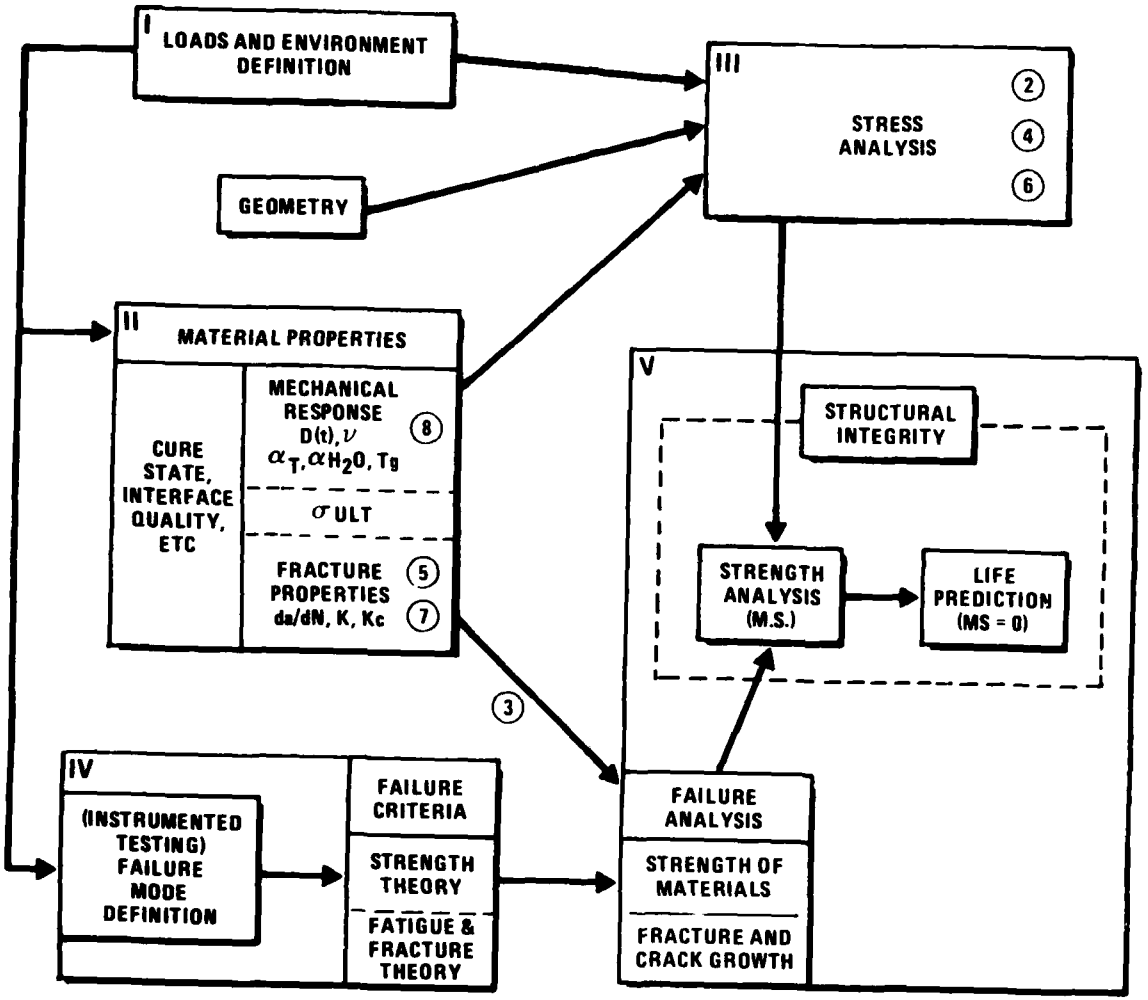

Figure 2 Modules and Flow Path of Predictive Method:
"Integrated Methodology for Adhesive Bonded Joint Life Predictions"(1)

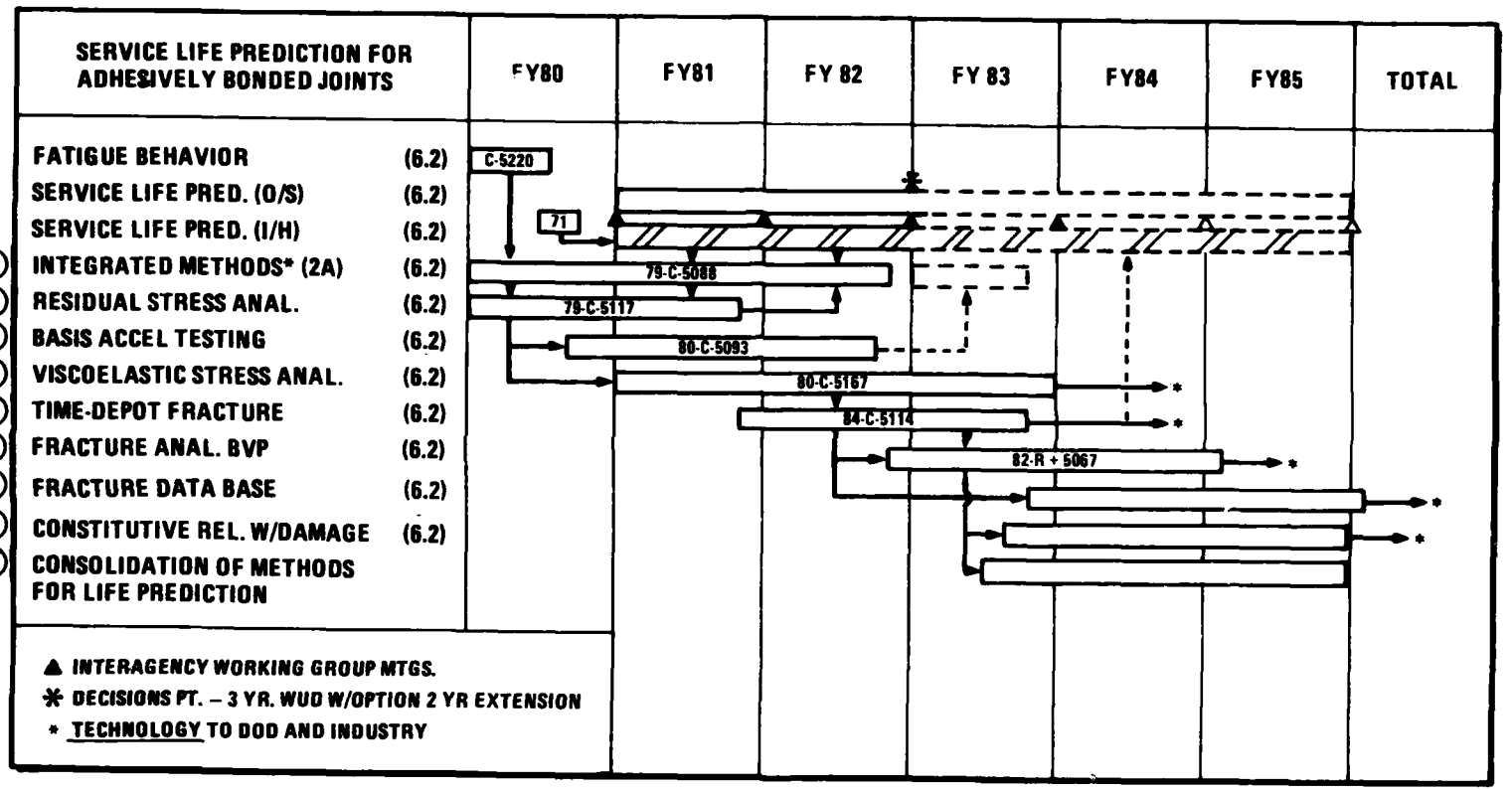

Figure 3 W-P AFB AFWAL/MLBC Program Plan on Service Life Prediction for Adhesively Bonded Joints

finite element program unique to bonded joints; program ⑤ would generate the fracture mechanics data base needed for the life prediction, and program ⑥ would develop advanced fracture mechanics solutions to relevant bonded joint geometries using the VISTA program developed in program ④; etc...

The overall plan of the IM program is to set up the technical and management framework and organize constituent tasks in modular format which would be used to make the life prediction(s). The IM program deals with the individual modules to some extent, with the specific details of the modules to be developed by the related roadmap contracts.

The I M program had the objectives to a) identify clearly the interacting subdisciplinary modules, b) to evaluate and to some degree further the state of the art of each one, and c) identify the major shortcomings so that further contractural efforts would improve the knowledge in each module so that the overall IM could proceed more reliably.

The goal of the IM program was to develop the methodology which can be used in the design stage to facilitate durable, reliable designs, and to improve cost of ownership, projections, etc.

The related roadmap contracts are marked ② through ⑧ in Figures 1 and 2. These must be accomplished for full implementation of the Integrated Methodology program. We outline and enumerate our five main modules by Roman numerals I through V. Of special interest is the central position of the Stress Analysis module (III) and the dominance of the Failure Mechanisms and Criteria module (IV) in focussing all related activities.

An outline of the five main modules of a life prediction methodology and their contents (viz., analytical methods and/or questions that the module needs to address) is first given. We then establish the inputs and outputs of each of the five modules. Futhermore, in Table VI we outline the experimental data required, and finally in Figure 4 we summarize the Overall Integration of the method, including the Management Plan, for a structural bonded joint.

We have established:

a) priorities

b) problems that are solved in this program

c) problems yet to be solved.

Material properties represent the only element sensitive to aging time although there is naturally a time element inherent in the environmental loading rate, duration and frequency. Since storage time is a primary variable in the service life prediction scheme, the overall rationale should apply as well to the zero-time design point which considers all material properties in the unaged condition. Another important breakout of material properties, when considering the impact of aging, is the separation of response properties from the fracture properties; response properties being a principal input to the stress analysis and fracture properties applying primarily to the strength analysis.

The response and fracture characteristics of bonded structures are known to be dependent on loading rate and history in such a complicated fashion that analytical procedures must be supplemented with adequate laboratory testing to provide the necessary design confidence. The guiding assumption in this integrated methodology scheme is that the useful life of a bonded structure is determined by the initiation and relatively slow propagation of cracks emanating from corner singularities and reaching a critical size at which time catastrophic failure occurs.

The emphasis in this integrated methodology scheme is on the "deterministic" approach, with full recognition that a "probabilistic" treatment will eventually have to be incorporated in the methodology to realistically predict mixes of missions and mission profiles and to account for experimental error in the data used. However, since a deterministic approach provides the basis for a statistical representation and in view of the time and budget resources of this program, the deterministic approach was the first priority.

We note that physical laws govern the contents of a number of the modules, with only engineering approximations possible in describing the phenomena involved. Also, basically there are no modifications possible for these except for economic trade-offs in these approximations. Modules in this category commanding top priority include "Stress Analysis" and "Failure Mechanisms and Criteria".

Modules which allow descriptions not directly governed by physical laws allow system choices which affect the final result. Two such modules include "Loads and Environments" and "Material Properties" which are of top priority in our

scheme. Geometry, if it can be considered a module at all, commands secondary emphasis at this time.

We proceed with a description of the contents of each of the five main modules. These are summarized in Tables IA through VA. This is followed by a description of the input and output information required for each, as summarized in Tables IB through VB. These are followed by a description of the experimental data required to validate the concepts in the modules as presented in Table 14 . Finally, an overall integration of the method for the analysis of a test joint or an "aircraft", with associated Management Plan is presented in Figure 4.

Order of priority of some items, insofar as being accomplished in the Integrated Methodology program is indicated by the designation P(n) after the item in question in the Tables, with n=1, 2, 3,... in order of decreasing priority. Of course, the aforementioned feeder sub-programs will eventually develop the necessary inputs for full implementation of the methodology for a general case.

3.2 Module Evaluation and Selection

3.2.1 Loads/Environments (Module I)

Often the types of loads are directly related to failure modes (as far as the way engineers do it); one tends to forget that often loads may produce different, possibly longer term failures. It is important to delineate the kinds of "loads" at an early stage so that the types of histories are accounted for in material characterization (stress and failure response).

For this program, loads and environments are important from the latter point of view. We believe priorities are as listed in Table 2 (IA), which summarizes the contents of this important module, emphasizing the time, temperature, moisture, stress level and sequence of events in defining the impressed loads, whatever their origins may be.

The Magnitude and Frequency of the Periodic Mechanical Load and Steady and Monotonic Non-Periodic Mechanical Loads are of concern in the Integrated Methodology program.

Table 3 (IB) summarizes the input and output information relating to this module. Traditionally, the Loads Group has developed an expertise in these types of problems for rate independent structures. Some modification to this has been

Table 2 (IA) Loads/Environments, Contents*

A. MECHANICAL LOADS LOAD HISTORIES (DEDUCED MISSION PROFILES) MISSION PROFILE MANEUVER SEQUENCE FLIGHT ENVELOPE (a) PERIODIC (FATIGUE) – MAGNITUDE FREQUENCY (b) NON-PERIODIC – STEADY MONOTONIC
B. THERMAL ENVIRONMENT (a) EFFECT ON $\underline{A}$ (THROUGH STRESS ANALYSIS) UNDER CONSIDERATION OF DIFFUSION TIMES (b) EFFECT ON MATERIAL BEHAVIOR (c) TIME/TEMP HISTORY SYNCHRONOUS WITH LOAD HISTORY
C. MOISTURE ENVIRONMENT (a) EFFECT ON $\underline{A}$ (THROUGH STRESS ANALYSIS) UNDER CONSIDERATION OF DIFFUSION (b) EFFECT ON MATERIAL BEHAVIOR
D. SEQUENCE OF MECHANICAL LOADS, THERMAL MOISTURE ENVIRONMENT

* Details are recorded in Reference 35

Table 3 (IB) Loads/Environments, Inputs and Outputs*

INPUT			OUTPUT
MECHANICAL			* TIME DEPENDENCE OF LOADS
AIRPLANE RECORDS ON ACCELERATION WITH EXPLICIT TIME			(A) STEADY
(A) GROUND REST			(B) CYCLIC WITH WHAT FREQUENCY
(B) TAKE-OFF			(C) "BLOCKS" FOR STATISTICAL ANALYSIS
(C) LANDING			
(D) IN-FLIGHT MANEUVERS			
DETERMINISTIC			
STATISTICAL (SPECTRA)			
THERMAL			* (TIME DEPENDENT)
GROUND STORAGE		TIME SCALE	TEMPERATURE DISTRIBUTION
FLIGHT: STAGNATION-INDUCED		TIME SCALE	TEMPERATURE GRADIENTS
ENGINE – DUCT INDUCED		TIME SCALE	(INCLUDING SKIN TEMPERATURE)
ATMOSPHERIC		TIME SCALE	RADIATION OF SUN
MOISTURE (AND OTHER SOLVENTS)			* TIME DEPENDENT
DIFFUSION AS A FUNCTION OF TEMPERATURE			H_2O (AND/OR SOLVENT)
GROUND STORAGE		STRESS DEPENDENCE	CONCENTRATION AND GRADIENTS
FLIGHT DRY-OUT			POWER SPECTRAL RESPONSE

*Details are recorded in Reference 35

effected by "composite" needs. For adhesives, we envisage the following relation between information required for failure analysis purposes (output from the module and raw loads data input): The results of this digestion process are delineated in Table 3 (IB). It must be noted that the listing of input and output items is not necessarily complete at this time, although we have tried to be as inclusive as possible.

3.2.2 Material Properties (Module II)

The local stress distribution developed in a bonded joint will be greatly influenced by the material properties which define their deformation characteristics. The "response" properties of the adhesive, such as the creep compliance and Poisson's ratio will dictate, by and large, these deformational characteristics of the bonded joint and in general will exhibit time, temperature, moisture and stress level dependence.

After cyclic loading of the environmentally-conditioned (temperature and humidity) bonded joints in environments representative of an aircraft mission, the "fracture" or "failure" properties of the adhesive will control the residual strength capabilities of the structure. Typical "fracture" properties of the adhesive (joint) include the crack growth rate with cyclic frequency, viz., $da/dn = a'$, or the equivalent $da/dt = a$ representation. Failure or fracture "properties" are dependent on the current knowledge of failure analysis. (Properties are determined in tests prescribed by failure analysis).

A comprehensive review was made of these time-dependent "response" and "fracture" properties of adhesives required for this program as summarized in Reference 59. The physical and mechanical behaviors considered included constitutive relations under monotonic and cyclic loading conditions, dilatations during cure, cooling and moisture infusion, aging, mechanisms of damage accumulation, fracture toughness and ultimate strength spectra, among others.

Table 4 (IIA) and Table 5 (IIA') summarize the response and fracture properties contents of the Materials Property module, and their sensitive dependence on time, temperature, moisture, and stress level, among other parameters (see Reference 59).

Physical, chemical and structural aging effects are distinguished and these effects are being covered in the

Table 4 (IIA) Materials Properties,* Contents (Response)

RESPONSE
D(t), or E(t) or J(t)
k(t) or υ (t) (WHAT MINIMUM ACCURACY REQUIRED?)
TRANSITION TEMPERATURE (GLASS OR MELT TEMP FOR CRYSTALLINE COMPONENTS IN AN ADHESIVE)
SHIFT FACTORS ϕ DUE TO TEMPERATURE ϕ_T
MOISTURE ϕ_p
STRESS LEVEL ϕ_σ
COEFF OF EXPANSION DUE TO TEMPERATURE α_T
MOISTURE $\alpha_{p(x,t)}$
STRESS LEVEL ($\equiv$ k(t))
CONSTITUTIVE FORMULATION; NON-LINEAR VE < VOLUME / OCTAHEDRAL SHEAR
AGING: PHYSICAL (STRUIK)
CHEMICAL (DARK EDGE)
STRUCTURAL (MICROCRACKING)
NEAT vs NEAT-NEAT BEHAVIOR*
*NEAT TAPE IS WITH MATTE DACRON SCRIM. NEAT-NEAT TAPE IS WITHOUT SCRIM.

* Details are recorded in Reference 59

Table 5 (IIA') Materials Properties,* Contents (Fracture)

FRACTURE

$\Gamma = \Gamma(\dot{a})$ COHESIVE / ADHESIVE P(1)

$\dot{a} = \frac{da}{dt}$

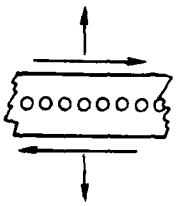

$\Gamma = \Gamma(a')$ COHESIVE / ADHESIVE P(1)

$a' = \frac{da}{dn}$

WHAT IS THE "PLASTIC ZONE" SIZE α, AS RELATED TO BONDLINE THICKNESS; AFFECTED BY MODE INTERACTION? P(1)

EFFECT OF PLANE σ vs PLANE ϵ
IS FATIGUE BEHAVIOR GOVERNED BY K OR ΔK? P(2)
IS SCRIM CLOTH IMPORTANT TO FIRST ORDER?

(a) SCRIM IN A BUTT JOINT UNDER NORMAL LOAD / SHEAR LOAD P(3)

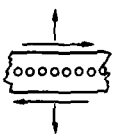

(b) SCRIM ORIENTED IN TEST PLANE (LABORATORY TYPE TEST & NEAT) P(2)

(c) NO SCRIM, NEAT-NEAT MATERIAL

IS TIME-TEMPERATURE-WATER (SOLVENT) "STIFF" BEHAVIOR SYNERGISTIC P(3)

EFFECT OF CURE LEVEL P(3)

EFFECT OF AGING (CHEMICAL, PHYSICAL) P(3)

ULTIMATE TENSILE PROPERTIES (SMITH PLOTS) P(3-4)

* Details are recorded in Reference 59

program on "Basis for Accelerated Testing" currently in progress at Texas Research Institute, Austin, Texas (Ref. 20).

The response and fracture properties of the adhesive layer will depend on whether it is neat-neat (without scrim), or neat (with scrim). A detailed inquiry into this matter is recommended, but is beyond the scope of this program. We have elected to approximate the out-of-plane response and fracture properties of the adhesive layer by the properties measured in-plane using neat (with scrim) specimens.

Table 6 (IIB) summarizes the input data required for the Materials Properties Module. The output data for this table is all that has been listed in Table 4 (IIA). Recorded also in Table 6 (IIB) is a section on instrumentation and testing considerations in generating the appropriate data. Also the sub-title to this chart suggests the importance attached to interface or interphase properties at the adhesive/adherend junction where material properties are far from homogeneous and isotropic. The fact that the initial failure mode in a bonded structure is a crack at the interface, initiating at the high (peel) stress corner singularity, highlights the importance of this part of the adhesive joint.

3.2.3 Stress Analysis (Module III)

A thorough stress analysis is vital to the success of the Integrated Methodology program. It allows point-by-point description of the displacements and stresses (both peel and shear) on a "micro level" in attempting to account for material displacements (creep) and damage mechanisms occurring in the adhesive interlayer on a realistic basis. Earlier studies which deal with averaging of stresses through the thickness of the adhesive are incorrect and lead to erroneous results.

Table 7 (IIIA) summarizes the requisite content of the Stress Analysis module, including the validation of the stress analysis by holographic interferometry as described in Appendix 1. This validation is an important part of the methodology since it will allow first hand confirmation of the finite element procedures adopted in this program.

Table 8 (IIIB) details the input and output information required for and expected from, respectively, the Stress Analysis module.

Table 6 (IIB) Material Properties and Interface Inputs and Outputs

INPUT	
ENVIRONMENT LOAD LEVELS HISTORIES STATE OF CURE TYPE OF MATERIAL	INSTRUMENTATION – A. CREEP APPARATUS OR RELAXOMETER TEMPERATURE CONTROL EQUIPMENT $\bar{P}(1)$ HUMIDITY CONTROL EQUIPMENT TMA B. TEST MACHINE FRACTURE SPECIMEN
OUTPUT	SAME AS ALL OF TABLE IIA

Table 7 (IIIA) Stress Analysis, Contents

HIERARCHY OF REQUIREMENTS AND CAPABILITIES:		WHICH PROGRAM:	
A. MATERIAL REPRESENTATION			
LINEARLY ELASTIC		MARC	VISTA
ELASTIC – PLASTIC (WITH AND WITHOUT STRAIN HARDENING)		M	
LIN VE		M	V
NON-LINEAR VE			V
GEOMETRIC NON-LINEARITY (GEOMETRY UPDATING)		M	V
DILATATIONAL BEHAVIOR OF MATERIAL DUE TO TEMPERATURE AND OR WATER (SOLVENTS)		M	V
B. GEOMETRY REPRESENTATION:	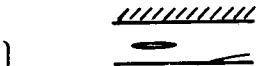		
CRACK TIP ELEMENT		M	V
INTERFACE CRACK TIP ELEMENT	DEAL WITH INTERACTION		V
END TERMINATION (CORNER SINGULARITY)	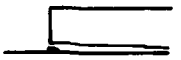	M	V
VOIDS AND POROSITY			
C. DISTRIBUTION OF a) TEMPERATURE b) WATER			V
–VALIDATION– (HOLOGRAPHIC INTERFEROMETRY)*			

* Details are described in Appendix 1

Table 8 (IIIB) Stress Analysis, Inputs and Outputs

INPUT			OUTPUT
A. GEOMETRY INCLUDING FRACTURE PATH (a) INTERFACE (b) COHESIVE	MARC	VISTA	ENERGY RELEASE RATE OR J INTEGRAL – (THICKNESS AVERAGED) – DETAILS
		V	STRESS INTENSITY FACTOR
B. MATERIAL RESPONSE CHARACTERISTICS		V	CORNER SINGULARITY STRENGTH
CONSTITUTIVE BEHAVIOR ACCOUNTING FOR TEMP AND WATER	M	V	STRESS DISTRIBUTION MAPS FOR STRESS COMPONENTS PLUS
C. BOUNDARY CONDITION ON (a) LOADS (b) TEMPERATURE (c) WATER			(a) PRINCIPAL STRESSES AND THEIR (b) ORIENTATIONS (c) OCTAHEDRAL (d) DILATATIONAL ($\sigma_1 \pm \sigma_2 \pm \sigma_3$)
D. EXTREME EXAMPLE: TIME MARCHING PROBLEM	M	V	NODAL DISPLACEMENTS
		V	ENERGY RELEASE FOR MINIMUM CRACK P(2) 
			DETERMINATION OF CRACK PATH TO BE ACCOMPLISHED BY TRIAL AND ERROR FOR MAXIMUM ENERGY RELEASE RATE AS A FUNCTION OF INCREMENTAL CRACK EXTENSION
NASTRAN WILL BE USED FOR GROSS ANALYSIS			

In Table 8 (IIIB), between the input and output requirements, is emphasized the use of the appropriate cost-effective, finite element stress analysis program for the calculation at hand. In some cases, the more extensive VISTA program with generalized boundary conditions being developed under C-5167 will be used. In other cases, the original MARC program or its recent PRONY series modification may be more cost-effective, and, of course, the much more cost-effective MacNeal Schwendler Corp. NASTRAN program will be used for gross analyses.

3.2.4 Failure Mechanisms and Criteria (Module IV)

Table 9 (IVA) outlines the contents of the Failure Mechanisms & Criteria module. Criteria of critical crack growth rate, instability and allowable crack length are considered using energy and displacement approaches.

Table 10 (IVB) delineates the input and output information pertinent to the Failure Mechanisms & Criteria module.

Table 11 (IVC) outlines the basic problems for defining the Failure Mechanisms and Criteria module.

3.2.5 Structural Failure Analysis (Module V)

Table 12 (VA) summarizes the expected content of this module.

Table 13 (VB) summarizes the applicable input and output information pertinent to the Structural Failure Analysis module.

Table 14 outlines the experimental data requirements of the Integrated Methodology.

Figure 4 shows the overall integration/test plan with the management plan indicated in heavy script.

Table 9 (IVA) Failure Mechanisms and Criteria, Contents

CRITERIA OF FAILURE – BRITTLE, "DUCTILE"; VISCOELASTIC			
	(A)	CRACK GROWTH RATE EXCESSIVE	P(1)
	(B)	AN INSTABILITY DEVELOPS (DISCONTINUOUS GROWTH RATE OF CRACK COALESCENCE)	P(2)
	(C)	CRACK SIZE EXCEEDS ALLOWABLE VALUE	P(3)
VIA	(A)	THICKNESS AVERAGED ENERGY RELEASE	P(1)
	(B)	LOCAL ENERGY RELEASE OR STRESS INTENSITY INCLUDING LOCAL CRACK TIP DISPLACEMENT CRITERIA FOR GENERATION OF SMALL BUT FINITE CRACK 	P(1)
	(C)	MINIMAL ENERGY PATH FOR ADHESIVE AND COHESIVE FRACTURE	P(2-3)
VECTORIAL DISPLACEMENT CRITERION:		$K_I^2 + K_{II}^2 = \Gamma E$ ALONG INTERFACE, OR ALONG SCRIM PLANE	

Table 10 (IVB) Failure Mechanisms and Criteria, Inputs and Outputs

INPUT	OUTPUT
ENERGY RELEASE RATE G	(A) CURRENT RATE OF CRACK GROWTH
STRESS INTENSITY FACTORS K_I, K_{II} AND ΔK_I, ΔK_{II}	(B) CRACK SIZE AS A FUNCTION OF TIME
FRACTURE PROPERTIES, $\Gamma(\dot{a})$, $\Gamma(a')$	(C) INTRODUCTION OF MULTIPLE CRACK LEADING TO INSTABILITY
FRACTURE PATH (COULD BE CALCUALTED AT GREAT COST) $\dot{a} = \frac{da}{dt}$ $a' = \frac{da}{dn}$	

Table 11 (IVC) Basic Problems for Defining the Fracture Mechanics & Criteria Module

	WE SHALL USE QUASI-ELASTIC CRITERIA (i.e., INSPITE OF VE DEFORMATIONS, TREAT MATERIAL AS ELASTIC FOR FRACTURE CALCULATIONS. ONE CAN THEN CALCULATE AN ENERGY RELEASE RATE; IF VE EFFECTS BECOME DOMINANT, RELEASE RATE USES E(α/$\dot{a}$) IN PLACE OF E(o))	
(1.)	IS THERE A BASIC DIFFERENCE BETWEEN MONOTONIC AND CYCLIC LOAD HISTORIES CAUSING FRACTURE? (CAN K(da/dt) BE CONVERTED TO K(da/dn))?	P(1) LOADING SEQUENCING MAY BE IMPORTANT +++ – +++ – ++ – – ++ – – Etc.
(2.)	IS da/dn A FUNCTION OF ΔK? TO WHAT EXTENT IS THE MEAN VALUE OF K IMPORTANT? WE CANNOT ASSUME THAT RESULTS FOR METALS HOLD	(NEEDS TO BE DONE BEFORE JOINT TESTS)
(3.)	WE WOULD LIKE TO DISREGARD SCRIM IN STRESS ANALYSIS. CAN SCRIM BE NEGLECTED IN FRACTURE THEN?	P(2-3)
(4.)	HOW MUCH OF TOTAL LIFE IS SPENT ON THE "INITIATION" PROCESS?	P(1)
(5.)	CRACK GROWTH PATH; AFFECTED BY HISTORY OF LOADING AND CHANGES IN CRACK SIZE	P(2)

Table 12 (VA) Structural Failure Analysis, Contents

IF A CRITERION EXISTS, IT CONTAINS THE ONSET OF FAILURE
SO PROBLEMS OF STRUCTURAL FAILURE ANALYSIS REALLY BECOME PROBLEMS OF REDUCING STRUCTURAL LOADS TO LOCAL STRESSES CAUSING BOND FAILURE; ONCE FAILURE HAS OCCURRED, ASK WHETHER THE OVERALL STRUCTURE WILL FAIL.
EXCEPT: EXTENT OF BOND CRACK GROWTH DOES THE CRACK STOP?

Table 13 (VB) Structural Failure Analysis,
Inputs and Outputs

INPUT		OUTPUT
(1.) FAILURE CRITERION (2.) OVERALL STRUCTURE (Airplane) AND PROBLEM AREA LOCATION REDUCTION TO STRESSES AT BONDED JOINT (3.) LOADS	MARGIN OF SAFETY: LET SERVICE LOAD BE L L GIVES RISE TO $\dot{a}_L$ LOOK FOR OVERLOAD L_o WHICH PRODUCES THE CRITICAL GROWTH RATE $\dot{a}_o$ AT THE EXISTING GROWTH GEOMETRY $MS = \frac{Lo}{L} - 1$	BOND OR JOINT (A) LIFE (B) YES OR NO ON FLY (C) MARGIN OF SAFETY

Table 14 Experimental Data Requirements of Integrated Methodology

R = 0.1

I MODEL JOINT	ΔK & $\overline{K}$ TESTS FOR FAILURE JOINT CRACK FRONT LOCATION a(N)	"K" vs a'
	FROM COMPUTER DETERMINE $\overline{K}$ vs CRACK LENGTH (K_I & K_{II})	THESE TESTS USED TO FOLLOW INVESTIGATION OF ΔK & $\overline{K}$ EFFECT SINCE THIS INTERPRETATION AND APPLICATION OF I & II TO III DEPENDS ON THAT
II CRACKED LAP SHEAR	(1) CHOOSE h_1/h_2 SO THAT THE SAME K_i & K_{II} AS FOR MJ	$K_I^2 + K_{II}^2 = \Gamma'(a')E$
	RESULTS: DOES IT LEAD TO SAME CRACK GROWTH LAW?	CHECKED
	(2) IF CHOICE IS MADE WITH MORE DIFFICULTY THAN THAT, ASK WHETHER A DIFFERENT K_I–K_{II} COMBINATION PRODUCES THE "SAME" FRACTURE RATE BY $K_I^2 + K_{II}^2 = \Gamma'(\dot{a})$	"IF NOT, WHAT WORKS?"
III STRUCTURAL LAP JOINT	NEED STRESS ANALYSIS TO DETERMINE LOADS SUCH THAT K_I & K_{II} ($K_I^2 + K_{II}^2$) ARE IN THE SAME BALL PARK AS FOR CLS & MJ. THEN PROCEED TO PREDICT NUMBER OF CYCLES TO FAILURE FOR GIVEN LOAD LEVELS	$\dot{a} = \frac{da}{dt}$
	USE DIFFERENT LOAD HISTORY	$a' = \frac{da}{dn}$
		$\overline{K}$ = AVERAGE K PER CYCLE

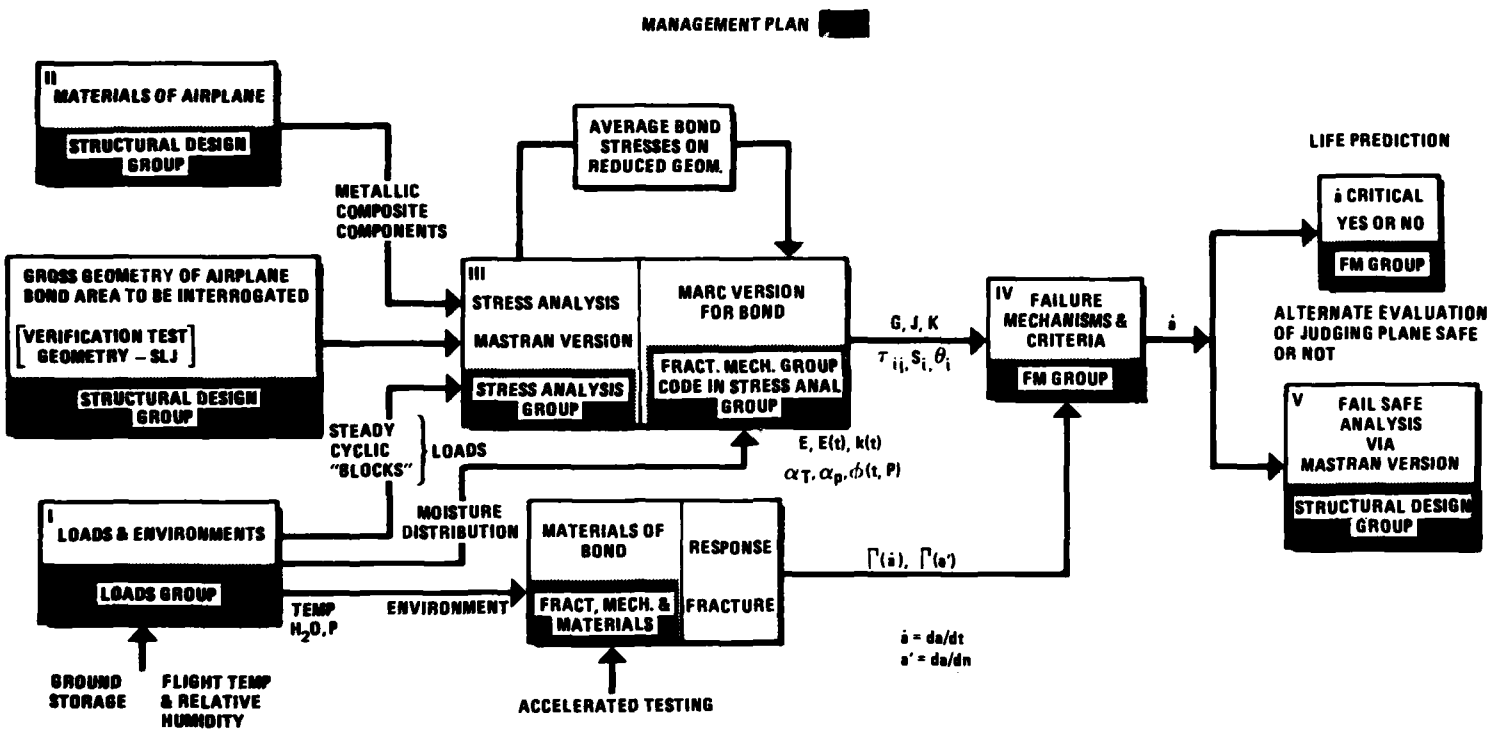

Figure 4 Overall Integration Methodology for Service Life Prediction of Adhesively Bonded Joints

IV. DEMONSTRATION OF THE INTEGRATION METHOD

4.1 Introduction

The discussions in the preceding sections concerning the integration of the different modules will now be demonstrated. The demonstration addresses the circumferential bonded splice (CBS) (Fig. 5) of the full-scale demonstration component in the PABST program (Ref. 8). In order to first verify the methodology, a comparison is made between results from fatigue testing of Structural Lap Joints (SLJ) and crack growth predictions that were made using the methodology. The predictions were made on the basis of fracture property measurements that were made through fatigue testing of Cracked Lap Shear (CLS) specimens. The verification of the methodology using the SLJ specimen is described in Section 4.2, followed by the demonstration of the methodology on the CBS full-scale demonstration article in Section 4.3.

4.2 Verification of Integration Method

4.2.1 Introduction

Recall that the fracture properties of the adhesive layer can be described by the relationship between a chosen fracture parameter and the crack growth rate in the adhesive layer. Thus, if the fracture properties of an adhesive and the variation of fracture parameter with crack length for a particular joint geometry are known, the history of the crack growth in that joint can be predicted by an integration of the crack growth rate/fracture parameter equation. Final failure can then be defined by the achievement of critical crack growth rate or crack length.

For the purposes of this investigation, the fracture properties of FM-73M were determined by fatigue testing of Cracked Lap Shear (CLS) specimens. Testing of Structural Lap Joints (SLJ) was conducted to provide a verification of the integrated method . The testing of both these joints is described in Section 4.2.2. The variation of fracture parameter with crack length is determined by stress analysis (module III). The stress analysis of the two joints is discussed in Section 4.2.3. The results of the testing and stress analysis of the CLS are combined in Section 4.2.4 to determine the fracture properties (module II). Section 4.2.5 discusses predictions of crack growth history in the

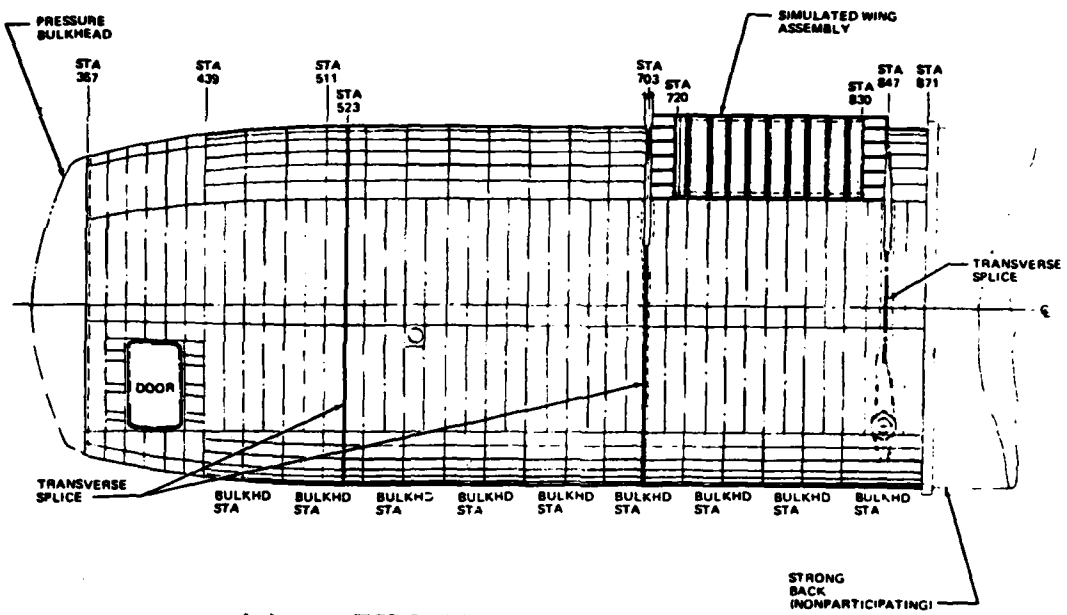

(a) FSDC Side View

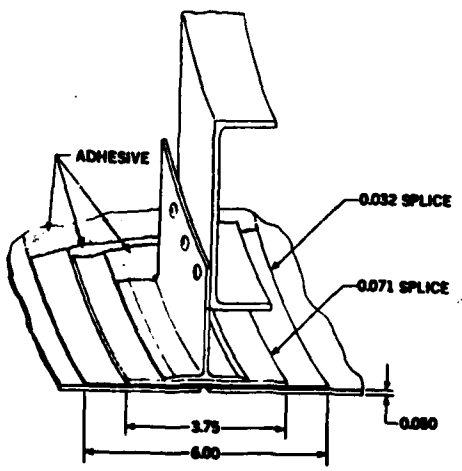

(b) Transverse Bonded Splice (Station 703 Only)

Figure 5 The PABST Circumferential Bonded Splice Joint (CBS)

(From Reference 63)

SLJ and compares the predictions with the actual test results that were reported in Section 4.2.2.

4.2.2 CLS, SLJ Fatigue Testing

The geometries of the CLS and SLJ are shown in Figures 6 and 7, respectively. They were all fabricated at General Dynamics, Fort Worth Division (GD/FWD) using the procedure described in Reference 32.

Testing of the specimens was conducted at GD/FWD and United Technologies, Chemical Systems Division (UT/CSD) (Ref. 61). At GD/FWD the specimens were fatigue tested using servohydraulic testing machines under load control. Environmental conditions of -65°F and 140°F were provided by a Cincinnati Subzero environmental chamber Model HTT-4. The location of the crack in the specimens was determined ultrasonically as described in Appendix B.

4.2.2.1 Test Results for CLS Specimens

The conditions under which the CLS1 and CLS2 specimens were tested are given in Table 15. Since the purpose of the tests on the CLS specimens was to obtain fracture properties without considering crack initiation effects, the specimens were precracked at 3 Hz according to the schedules given in Table 16 (CLS1) and Table 17 (CLS2).

The da/dN data generation schedule consisted of starting the test using the final precracking loads. The test temperature and cycling rate for each specimen were taken from the test plan and were held constant for the entire test on that specimen. For the room temperature tests, after the crack had grown 1.5 inches, the load amplitude was increased in 1000-pound steps after each increase in crack length "a" of at least 1.5 inches for the CLS1 specimens. For the CLS2 specimens, this was usually a 500 pound change. This stepping of the load provided for three magnitudes of crack growth rate (da/dN) on each specimen covering the range from a new microinches per cycle to over 1000 microinches per cycle.

When testing at temperatures other than room temperature, some variations in testing procedure were necessary: At -65°F, if no crack growth was noted after 300,000 to 500,000 cycles, the load was increased in 1000 pound increments until crack growth occurred. The standard 1000-pound load increase after each 1.5 inches of crack

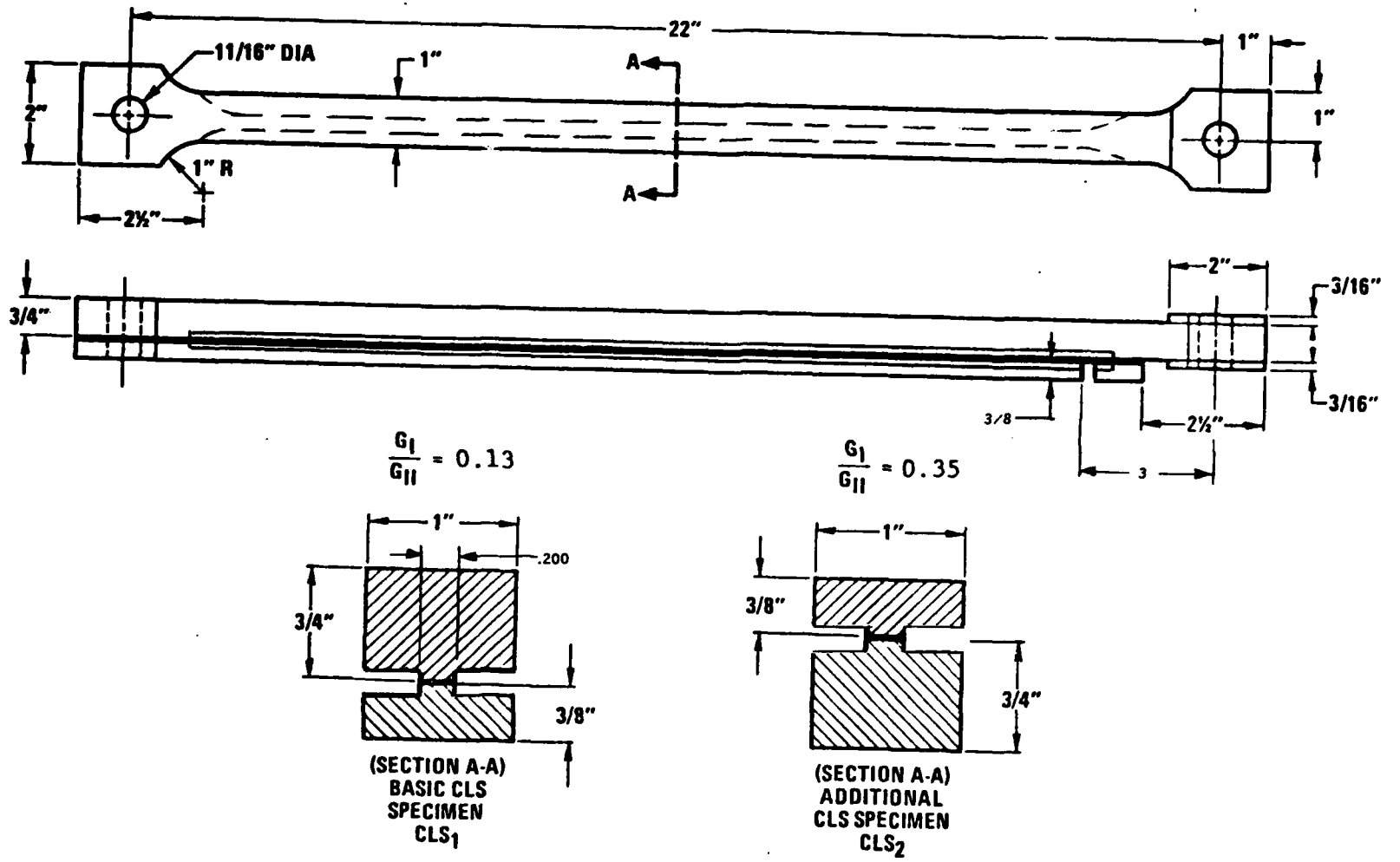

Figure 6 Cracked Lap Shear (CLS) Test Geometry

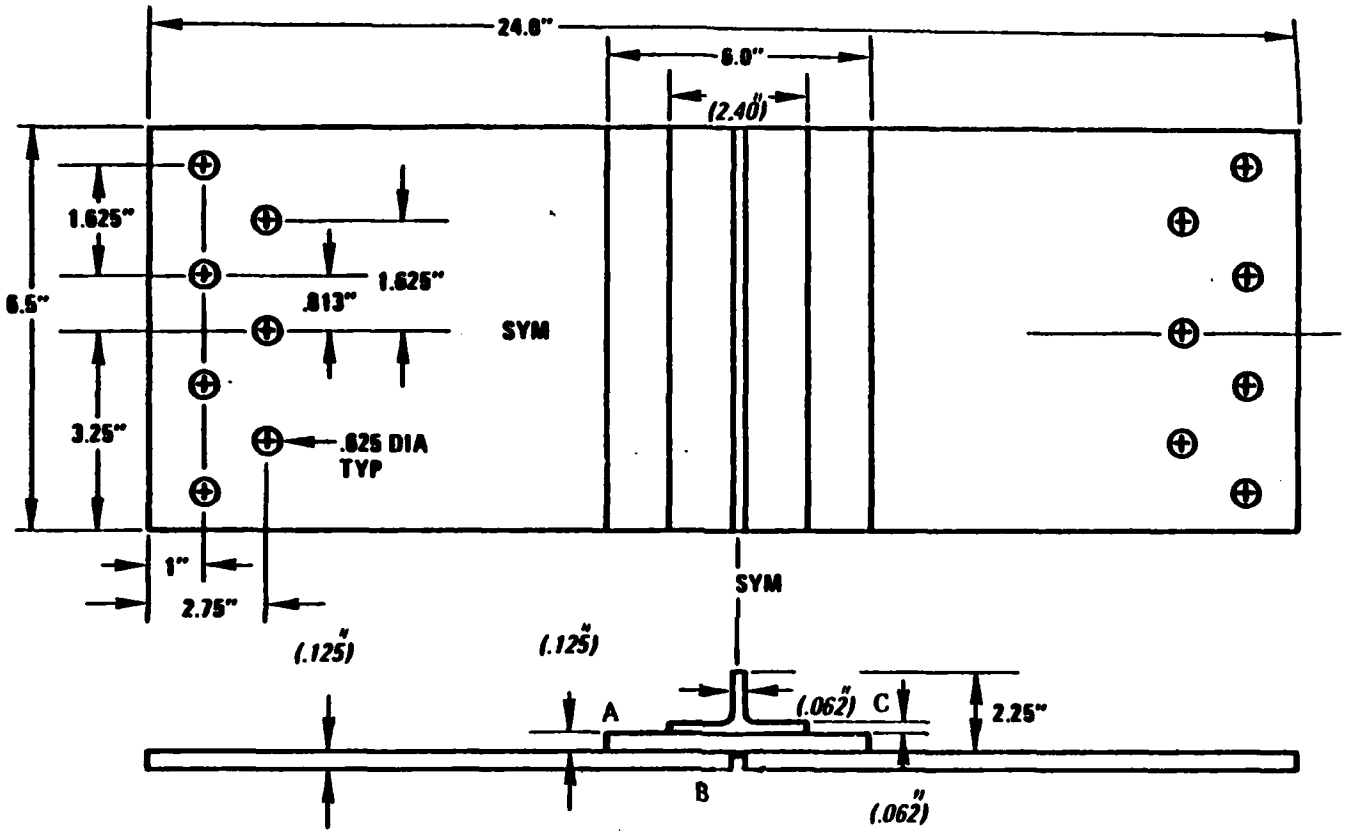

PHOSPHORIC ACID ANODIZE SURFACE TREATMENT
BOND WITH FM-73M ADHESIVE

(INTERMEDIATE) Adherend SLJ Specimen

Figure 7 The Structural Single Lap Strap Joint (SLJ)

Table 15 Test Conditions for CLS_1 and CLS_2 Bonded Joints

Specimen Number	Test Frequency	Test Temperature
CLS_1-5	3 Hertz	R.T.
CLS_1-7	10	R.T.
CLS_1-6	0.3	R.T.
CLS_1-8	10	-65°F
CLS_1-4	3	140°F
CLS_1-9	3	-65°F
CLS_2-4	3	R.T.
CLS_2-6	10	R.T.
CLS_2-8	0.3	R.T.
CLS_2-7	3	140°F

Table 16 Precracking Schedule for CLS_1 Bonded Joints

Load Amplitude Pounds	Load Ratio "R" Max/Min	"A" Inches
7000	0.1	0 to 1.5
6000	0.1	1.5 to 2.25
5000	0.1	2.2 to 2.5
400	0.1	2.5 to 3.0

Table 17 Precracking Schedule for CLS_2 Bonded Joints

Load Amplitude Pounds	Load Ratio "R" Max/Min	"A" Inches
3300	0.1	0 to 1.5
2800	0.1	1.5 to 2.25
2400	0.1	2.25 to 2.5
2000	0.1	2.5 to 3.0

Table 18 Test Results for SLJ Bonded Joints

Specimen No.	Max. Test Stress KSI	Adherend Thickness	Cycles To Failure
7	15	.125"	203,786 M-G
9	20	.125"	36,479
6	25	.125"	7,957
8	15	.375"	377,579
10	20	.375"	14,258
13	25	.375"	1,744

Notes:

M = Failure Through Metal

G = Failure At Edge Of Gripping Fixture

growth was then followed. For the 140°F specimens, the crack growth rate for the first 1.5 inches was calculated and the load was reduced to obtain a growth band in the lower microinch range. Adequate crack length readings were made during this growth band to identify any retardation. The test was then continued using the 1000 pound increase after each 1.5 inches of crack growth for the CLS1 specimens.

The crack growth rates at the various load levels are summarized in Tables 19 and 20 for the CLS1 and CLS2 specimens, respectively. These data will be used in conjunction with the stress analysis to be discussed in Section 4.2.3 to generate fracture properties (Section 4.2.4).

4.2.2.2 Test Results for SLJ Specimens

A total of six SLJ specimens were tested at GD/FWD. The tests were conducted at room temperature at a cyclic rate of 3 Hertz with a stress ratio, R = 0.1. Three of the specimens had 1/8" thick adherends and are designated SLJ1. The other three specimens (SLJ2) had 3/8" thick adherends. Table 18 records the loads at which the tests were conducted and the corresponding lifetimes in terms of cycles to failure.

Figures 8 and 9 show two opposite views, respectively, of two different failed specimens. In each case, the failure occurred between the splice and one end plate, with the almost symmetrical lighter portions in Figure 8 representing the slow fatigue crack. The latter initiated from the corresponding stress singularities at the overlap ends and propagated towards the center of the overlap until final fast, cohesive fracture occurred, as indicated by the darker regions. The progress of the advancing crack front with cycle number is indicated by the pencilled lines drawn after locating the discontinuity (i.e., crack front) with the ultrasonic detector.

The details of the crack growth histories of the six SLJ specimens were presented in Reference 32. The ultrasonically determined crack fronts were averaged to define effective crack lengths which were plotted against the number of cycles at which the crack front determination was made. With reference to Figure 10, cracks always grew from the center of the doubler plate, in either the positive or negative y-direction and, in the case of the SLJ1

Table 19 Crack Growth Rates in CLS_1 Specimens

Specimen Designation	CLS_1-4	CLS_1-5		CLS_1-7	CLS_1-8	CLS_1-9	CLS_1-10
Delta Load (kN)	Crack Growth Rate (m/cycle)						
13.34	0.03						
17.79	0.20	0.05		0.08		0.05	0.10
22.24	0.81	0.22		0.44	0.16	0.21	0.52
26.69	2.01	0.79		1.47	1.37	0.49	1.15
31.14	4.76	2.08		4.41	9.20	2.13	2.35
35.58	25.4	7.56		7.24	30.48	5.08	6.65
40.03		22.63		22.83			

Table 20 Crack Growth Rates in CLS_2 Specimens

Specimen Number	CLS_2-4	CLS_2-6	CLS_2-7	CLS_2-8
Delta Load (kN)	Crack Growth Rate (m/cycle)			
8.90	0.06	0.05	0.26	0.17
11.12	0.31	0.51	1.40	0.79
13.34	1.02	3.21	5.56	1.74
15.57	11.66	9.21	18.03	5.65
17.79	14.29	23.29	34.29	49.73

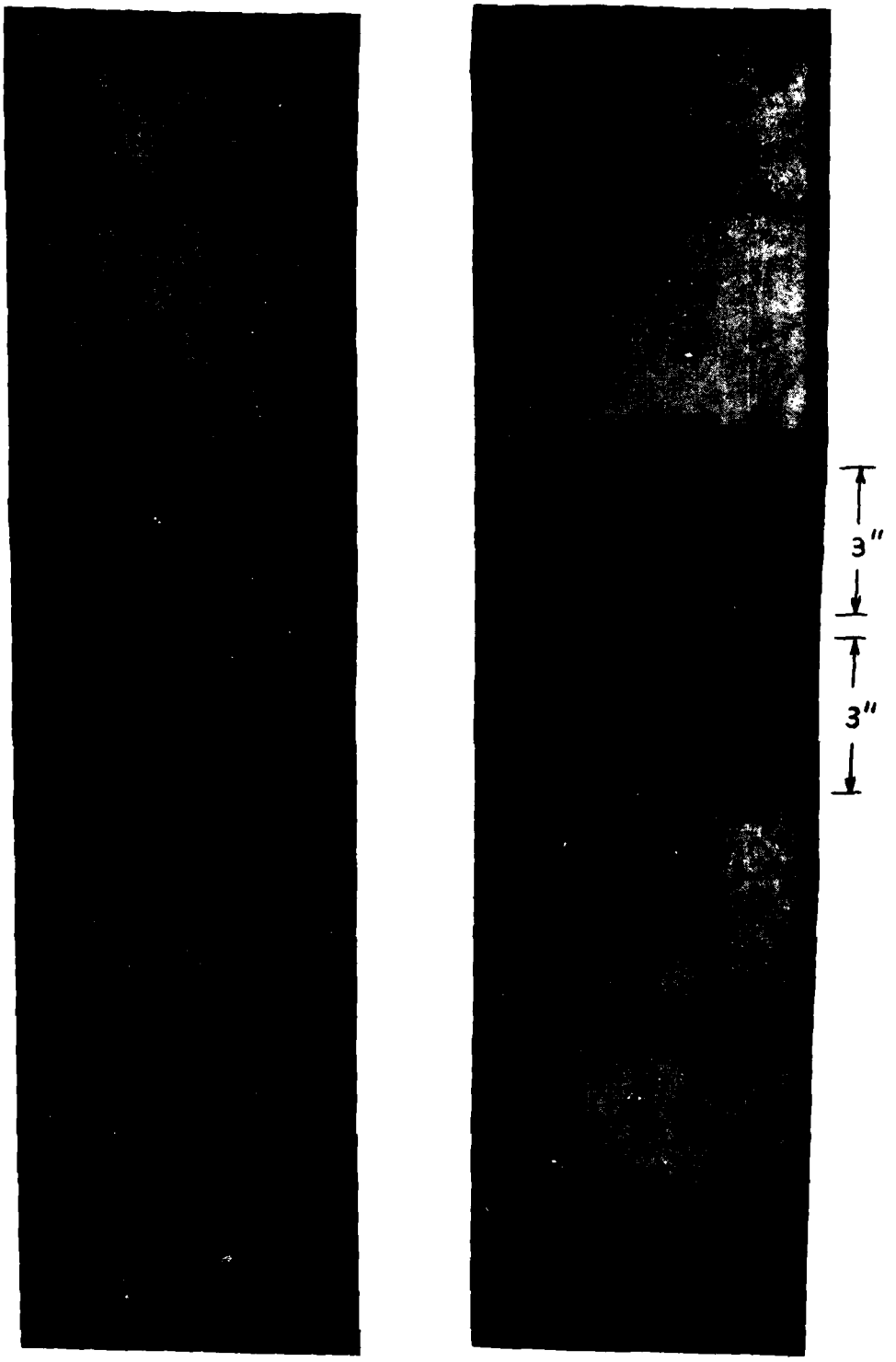

Figure 8 Failed Thick Adherend SLJ Specimens With Measured Crack Fronts.

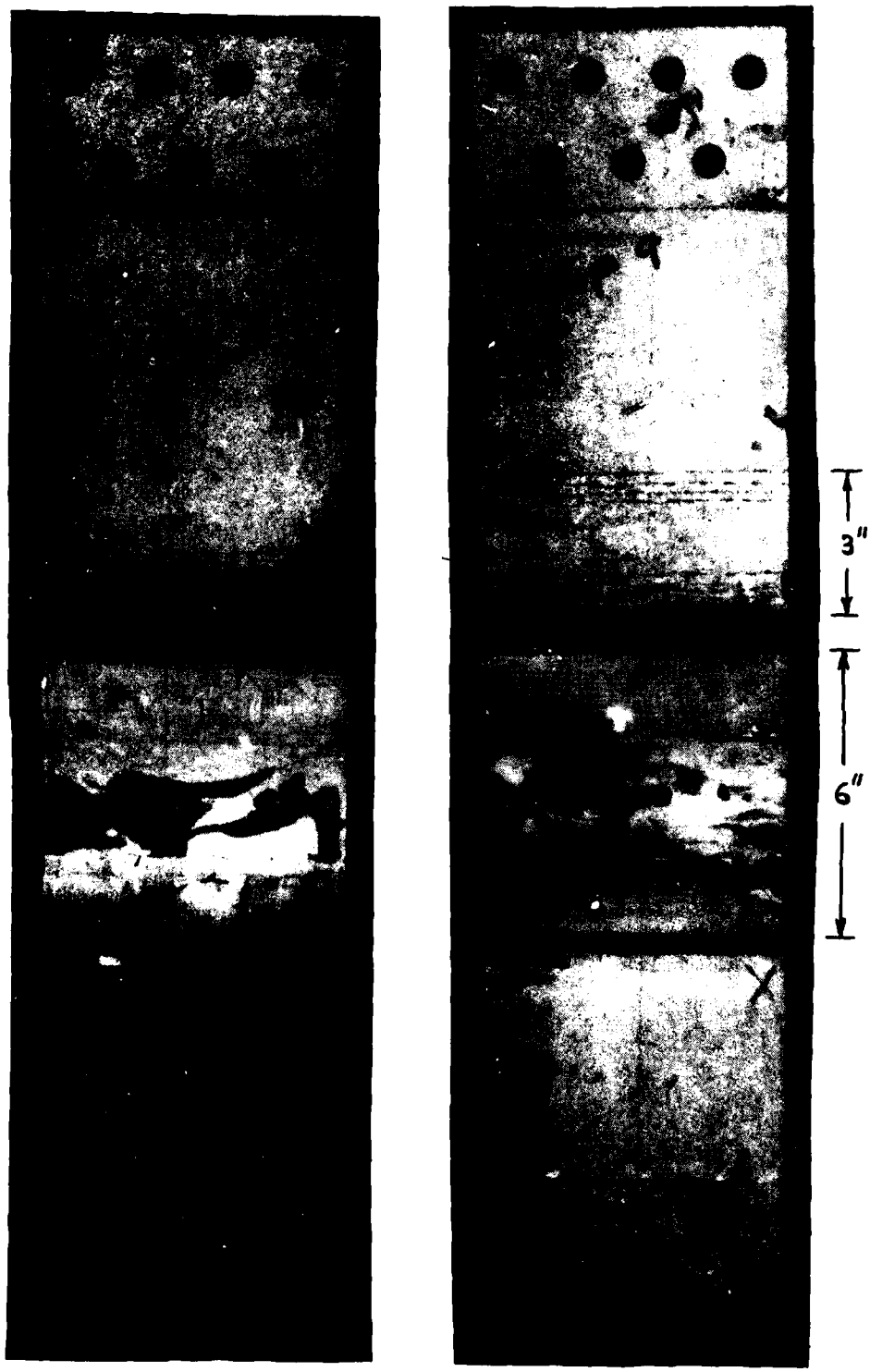

Figure 9 Failed Thick Adherend SLJ Specimens With Measured Crack Fronts. (Other Side)

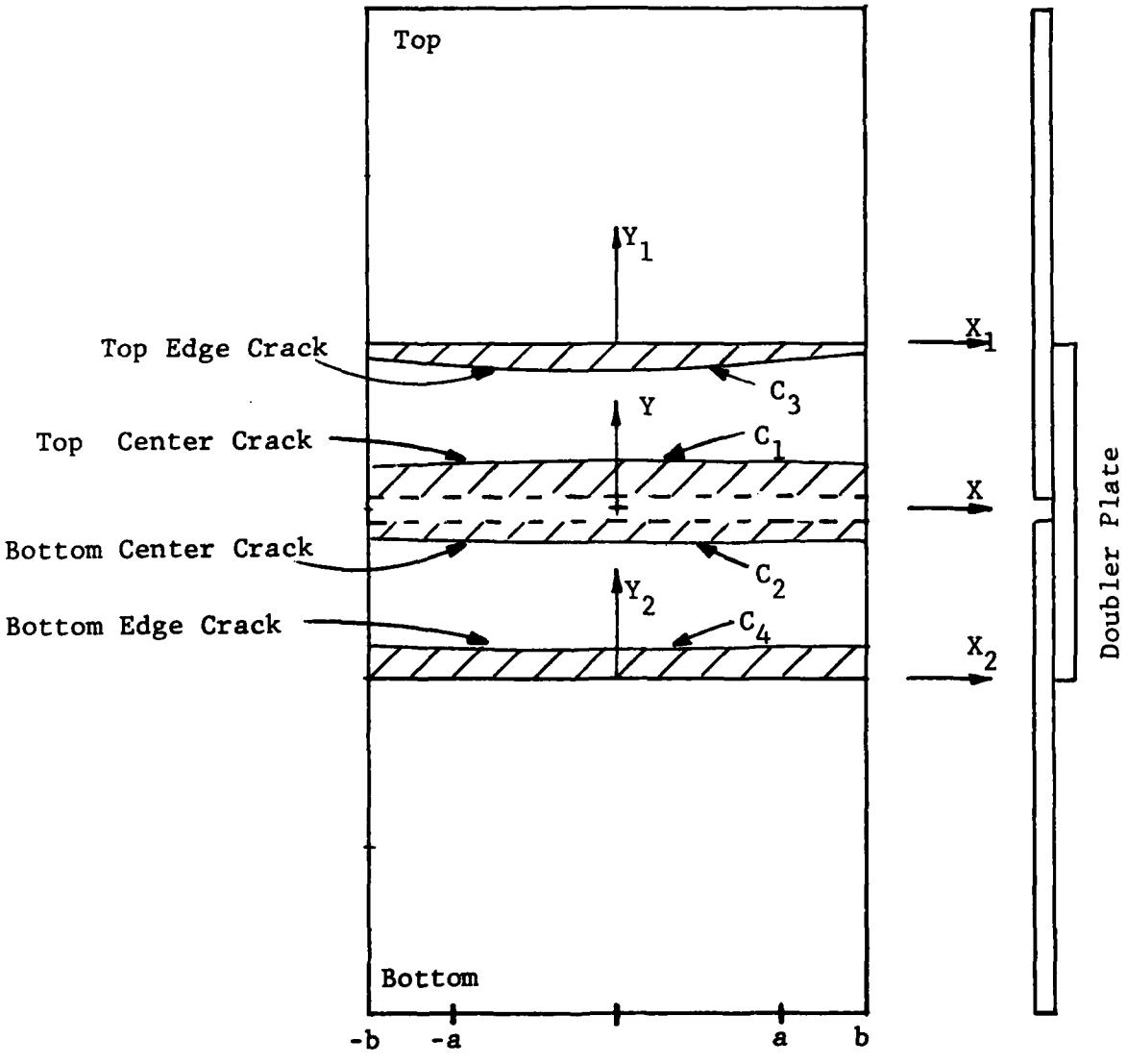

Figure 10 SLJ Crack Geometry.

specimen, from the top and bottom edges of the doubler plate.

Symmetric crack growth would be manifest as $c_1(N) = c_2(N)$ and $c_3(N) = c_4(N)$ where N is the number of cycles. Within experimental error, this occurred only for the SLJ_1-2 test. That test also indicated that the center cracks (c_1, c_2) grew initially at a faster rate than the edge cracks (c_3,c_4). However, after about $1x10^4$ cycles, the crack growth rates were the same for the two sets of cracks.

In view of difficulties that were experienced in the stress analysis of the SLJ, the crack growth histories of the SLJ1 and SLJ2 specimens that were recorded in Reference 32 have been further averaged to reflect only symmetric crack growth from the center of the doubler plate. Figures 11 and 12 summarize these simplified crack growth histories for the SLJ1 and SLJ2 specimens. the effect of load level on crack growth history is clearly seen.

4.2.3 Stress Analysis

4.2.3.1 Validity of Finite Element Stress Analysis

The question of the validity of a finite element stress analysis always arises. Based on mesh refinement studies that were conducted when the MARC finite element code was first used in the Fatigue Behavior Program (Ref. 19), the most ideal validation would come from an analytical, closed-form solution which included the bondline. However, because of the complexity of the joint geometry, such analytical solutions are not, and are not likely to become, available.

In Reference 5, Brussat conducted a beam theory analysis of the specimen which neglected the adhesive layer. The beam theory result for each specimen geometry is compared with the MARC results in Figures 14 and 15 in Section 4.2.3.3, and predicts a constant value of G with crack length that is on the order of 5 times greater than the MARC results. The greater values of J integral are a consequence of neglecting the adhesive layer in the beam theory analysis.

Another means of validating the MARC results is to compare them with other finite element analyses. One such analysis was conducted using the GAMNABS finite element code which has been developed by Dattaguru at NASA Langley (Ref. 66). The relatively close agreement between the two analyses

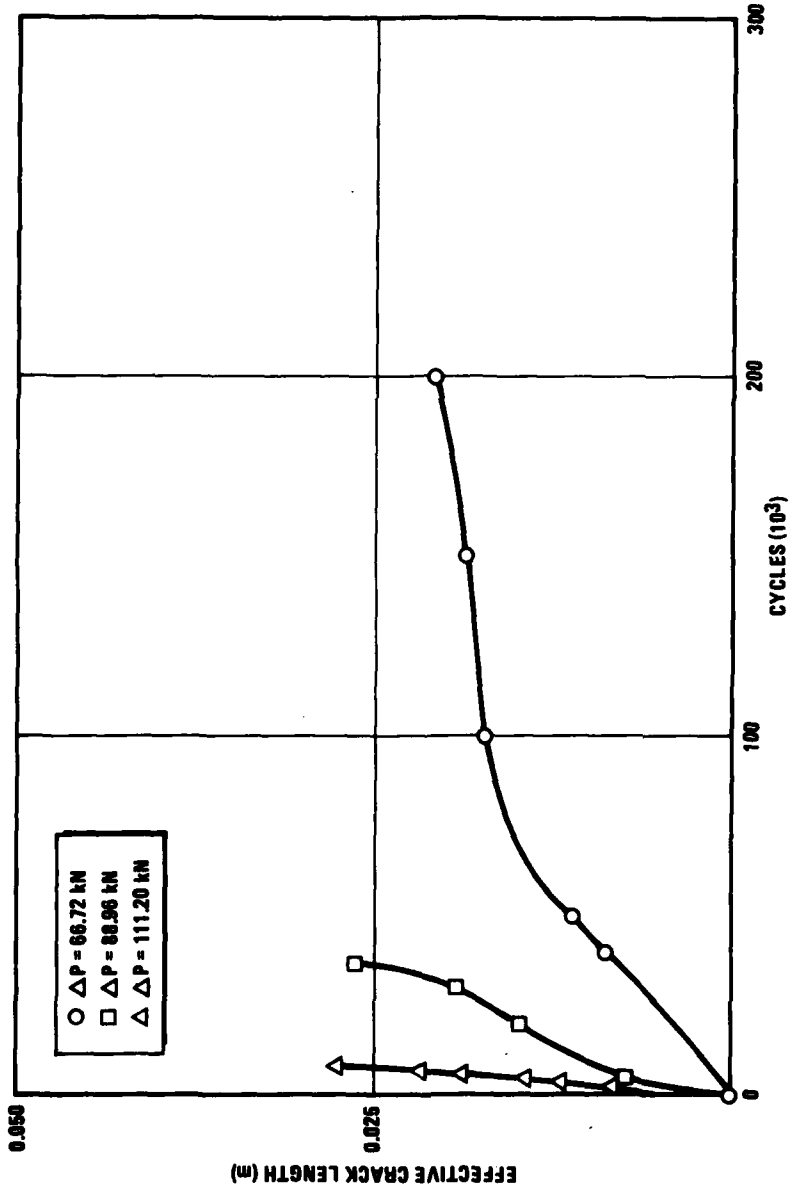

Figure 11 Crack Growth History in SLJ_1 Specimen

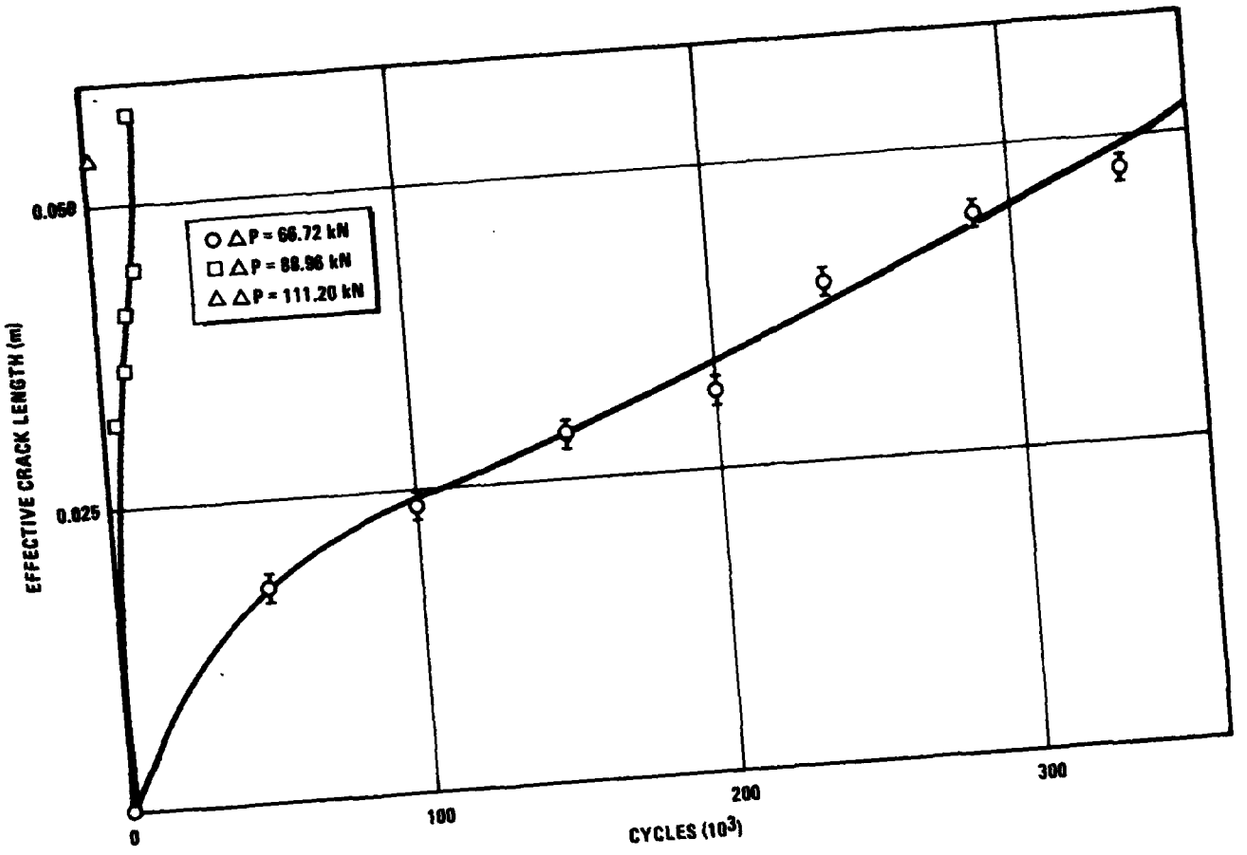

Figure 12 Crack Growth History in SLJ_2 Specimen

(Figures 14 and 15) provides greater confidence in the MARC analysis.

The ultimate standard with which to evaluate the finite element codes would be an experimental investigation. The means of such a validation is described in Appendix 1 using the technique of holographic interferometry with fictitious fringe-moire' in real time.

4.2.3.2 Stress Analysis of the Cracked Lap Shear Specimen

Finite element analyses of the cracked lap shear (CLS) specimen were conducted for two GI/GII ratios. J-integral calculations were performed for each ratio to determine the variation of the J-integral with crack length. The finite element models used for the analysis were generated by a small program created specifically for generating finite element models of the CLS. Input for the model generation program allowed models with various crack lengths and adherend thicknesses (also adhesive thickness) to be quickly generated without the time-consuming debug phase typically required when a finite element model is developed by hand.

All models were generated with the 8-node, plane strain, isoparametric quadrilateral element as used in prior analyses. Since the models were to be used for J-integral analysis, the area around the crack tip had to be a relatively fine mesh. This region, shown in Figure 13, is basically the same for all models. The triangles shown around the crack tip are 8-node quadrilateral elements that have been compressed to triangles. The midside nodes that fall on the sides radiating from the crack tip are placed at the quarter points of the elements to create the $r^{-\frac{1}{2}}$ strain singularity that is characteristic of elastic fracture mechanics problems.

Figure 6 shows the actual test geometry and the cross sections for the two GI/GII ratios. The models used in the analysis represented the distance between the mounting lugs of 55.88 cm (22 inches). The ends of the specimens were rigidly attached to the test frame so that fixed boundary conditions were assumed for the analysis. A 4448 N (1000 lb) load was considered in the analysis. The models that were generated for the analysis typically contained some 120 elements and 450 nodes. This allowed an adequate mesh refinement around the crack tip but only a very coarse mesh outside of this region. Even though some elements in this coarse region approached an aspect ratio of 300:1 (in the adhesive layer), ill-conditioning of the stiffness matrix

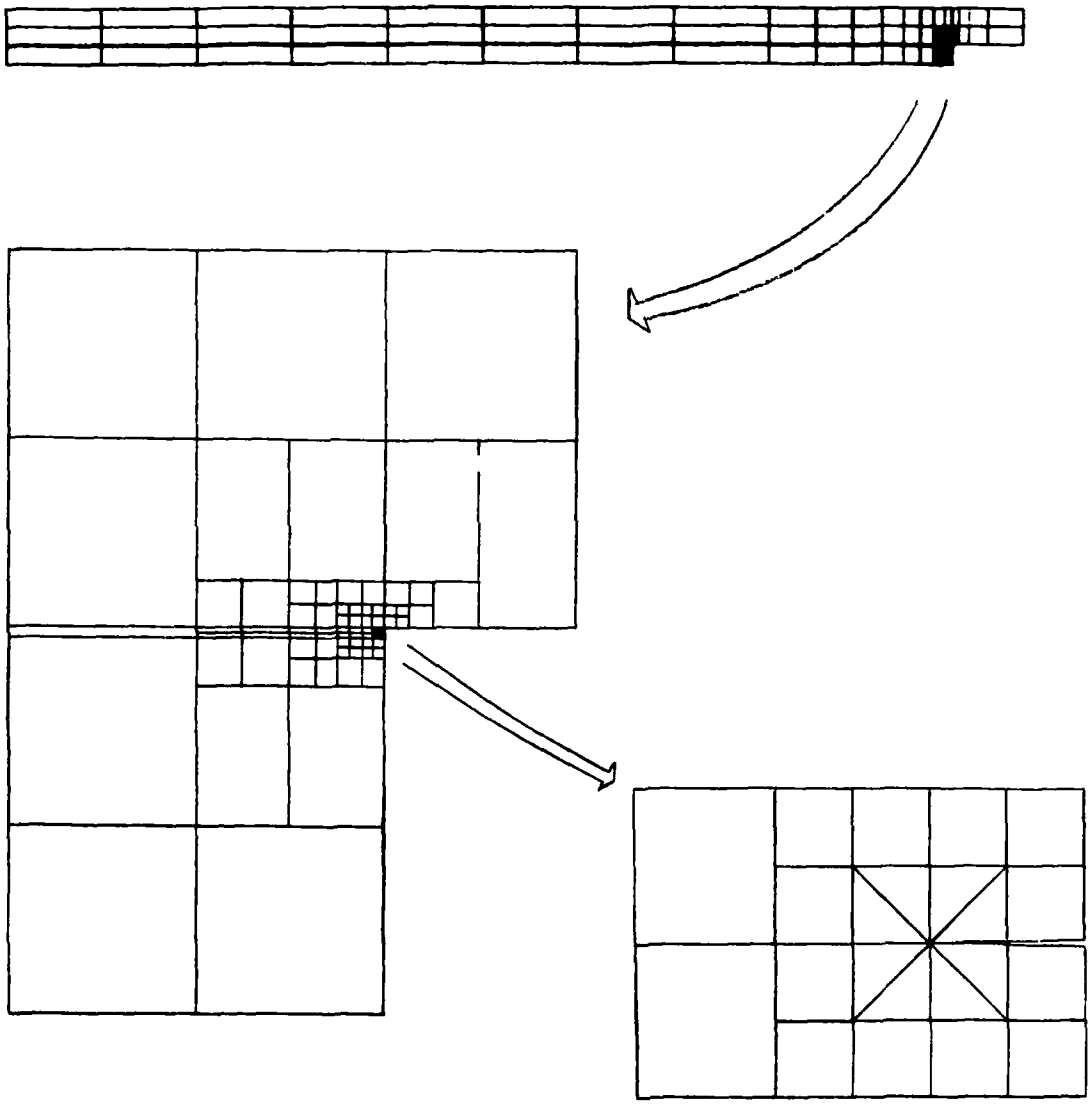

Figure 13 Finite Element Model of Cracked Lap Shear Specimen, CLS_1

did not appear to be a problem as the element force balance obtained from the analysis was very good.

Plots of the J-integral versus crack length are shown in Figures 14 and 15 for both GI/GII ratios. The J-integral for the analysis in which the thicker adherend is loaded (G_I/G_{II} = 0.13) is fairly flat while the other case (G_I/G_{II} = 0.35) has a significant peak.

For purposes of comparison, the results of beam theory and GAMNABS analyses are also shown in Figures 14 and 15. The beam theory analysis was used by Brussat et al. (Ref. 5) and GAMNABS is a finite element code developed by Dattaguru at NASA Langley (Ref. 66).

The reason for this sizable discrepancy between the MARC (or GAMNABS) and beam theory results is, of course, the relatively large compliance offered by the thin adhesive layer. It provides poor load transfer from the loaded member to the other one. This statement is best understood if one assumes that the adhesive has zero rigidity; then growth of a crack in this very compliant layer brings about absolutely no change in stored energy. Maximum change is stored energy results if the adhesive is assumed infinitely rigid (thickness-averaged fracture mechanics). The beam theory analysis does not account for the presence of the adhesive layer. It should be noted that the J integral does vary with crack length when the adhesive layer is modeled.

4.2.3.3 Stress Analysis of the Structural Lap Joint Specimen

The MARC analysis of the structural lap joint designed to model the effects of geometric nonlinearities is reported herein. Problems designed to establish the significance of other factors such as grip length, adhesive thickness, and crack location (interface or cohesive) are recorded in Ref. 32. Those analyses also attempted to include examining the interaction of cracks emanating from both the edge and center of the doubler and observing the effect of cracks that are no longer symmetrically positioned about the centerline of the model.

The basic model analyzed and representing the circumferential bonded splice (CBS) at station 703 of the PABST Full Scale Demonstration (FSD) component is the structural lap joint with 3.175mm (1/8 inch) adherends (Fig. 7). The finite element models of the joint are typical of those used in other analyses in this program. Eight node,

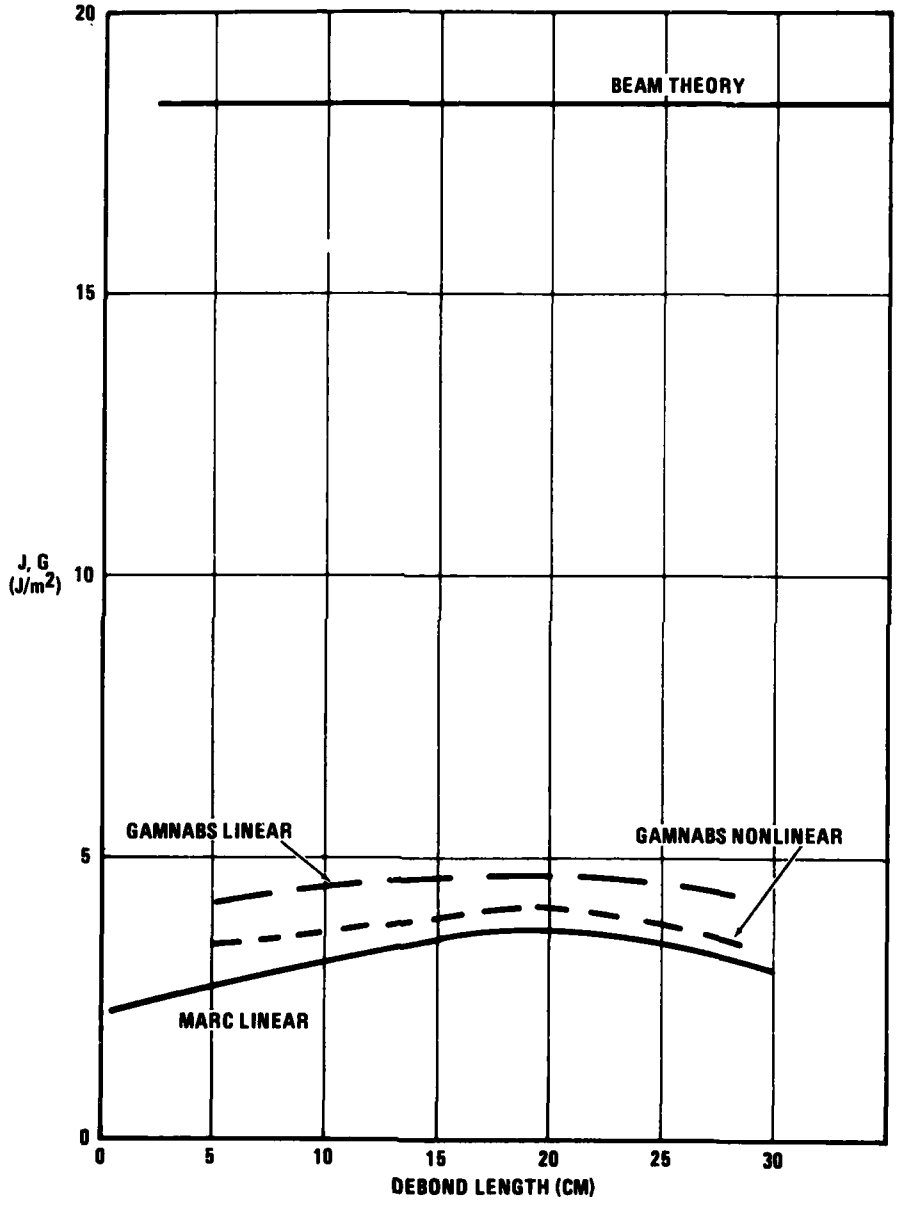

Figure 14 J,G Integral versus Crack Length for CLS_1 Specimen

AD A124 324 INTEGRATED METHODOLOGY FOR ADHESIVE BONDED JOINT LIFE PREDICTIONS(U) GENERAL DYNAMICS FORT WORTH TX FORT WORTH DIV J ROMANKO ET AL. NOV 82 AFWAL-TR-82-4139 2/2

UNCLASSIFIED F33615-79-C-5088 F/G 13/5 NL

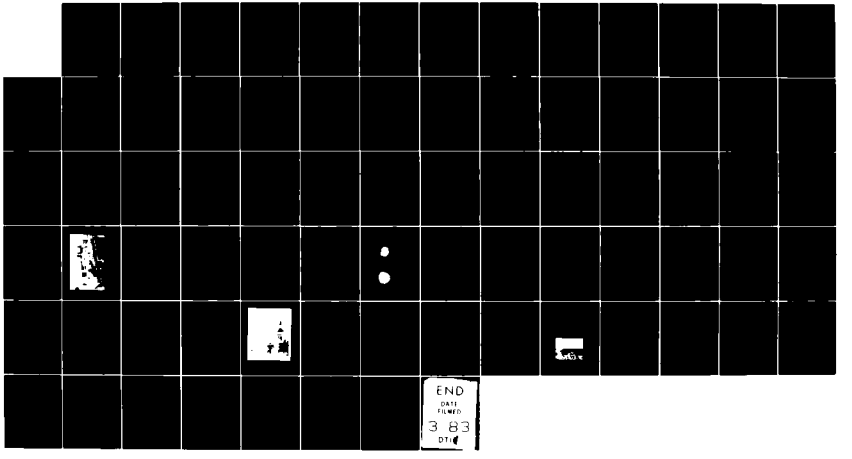

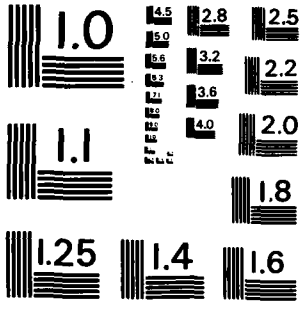

MICROCOPY RESOLUTION TEST CHART
NATIONAL BUREAU OF STANDARDS - 1963 - A

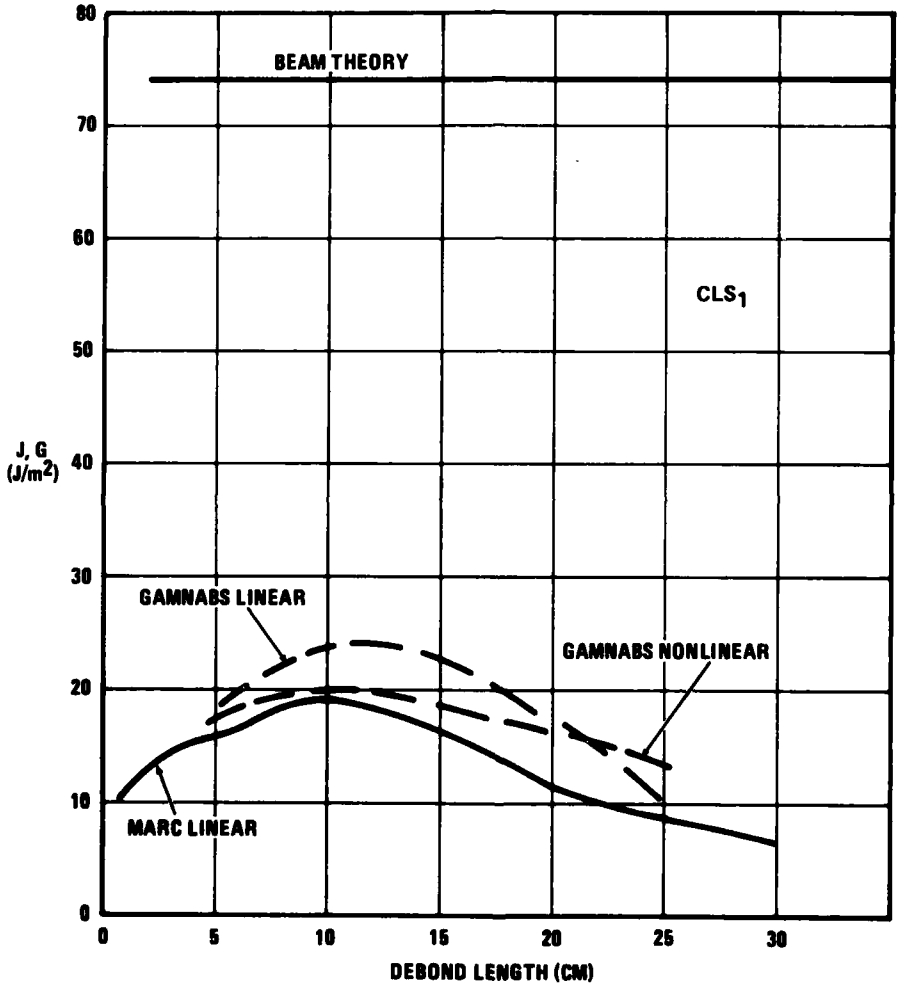

Figure 15 J,G Integral versus Crack Length for CLS_2 Specimen

isoparametric quadrilateral elements are used throughout. Elements around the crack tip are collapsed quadrilaterals with the midside nodes positioned at the quarter points to create the $1/\sqrt{r}$ singularity common to fracture problems (Figure 16).

The properties of the adhesive material are typical for FM-73 at room temperature; Young's Modulus = 2068 MPa, Poisson's ratio = 0.32. The material properties of the adherend are typical for aluminum; specifically, Young's Modulus = 72400 MPa, Poisson's ratio = 0.33. A linear stress-strain law was assumed for both the adhesive and adherend.

For all of the analyses, cracks were assumed to be symmetrically located so that symmetric boundary conditions could be applied. Various load levels were considered in the initial series of analyses to observe the effects of geometric nonlinearities. The load levels considered created average stresses in the aluminum adherend of 84.9 MPa (12300 psi) to 254.7 MPa (36900 psi). However, all subsequent analyses were performed at the lowest load level corresponding to an average stress of 84.9 MPa.

It was initially assumed that a J-integral analysis would be performed for the structural lap joint as was done in the analysis of the model joint and the cracked lap shear joints. However, the use of the large displacement option in MARC to account for the effects of geometric nonlinearities ruled out the use of the J-integral option. Thus it was decided to calculate the stress intensity factors k_I and k_{II} from the numerical crack flank data. For the case of a cohesive crack, the stress intensity factor may be calculated by

$$k_{II} = \frac{E\Delta u}{4\sqrt{2r}\,(1-\nu^2)}\,, \tag{18}$$

and

$$k_I = \frac{E\Delta v}{4\sqrt{2r}\,(1-\nu^2)}\,. \tag{19}$$

k_I and k_{II} are the mode I and II stress intensity factors, respectively,

Δv and Δu are the normal and tangential crack opening displacements, respectively,

E is the Young's modulus of the adhesive layer,

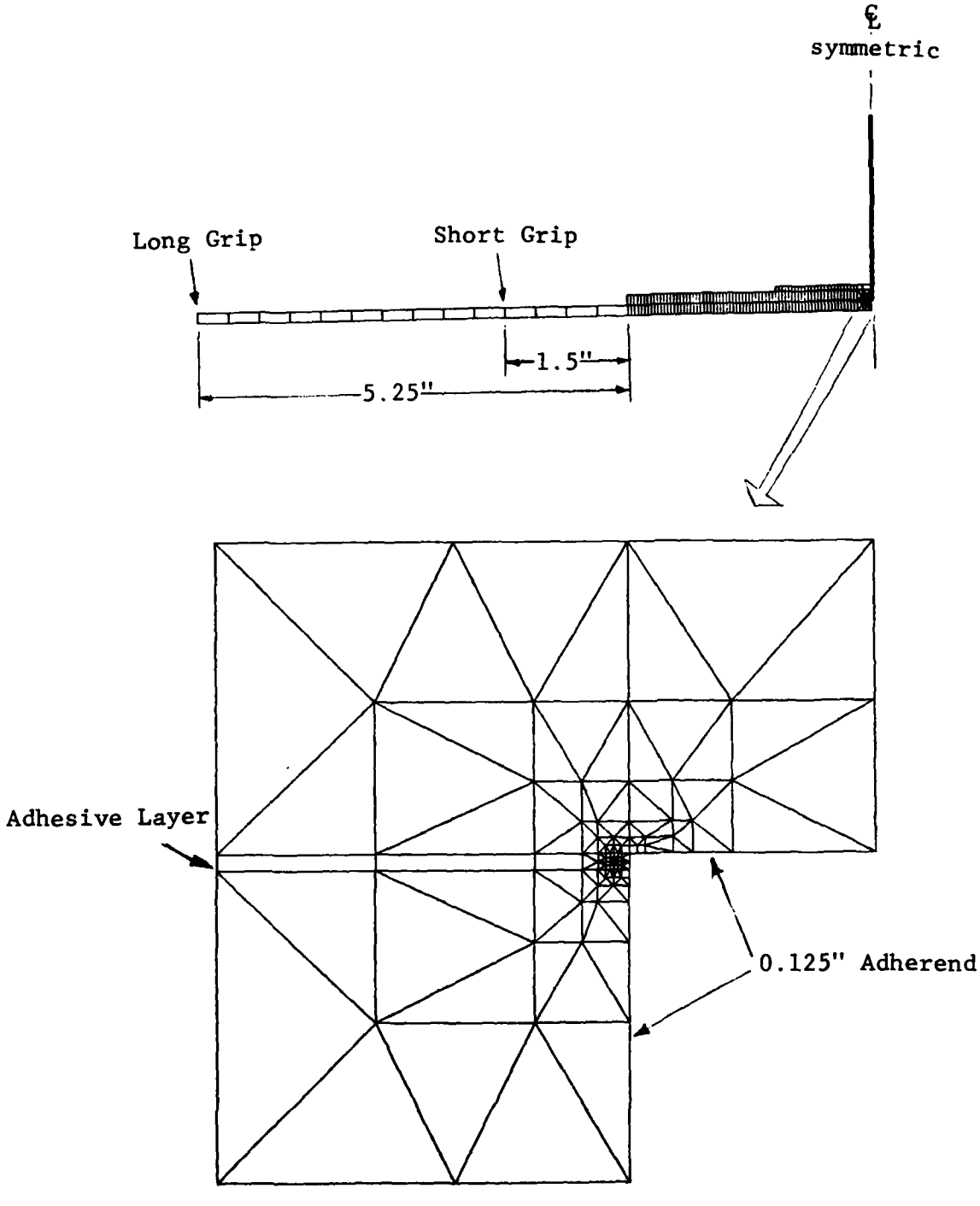

Figure 16 Finite Element Representation of the Structural Lap Joint

ν is the Poisson's ratio of the adhesive layer,

and r is the distance from the crack tip at which Δu and Δv are taken.

The strain energy release rate, G, is given by:

$$G = \frac{\pi(1-\nu^2)}{E} (k_I^2 + k_{II}^2) \quad . \tag{20}$$

It was desirable to assess the effect of geometric nonlinearities on the response of the structural lap joint early in the analysis. Problems where the effect of large displacements are significant are typically more complex and more expensive to analyze. Hence, it was desirable to use small deflection, linear elastic theory whenever possible.

4.2.3.4 Effect of Large Displacements

In order to determine the effect of geometric nonlinearities, the first set of problems were analyzed using the large displacement option available in MARC. The structural lap joint model used in the analysis represented a joint with a 2-mil adhesive layer. Both short and long grip lengths were considered in combination with crack lengths of 0.127, 2.54, and 25.4mm. Three load levels were considered in each run so that the effect of load level could also be observed. When the stress intensity factors are calculated as described earlier, it is necessary to determine the difference in displacement between two nodes. Since the displacements are only printed out with six digits maximum, problems arise when the difference in displacements occurs in the last digit. Calculations of stress intensity values for these cases could have errors of as much as 20%. This was often seen when the displacements varied practically linearly with load but the difference between displacements varied considerably. Since the load versus displacement is nearly linear, it has been assumed that geometric nonlinearities are not significant for this joint configuration and small deflection analyses have been used on all subsequent problems.

4.2.3.5 Effect of Adhesive Layer Thickness

The effect of adhesive thickness variation is shown in Figure 17 for the structural lap joint with long grips. The two adhesive thicknesses considered in the analysis were 0.0508 mm (0.002 inches) and 0.254 mm (0.010 inches). The plot shows a general increase in KI and KII for the thick adhesive layer as compared to K_I and K_{II} for the thin adhesive layer at corresponding debond lengths. The K_I and K_{II} curves appear to cross at around 28 mm for both adhesive thicknesses. It is also probable that both curves cross at smaller debond lengths although it cannot be confirmed for the model with the thicker adhesive layer since the smallest crack length is only 0.254 mm compared to .0508 mm for the model with the thin adhesive layer.

The variation of J-integral with crack length is shown in Figure 18 for the case in which the adhesive layer is 0.254 mm. thick.

4.2.4 Fracture Properties

The testing (Section 4.2.2) and stress analysis (Section 4.2.3) of the CLS specimen are now brought together to generate fatigue fracture properties.

The fracture properties are presented in terms of the crack growth rate (da/dN) vs. the change in J Integral per cycle (ΔJ). The loads that gave rise to crack growth rates were recorded in tables and must therefore be converted to J-integrals using the finite element stress analysis of Section 4.2.3.

Thus, the change in J-integral per cycle, ΔJ, is given by

$$\Delta J = J_{max} - J_{min} \quad . \tag{21}$$

Since the MARC analysis was linear, the J-integral can be scaled for different loads:

$$J = \left[\frac{P}{P_m}\right]^2 J_m \quad , \tag{22}$$

where P_m and J_m are the load and resulting J integral from the finite element analysis.

Testing was conducted at a stress ratio, R = 0.1. Thus

$$P_{min} = RP_{max} \quad , \tag{23}$$

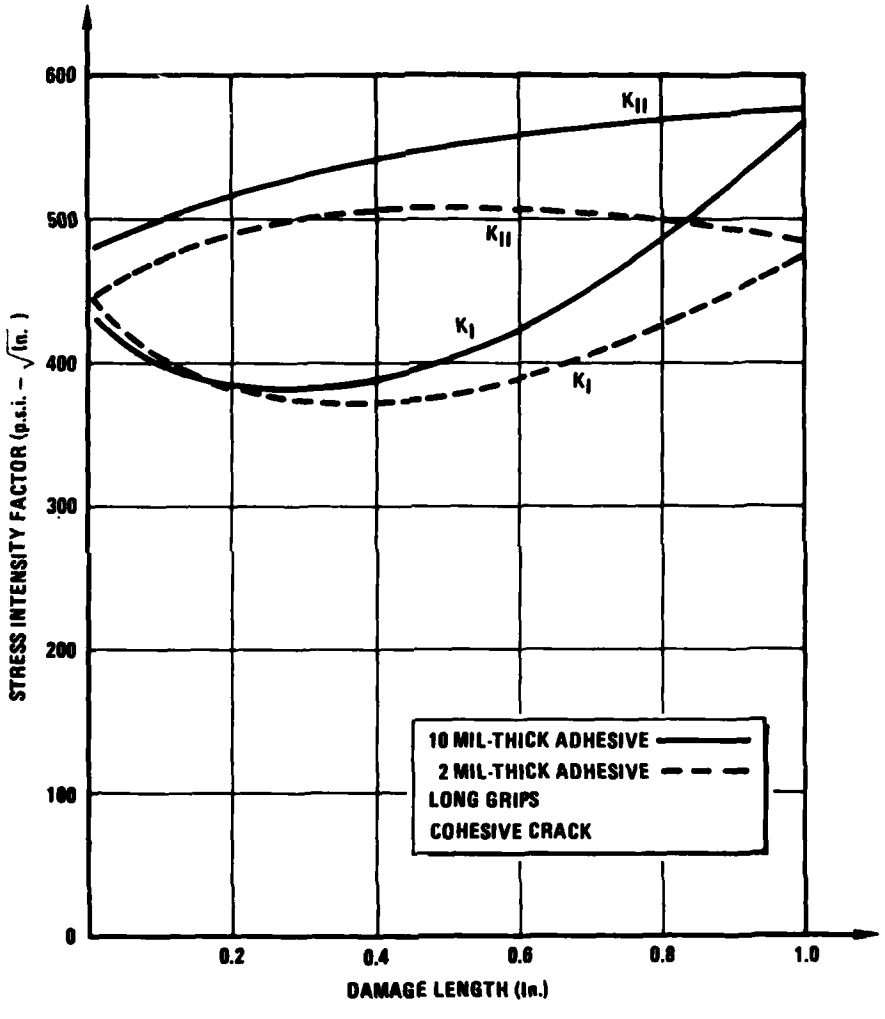

Figure 17 Variation of Stress Intensity Factors for Two Adhesive Layer Thicknesses

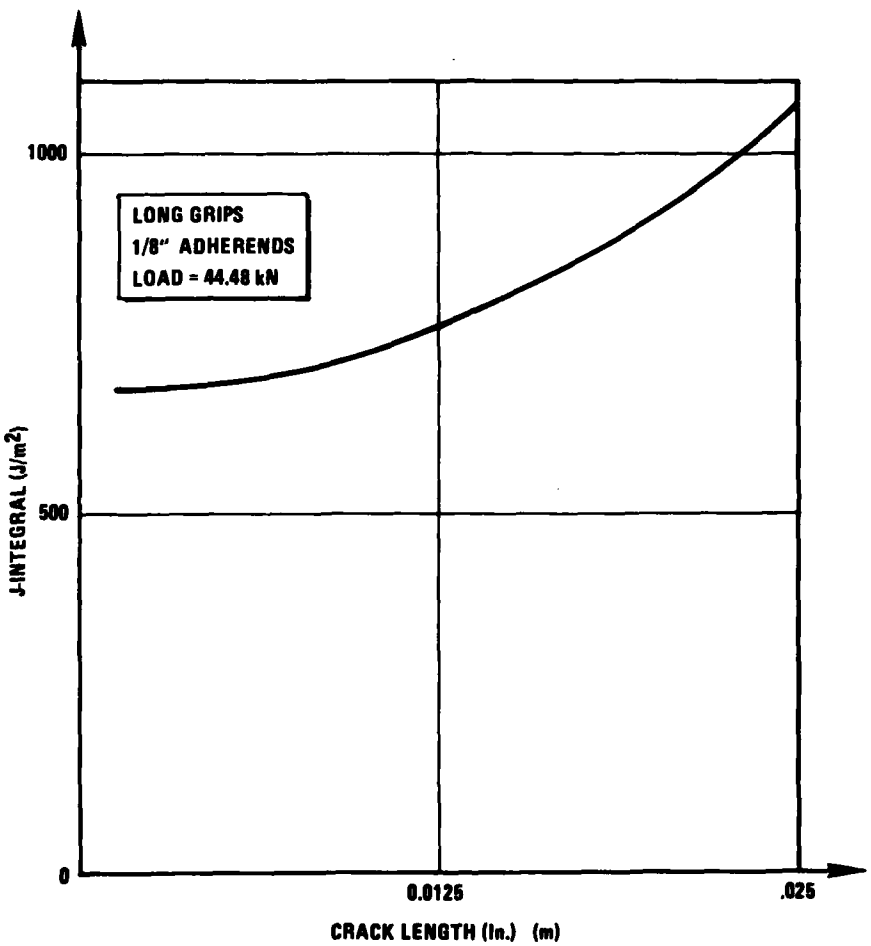

Figure 18 J Integral versus Crack Length for SLJ Specimen

or $\Delta P = (1-R) P_{max}$. (24)

Combining equations (21), (22), (23), and (24) yields

$$\Delta J = \frac{1+R}{1-R} \left[\frac{\Delta P}{P_m}\right]^2 J_m \quad . \tag{25}$$

Since the J-integral, J_m, was a function of crack length, the crack location at which da/dN measurements were made must also be taken into account in calculating ΔJ.

Logarithmic plots of da/dN vs. ΔJ are shown in Figures 19-21. The effect of temperature on the CLS1 results is shown quite clearly in Figure 19 as the increased temperature increases the crack growth rate for a given ΔJ. A comparison of the results in Figures 19 and 20 for the CLS1 specimens indicate that frequency effects are small. The slope of the da/dN vs. ΔJ curves for the CLS2 specimens (Figure 21) is very large, indicating that, at the higher GI /GII ratios , fracture is governed by static fracture properties. Linear regressions of the data presented in Figures 19-21 were conducted.

Straight lines in the logarithmic plots imply a power law relationship between the crack growth rate and change in J-integral per cycle. This is given by the relation

$$da/dN = B\ (\Delta J)^n \quad , \tag{26}$$

The correlation coefficient of the least squares fit, the power law exponent, n, and the power law coefficient, B, for each test condition are shown in Table 21. For the CLS1 specimens, the crack growth law exponents are approximately the same as those that were measured for neat FM-73 during the Fatigue Behavior program (Ref. 19) when a factor of two is accounted for because the J-integral is proportional to the square of the stress intensity factor.

4.2.5 Failure Criteria and Flaw Growth Modeling

4.2.5.1 Failure Criteria

Fatigue crack growth leading to final fracture is a commonly observed mode of failure in adhesively bonded

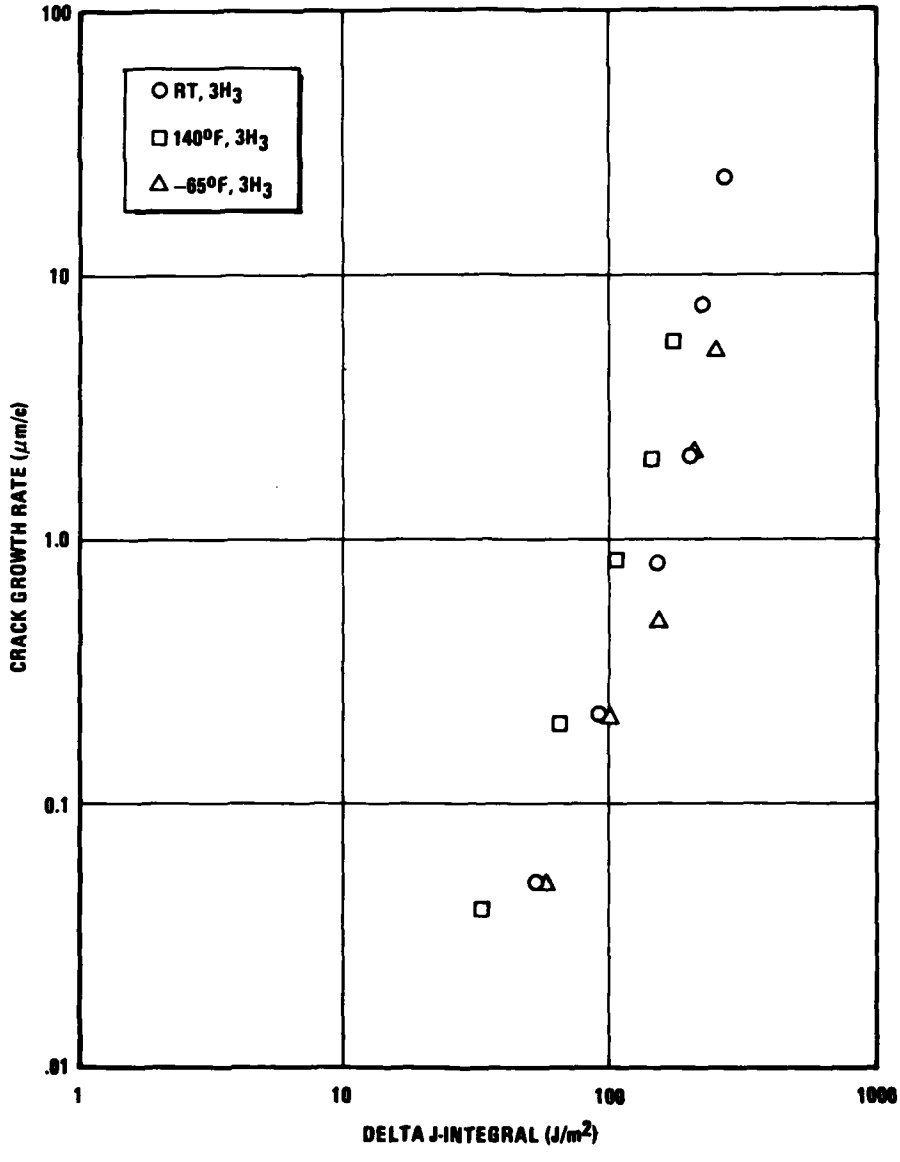

Figure 19 da/dN versus ΔJ for CLS_1 Specimen

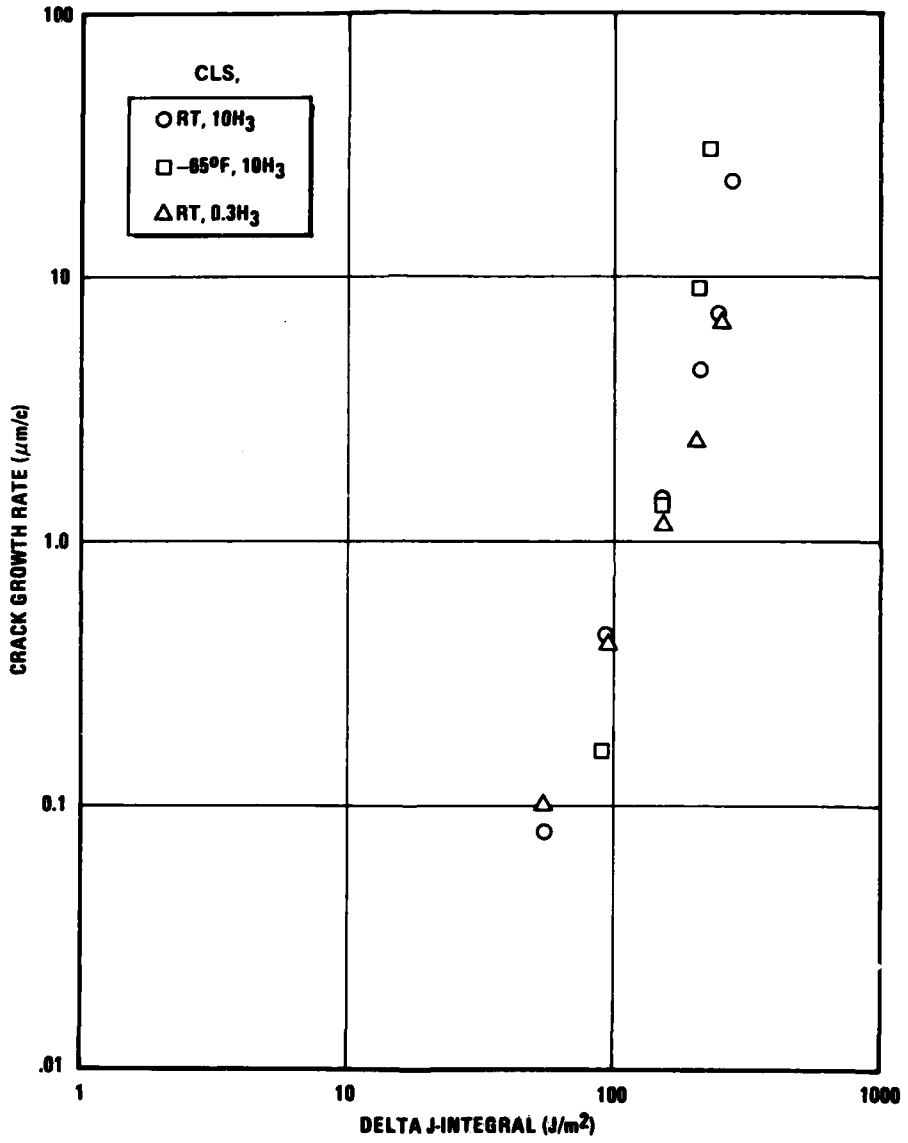

Figure 20 da/dN vs. Delta J. for CLS_1 (Continued)

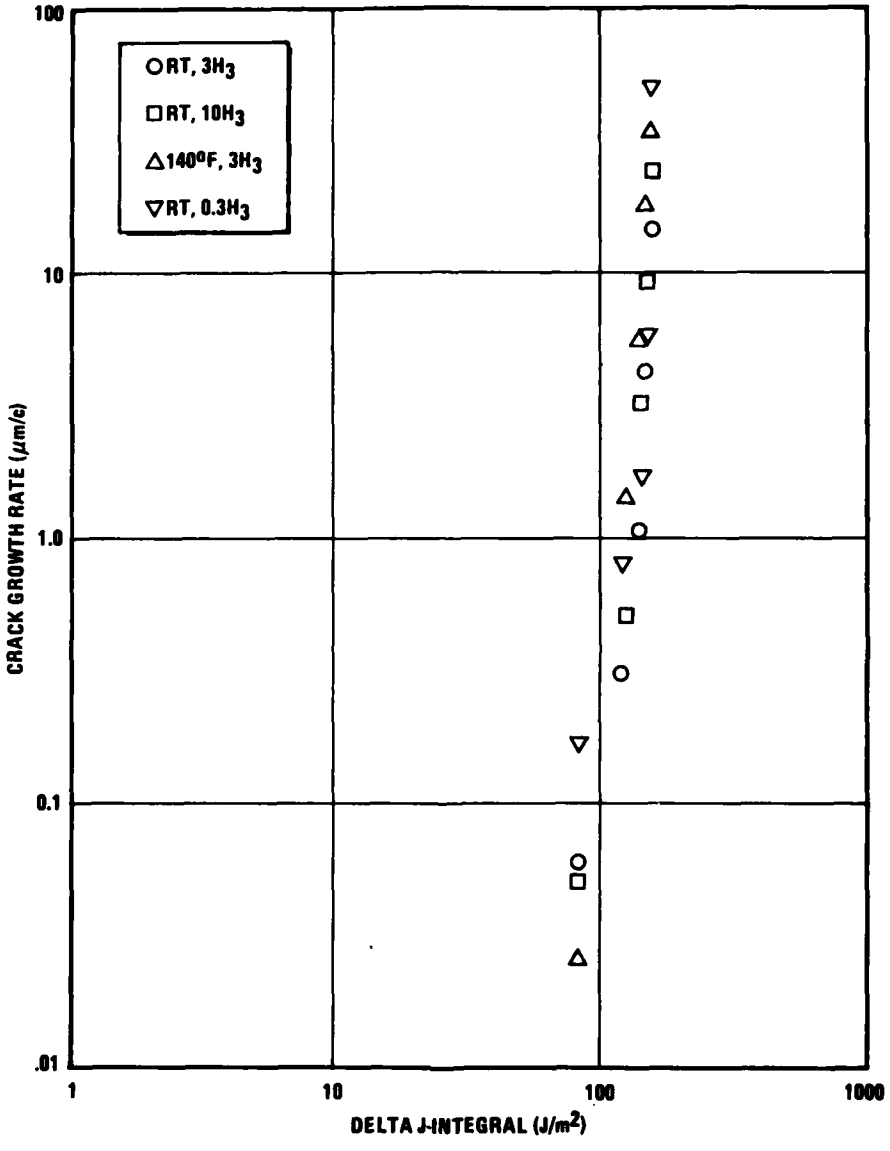

Figure 21 da/dN versus ΔJ for CLS_2 Specimen

Table 21 Crack Growth Laws for CLS Specimens

$$da/dN = B(\Delta J)^n$$

Specimen Number	Temperature (^{o}F)	Frequency (Hz)	Correlation Coefficient	Power Law Exponent n	Power Law Coefficient B
CLS_1-4	140	3	.974	3.55	$2.41x10^{-8}$
CLS_1-5	RT	3	.997	2.98	$8.4x10^{-7}$
CLS_1-7	RT	10	.988	3.24	$1.6x10^{-7}$
CLS_1-8	-65	10	.992	5.39	$4.64x10^{-12}$
CLS_1-9	-65	3	.985	3.05	$1.88x10^{-7}$
CLS_1-10	RT	0.3	.992	2.58	$3.41x10^{-6}$
CLS_2-4	RT	3	.949	8.13	$1.14x10^{-17}$
CLS_2-6	RT	10	.963	9.28	5.37x10-20
CLS_2-7	140	3	.937	7.48	$7.99x10^{-6}$
CLS_2-8	RT	0.3	.858	7.53	$3.40x10^{-16}$

joints. Accordingly, the failure criteria developed in this program are the results of a fracture mechanics approach.

Linear elastic fracture mechanics (LEFM) concepts have found successful application in the modeling of crack growth in metals. Parameters such as strain energy release rate, G, and the stress intensity factor, K, have been widely used to characterize both fatigue crack growth and final fracture for Hookean materials. The question then arises as to the extent of applicability of LEFM to the prediction of fatigue crack growth in adhesively bonded joints.

There are a number of reasons that crack growth in an adhesive bond could differ from that in metals. First, we recognize that adhesives are polymers and therefore potentially viscoelastic and time-dependent. Secondly, the adhesive layer is heavily constrained by the metal adherends, giving rise to the possibility of geometric and material non-linear behavior. Finally, fatigue crack growth must be understood under conditions of varying degrees of mode interaction.

The fracture parameter chosen to characterize fatigue failure in adhesively bonded joints in this program is the J-integral. Not only can it be compared directly with the LEFM approach, but it is also defined for cases of nonlinear elastic, nonlinear elastoplastic and, more recently, nonlinear viscoelastic behavior (Ref. 30). The J-integral has also been found to be equivalent to the vectorial crack opening displacement, a fracture criterion which was successfully used to characterize interfacial crack propagation in an adhesive joint subjected to loading normal to or tangential to the bondine (Ref. 54).

Slow fatigue crack growth has been observed in the CLS and SLJ specimens whose testing was reported in Section 4.2.2. In the Fatigue Behavior program (Ref. 19), fatigue testing of thick-adherend lap-shear model joints (MJ) also revealed a slow crack growth portion of the crack growth history.

The slow crack growth portion of the crack growth history has been characterized by a crack growth law which relates the rate of crack growth per cycle (da/dN) to the change in J Integral (ΔJ) during a cycle. Catastrophic failure following slow fatigue crack growth has been observed in the MJ and SLJ. The criterion for this mode of failure is that the shear strength of the adhesive has simply been exceeded due to the shorter overlap produced by an increase in crack length. Prediction of the crack growth

history is thus obtained by a cycle-by-cycle integration of the crack growth law for the fatigue crack growth portion subjected to the condition of a critical crack length for catastrophic failure.

4.2.5.2 Crack Growth Prediction - Model Development

The scheme that has been used in the cycle-by-cycle integration is shown in Figure 22. A finite element analysis of the geometry of interest is conducted to determine the variation of J integral with crack length.

If the finite element analysis was conducted at load levels different from the actual loading, then the results of the finite element analysis must be scaled as they were in the case of the CLS specimen. That is:

$$\Delta J(a) = \frac{1+R}{1-R} \left[\frac{\Delta P}{P_m}\right]^2 J_m \quad . \tag{27}$$

Recall that the fatigue test results gave rise to a fatigue crack growth law of the form

$$da/dN = B\ (\Delta J)^n \quad . \tag{28}$$

Cycle-by-cycle integration of (28) in conjunction with(27) yields

$$\Delta a = B \left\{ \frac{1+R}{1-R} \left[\frac{\Delta P}{P_m}\right]^2 J_m \right\}^n \quad , \tag{29}$$

where Δa is the increase in crack length per cycle. The crack length after N cycles is given by

$$a = \sum_{i=1}^{N} a_i \quad . \tag{30}$$

The cycle - by-cycle integration of the fatigue crack growth law (Equation 29) requires values of J integral at crack lengths not necessarily determined in the finite element

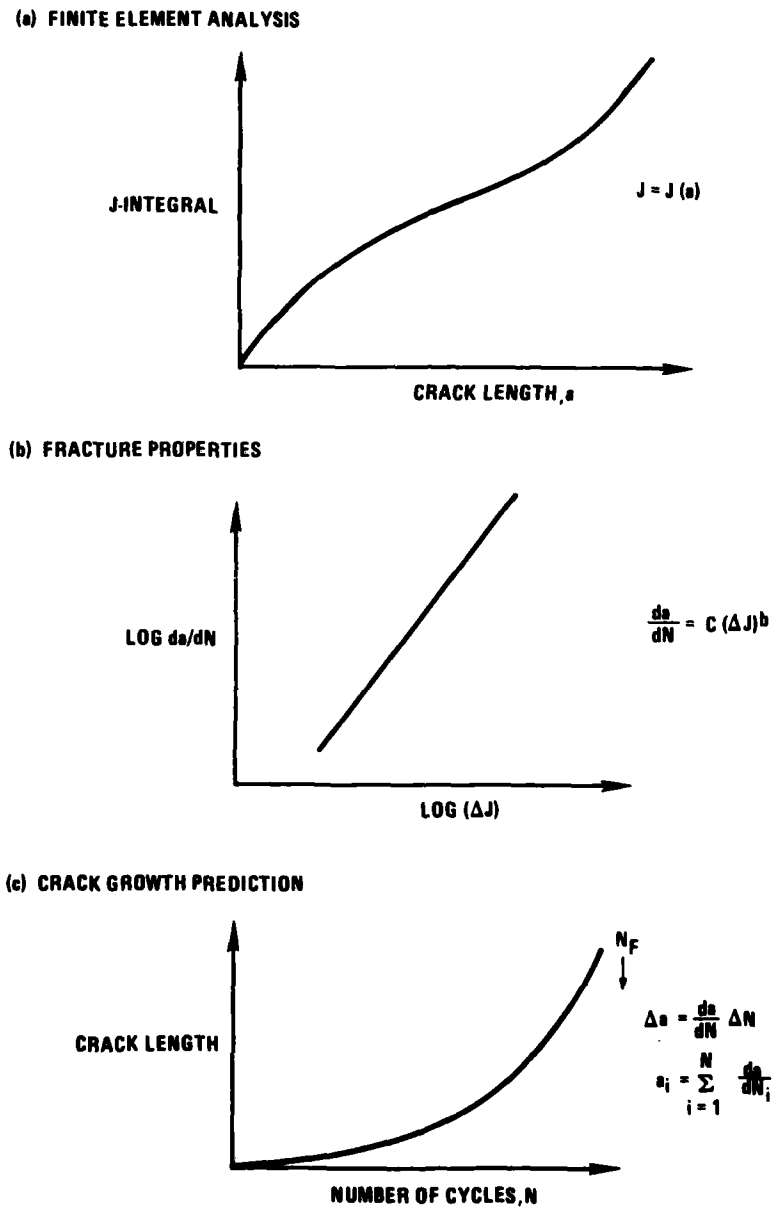

Figure 22 Crack Growth Prediction Scheme

analysis. Interpolated values of J integral were therefore obtained using the Hermite interpolating polynomial.

The scheme outlined in Figure 22 and formulated in Equations (27) through (30) has been computer programmed. The code has been validated using results obtained from the fatigue testing of center-cracked panels of neat FM-73M adhesive in the Fatigue Behavior program (Ref. 19). Figure 23 shows the crack length vs. number of cycles for a center cracked panel of neat FM-73M at room temperature subject to constant amplitude cyclic loading at a frequency of 1.0 Hz and R factor R = 0.1. The points are obtained from the actual fatigue testing and the full line is the result of the cycle-by-cycle integration. If the critical crack length is arbitrarily set at 17.75mm, we see that the predicted and actual lifetimes differ by 6.5%. In view of the large exponent in the crack growth law which was curve fit to the original data, this variation in lifetimes is not unreasonable and the code is therefore considered to be validated.

4.2.5.3 Verification of Crack Growth History in SLJ Specimens

The procedures outlined in the previous section were attempted for the SLJ. However, it soon became clear that the J-integrals obtained through the stress analysis using the MARC finite element code resulted in predicted crack growth rates based on CLS data that were orders of magnitude greater than those that were measured during the testing of the SLJ specimens.

To see this in more detail, consider Figure 18 which depicts the variation of J-integral with crack length. Values of J-integral there are greater than 600J/m² for a load of 44.48 kN. The peak to peak loading during testing of the SLJ1-1 specimen was 66.72 kN, resulting in a change in J-integral per cycle on the order of 1500 J/m². A look at the da/dN vs. ΔJ curves (Figs. 19-21) indicates that the specimens should have failed on the first cycle! Table 18 which records the lifetimes of the SLJ specimens that were tested indicates that the lifetime of the SLJ1-1 specimen was approximately 200,000 cycles.

The discrepancy could arise either from the representation of the material properties or from the stress analysis of the SLJ specimen. The fracture property measurements were consistent with measurements made on neat FM-73, making the stress analysis suspect. Unfortunately,

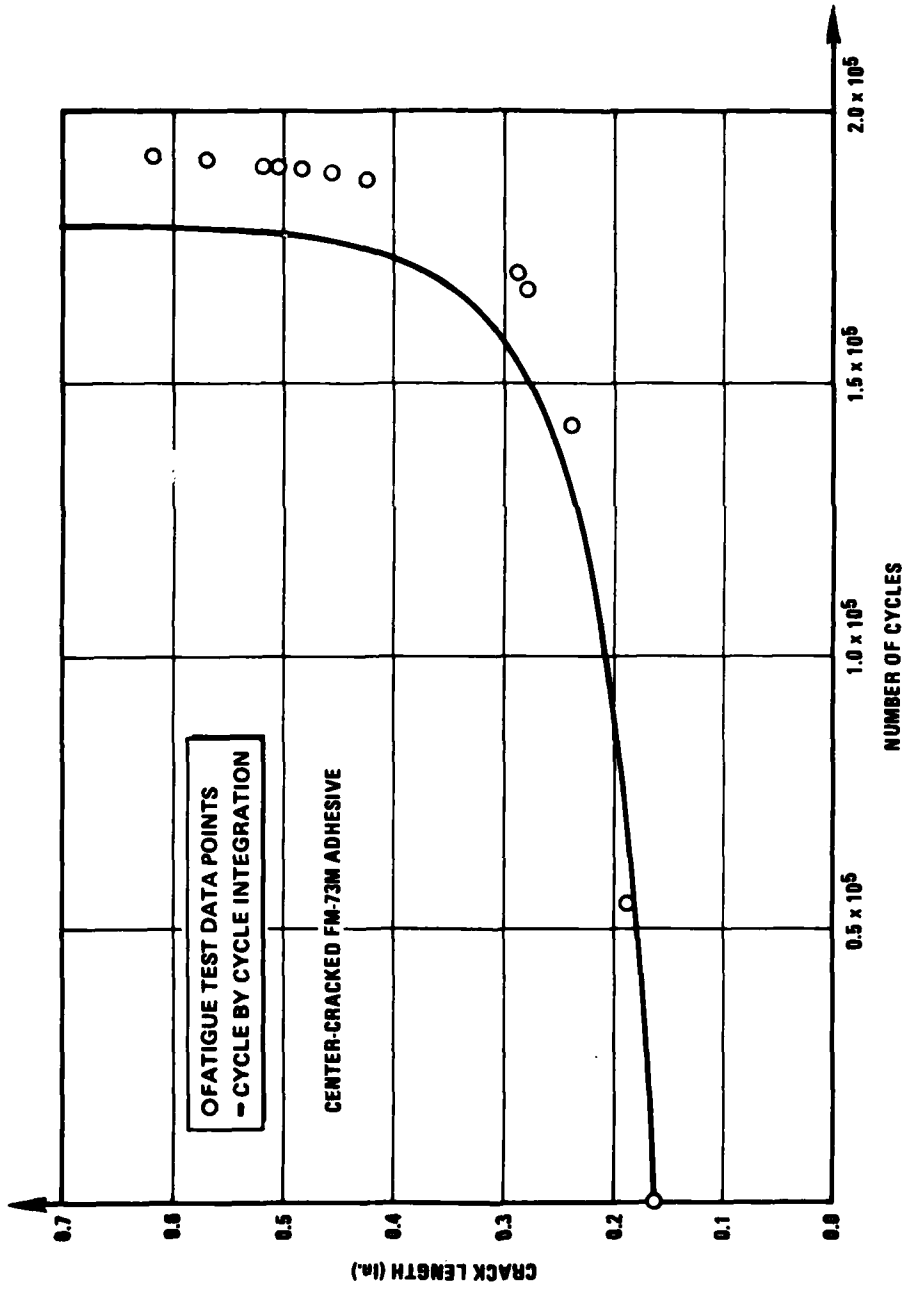

Figure 23 Crack Length versus Number of Cycles for Center-Cracked FM-73M Adhesive

time and funding constraints have not permitted a conclusive evaluation of the MARC finite element analysis of the SLJ. Stress analyses of the SLJ using NASTRAN and GAMNABS are available but are of a tentative nature.

The results of these analyses are compared in Table 22. The MARC and GAMNABS analyses were conducted for loads of 44.48 kN and have been scaled to the 73.39 kN level at which the nonlinear NASTRAN analysis was conducted (corresponding to the peak load applied during testing). No lateral constraint was modeled in the MARC analysis. The MARC and NASTRAN results are in closest agreement and if lateral constraint had been modeled, the agreement would have been better since the constraint acts to lower J-integral values. However, the GAMNABS analysis predicts levels of J-integral that would result in crack growth rates that are of the same order as those that were experimentally observed.

Although the GAMNABS results are much lower than the MARC and NASTRAN results, the GAMNABS results do predict crack growth rates that are of the same order as those that were experimentally observed. Because of the tentative nature of these analyses, the source of the discrepancy is not clear.

In fact a prediction of the crack growth history of the SLJ1 specimens was conducted using the GAMNABS analysis. It was assumed that the value of J-integral of 20 J/m^2 that was obtained for the load of 44.48 kN and a crack length of 0.0254m was the same for all crack lengths. The value of J was scaled to reflect the loads of 66.72, 88.96 and 111.20 kN that were used in the testing of the SLJ1 specimens. The assumption of a constant J-integral does not seem too severe in view of the NASTRAN results. The critical crack length marks the onset of catastrophic failure.

A comparison between the predicted and actual crack growth histories is made in Figure 24. The predicted growth is shown by the full line with the experimental points shown by the data points. The actual lifetimes are indicated by the arrow. It can be seen that the agreement in crack growth history and lifetimes is fairly good. The straight lines obtained by prediction are a consequence of choosing a constant value for J. The discrepancy in the initial crack growth rates may be due to the fact that the J-integral rises sharply to a maximum for very small crack lengths. A detailed stress analysis of the overlap region should resolve this possibility.

Table 22 Comparison of Finite Element Analyses of SLJ Specimen

Code	Analysis	Crack Length (m)	J-Integral (J/m^2)
MARC	LINEAR	.0025	1837
MARC	LINEAR	.025	2913
GAMNAS	LINEAR	.025	55
NASTRAN	NONLINEAR	.0025	1395
NASTRAN	NONLINEAR	.025	1358

*No lateral constraint was modeled in the MARC analysis.

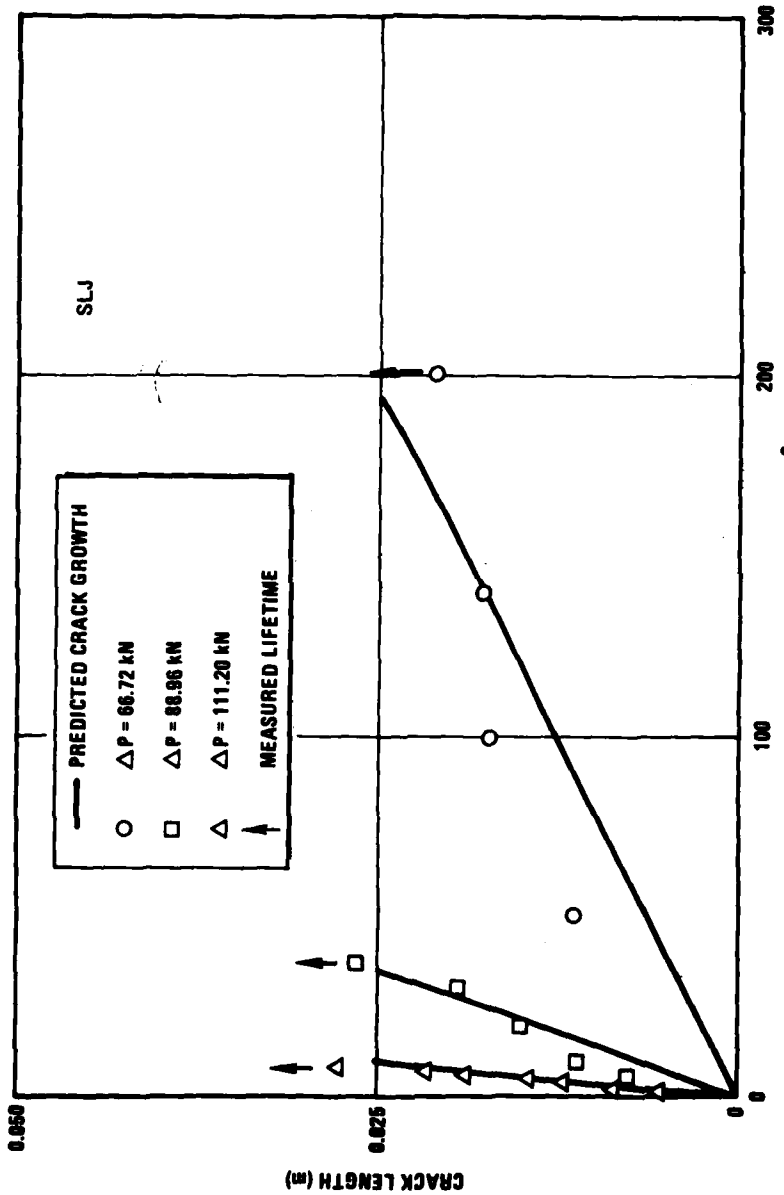

Figure 24 Actual and Predicted Crack Growth Histories for SLJ Specimen

A further source of the discrepancy could arise from the fact that the mode I/mode II ratio decreases in the SLJ as the crack grows, whereas it is approximately constant in the CLS geometry (Ref. 31). When the crack growth rates in the two CLS configurations are compared, the rates in the CLS2 specimens (higher modeI/mode II ratio) are greater. The initially higher mode I/mode II ratio at shorter crack lengths would give rise to the initially higher crack growth rates observed in Figures 11 and 12. The crack growth prediction scheme does not account for these mode interaction effects.

4.3 Demonstration of Integration Method for the PABST Test Article

The bonded joint to be used for the Integrated Methodology Demonstration Article is similar to the structural lap joint. The actual joint being modeled is part of the PABST Full-Scale Demonstration Component (FSDC) shown in Figure 5 (from Ref. 63). This particular joint is located at Fuselage Station 703 between longerons 14 and 19. The skins at this point are 1.27mm (50 mils) thick. Two splice plates are used in the joint. The first plate is 0.81mm (32 mils) thick and the next plate is 1.80mm (71 mils). To this is bonded a T-section which is part of the frame at Section 703.

The finite element model that was to be created represented a plane section perpendicular to a line that is (1), tangent to the outside surface of the fuselage and (2), normal to the fuselage centerline. Since this was a 2-D model and membrane elements were used, the effects of the joint curvature normal to the assumed section were considered. This would have required the use of solid elements to accurately account for the curvature. The cost incurred in a solid analysis would probably be large and was not feasible at this time.

Due to the thin skin thickness used, it is possible that geometric effects could be important for this particular joint geometry. If so, the cost per analysis would increase by a factor of 5 to 10 dependent on the finite element program used to perform the geometrically nonlinear solution. It is possible that these effects may not be important if sufficient boundary conditions are applied to simulate the support of surrounding structure. In this specific case, there are longerons and frames at regular locations which could prevent significant out-of-plane deflection in the real airplane.

Models of this joint were generated using a program which runs on a VAX 11/780, utilizing a refresh graphics tube and light pen to allow rapid development of models of joints. All element definitions are immediately drawn on the screen as the element is created. Thus errors are easily seen and rapidly corrected. There is roughly a factor of 10 savings in time required to create a model. There are additional time savings since the model is usually correct and little time (if any) is required to debug the model.

Problems with the MARC program itself did not allow any analysis of the models generated above.

One beneficial outcome of the predictive methodology is that the effects of different loading and environmental conditions can be assessed more cost effectively than recourse to a substantial amount of proof testing.

As an example, we consider the effects of loading on temperature on the lifetime of the SLJ1 specimens. The influence of different load levels was determined in the testing and prediction of the SLJ1 specimen (Figure 24). An influence curve obtained from those results is shown in Figure 25 where lifetime is plotted versus load levels. Again for the SLJ1 specimen, it was thought that temperature effects could be accounted for by substituting the appropriate crack growth law (Table 21) in the crack prediction scheme. However, the effect of temperature was not accounted for in the stress analysis. At a temperature of 140°F, the predicted lifetime of the SLJ1 specimen was longer than that at room temperature; a fact which is not intuitively reasonable and which has not been borne out by recent tests conducted at UT/CSD. The simplest way to account for the higher temperatue in the stress analysis would be to lower the modulus of the adhesive. Analyses of the model joint indicated that lower moduli resulted in higher values for J integral. The increase in J-integral could raise the predicted crack growth rates at 140°F above those at room temperature. A schematic of the possible effect of temperature on crack growth history is shown in Figure 26. The effect on lifetime would then be determined by noting the critical crack lengths to produce an influence curve similar to that for load effects.

4.4 Remarks

The details of the different aspects of the integrated methodology that were discussed in previous sections have

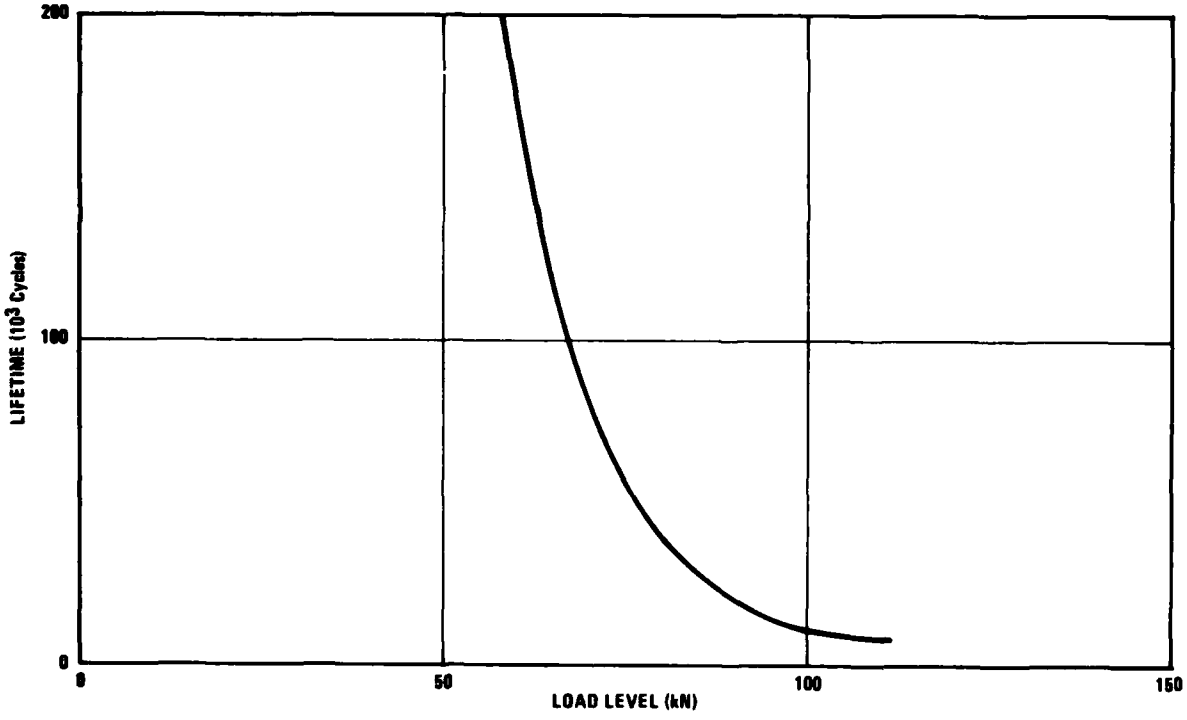

Figure 25 Influence of Load Level on the Lifetimes of SLJ Specimen

been developed. While further refinements will improve the accuracy of the predictions (and use), the methodology has been demonstrated in principle and has been shown to be sound.

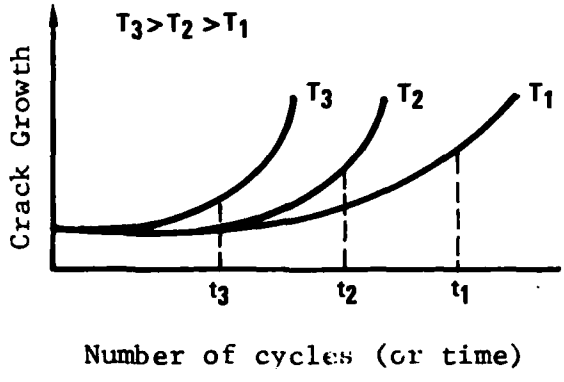

Figure 26 Example of Effect of Temperature on Lifetime for Bonded Joint

V. IDENTIFICATION OF EXPANDED REQUIREMENTS

The present program has been developed and laid out with consideration given to thorough coverage of the needs for a reliable bonding technology. Accordingly, the modules with which the whole field has been subdivided represent fairly clearly and totally the needed subject disciplines. Therefore, in this section we shall point out the most pressing problems that need to be attacked within the modules, plus some general remarks.

The areas that we have identified to require additional effort are as follows:

a) loads/environments definition
b) adhesive constitutive behavior
c) stress analysis
d) fracture mode interaction.

We have come to believe during the course of this investigation that apart from item a) above, these subjects contain the major shortcomings in predictive bonding technology at this time. Some general comments on these items are given below.

a) Since loads definition was not the central focus of this program, and there was finite funding, only a minor effort was directed in the area. In order to establish more definitely the time scale of loading that will affect the time-dependent bond failure processes, a more thorough study/survey should be conducted. We believe that enough information is now available on the time scale of the thermo-mechanical response of adhesives so that the pertinent ranges of time dependent loads for aircraft can be discussed, and which types of bonds are important in the time-dependent failure process.

b) Under this program, the adhesive was considered basically a linearly elastic solid for analysis purposes, although viscoelastic efforts were continuously monitored, measured and considered. In reality, the material is non-linearly viscoelastic, especially due to the presence of the scrim cloth. These nonlinear effects, largely due to time dependent microfracturing, are particularly of concern in the failure process and will need to be considered in more detail in the future.

c) There are some serious questions regarding application of currently-available computer codes to bond

type geometries. Let us recognize that much of the interpretation as to whether a code provides realistically computed answers depends primarily on our ability to visualize or otherwise estimate the stress and/or displacement field. With regard to stresses near cracks in the bondline, we have relatively little information or intuition as to what values are appropriate. The MARC computer code appears to possess some serious shortcomings in this regard, although the source of this shortcoming could not be ascertained.

d) A limited amount of testing has been directed in this program to elucidate the effect of Mode I, II, III interaction on fracture of bonded joints. There is no basic information on how much interaction occurs, and hence our predictive capability in this regard is - and is likely to continue to be - rather poor. Efforts directed at eliminating this problem are necessary for a predictive methodology with a still smaller range on the error bound.

There are other observations that should be made, and that is that it has been presumed throughout that a certain standard of quality is maintained between the characterizing specimens and the design or evaluation geometries. In order to verify this, NDI methods are required which have not been incorporated into the present Integrated Methodology program, but which should be considered a part of it in order to make bonding an acceptable way of manufacturing. Nondestructive inspection (NDI), and possibly Quality Control on surface properties in general must be implemented for reliable and fast "on-line" inspection. Periodic NDI, coupled with the Predictive Methodology, would facilitate disposition (also such as MRB in Factory) of parts containing imperfections.

The reason that NDI was not made a part of the present Integrated Methodology program was that a) efforts on this subject are well underway in this institution of structural research, and b) that in light of that fact the present program should not be burdened by additional concern. Future programs or efforts on bond technology should keep in close touch with developments on NDI.

Our concern with the quality control on surface preparation results from the observation that interface separation cannot be measured in a non-destructive way. Achieving a required bond strength cannot, therefore, be measured except through a proof test. While proof testing is undoubtedly an important aspect of implementing bonding in structural manufacturing, the assurance for the safety of

the execution will undoubtedly rest strongly on a reliable demonstration of optimal manufacturing care.

To summarize then, we believe that the present investigation modules of

a) Loads/Environments Definition
b) Material Characterization
c) Stress Analysis
d) Failure Criteria
e) Structural Integrity (Strength) Analysis

are mature and well manageable investigative entities that require additional work in detail. Other than such greater detail definition, there appears to be a need for a more careful loads definition and education on the importance of time dependence of loads and their effect on the bond failure process.

In particular, there are certain areas in each one of the modules that need more detailed attention: we would rate these, listed below, as first priorities in any serious effort to further improve bond predictability.

A. Loads and Environment

1) The effect of mission profile and time history of loading needs to be better clarified (including maneuver sequence and flight envelope).

2) The periodic content of the mission profile needs to be determined with emphasis on the frequency content, clearly separating out the steady or monotonic loads.

B. Material Properties

1) The effect of load level on accelerated time response needs to be better clarified. This phenomenon can be combined with a lack of knowledge of the non-linearly viscoelastic material behavior.

2) Physical aging, by which the material changes its mechanical response with time, needs to be better understood so that failure predictions with appropriate long time properties can be accomplished.

3) Microfracture preceding bond failure is an important phase in the failure process, yet very little is known about

it, its causes (other than high stress), its growth and dependence on stress state.

4) The intrinsic strength of a bond derives from the adhesive per se (not including the scrim cloth) and more knowledge regarding these intrinsic adhesive properties is necessary.

C. Stress Analysis

While the currently-developing computational code VISTA addresses many of the needs of bonded joint analysis, perhaps the greatest need exists in evaluating the code capability for non-linear stress analysis; the material representation now developed needs to be checked out and its limitations at large strain (over 5%) needs to be estimated.

D. Failure Criteria

So far, possible criteria for incipient failure have been identified; they are listed in Table IV A. Those that are associated with cracks are well understood, if not completely evaluated. However, criteria that address the growth and/or initiation of cracks are virtually non-existent. Work in this area is needed, particularly addressing the generation of failure from bond terminations (end of adherend region). A possible criterion for this purpose might be crack generation over a finite area (length) along a path requiring minimal energy expenditure. Along with this requirement there are several questions of a fundamental nature that must be resolved in order to develop a satisfactory predictive framework; these are:

1) Is there a basic difference between failure in monotonic and cyclic load histories or can fatigue fracture be predicted from steady crack propagation tests?

2) What is the limitation in considering fatigue failure to depend on ΔK?

3) What is the effect of disregarding the presence of the scrim in the adhesive?

SECTION VI

CONCLUSIONS AND RECOMMENDATIONS

A detailed review was conducted of existing analytical and experimental structural mechanics procedures required to perform accurate and rigorous structural analysis of adhesively bonded joints. Four main analytic concepts were encountered during the course of this review: P-over-A analysis; strength of materials approach; thickness-averaged fracture mechanics; and (true) fracture mechanics. It is argued, and substantiated by finite element calculations, that it is only with the (proper) application of the fourth analytical procedure, viz., fracture mechanics, that a suitable vehicle is obtained to organize and rationalize problems of bonded joint performance.

Use of the thickness-average fracture mechanics approach provides a non-conservative prediction of failure, and is not recommended for use. In citing only one case, the J-integral calculations versus crack length were considerably higher than the two cases modeling a realistic modulus (Ref. 62). On the other hand, the strength of materials approach leads to unnecessary conservative estimates and thus leads to designs having longer-than-needed overlap lengths. This is an acceptable approach although the associated weight penalties may be troublesome for some systems (Ref. 7). The fracture mechanics approach emphasizes the use of information on the effects of interactions with mechanical loads of time and environment (temperature, moisture) reflecting the viscoelastic (polymer) nature of the adhesive interlayer of bonded structures, in the formulation of the stress analysis methods and crack growth modeling to accomplish the goals of this program.

Based on the findings of the aforementioned review of structural mechanics procedures, a comprehensive integrated methodology for adhesive bonded joint life predictions is developed. The guiding assumption is that the useful life of bonded joints is determined by failure in the adhesive interlayer, and this is the basis for a systematic analysis of information and the techniques required to provide valid predictions. Emphasis is placed on time-dependent fracture mechanics procedures, including detailed through-the-adhesive thickness viscoelastic finite element calculations of the stress-strain distributions, and on analytical methods involving the constitutive relations of the adhesive interlayer. Use is made of instrumented bonded joint data

obtained from structural overtest methods under a number of U.S. Air Force-sponsored program. A logical program rationale is outlined which has sufficient generality to apply to any adhesive bonded joint structure including metal and composite adherends, and various loading/environmental conditions, which apply to high-performance aircraft.

Five main modules of the integrated methodology are established: (Definition of) Loads/Environments; (Adhesive) Material Properties; Stress Analysis; Fatigue Mechanisms and Failure Criteria; Aging Structural Failure Analysis (Life Predictions). The necessary contents of each module, including input and output data, are specified and a systems approach is taken interconnecting the modules into a logical sequence suitable for making service life predictions for bonded structures.

The various feeder sub-programs, which must be accomplished for full implementation of the Integrated Methodology program, are identified and it is recommended that they all be carried to completion to generate the contents identified in each of the interconnected modules constituting the integrated method. Since the Stress Analysis module(III) and Failure Criteria module (IV) occupy dominant positions in this methodology, it is recommended that the feeder sub-programs developing information for these two central modules should command top priority.

This backbone program, the Integrated Methodology program, is ending before completion of a number of feeder sub-programs, some of which haven't even been initiated. Under these circumstances, the life prediction of the verification test article, the circumferential bonded splice of the PABST FSD component, is a first attempt and is done for demonstration purposes. It is recommended that all the feeder sub-programs be initiated and carried to completion so that more reliable predictions of service life can be achieved.

In particular, an accurate stress analysis of the verification test article is required using a working viscoelastic code. There are apparently errors in the MARC program which need correcting. The VISTA program must be ready for use, before the stress analysis can be performed.

Also, additional fracture response properties are required from a feeder sub-program before reliable da/dN versus J data can be obtained over the broad range of temperatures and moisture mission profiles of advanced aircraft.

Important major payoffs resulting from the use of adhesive bonding, already successfully demonstrated in the PABST program, include: improved joint fatigue life (by avoiding rivet holes); elimination of corrosion (by avoiding fretting of faying surfaces); reduction of weight of the joint, and reduced cost through smaller part count.

There is no doubt that adhesive bonding will eventually play a significant role in the joining and/or repair of primary structural members of high performance military aircraft of the future.

Of course, the parallel development of adequate nondestructive inspection (NDI) techniques and repair procedures for bonded structures will further expedite the acceptance of this joining technique in military aircraft of the future.

The structural and performance characteristics of the advanced technology fighter (ATF), the so-called "stealth" aircraft, could be most efficiently realized using this joining technique, since its design will probably feature thin gage, lightweight, extremely aerodynamically smooth surfaces (for non-visibility) and a low (load transfer) density of primary joints, all ideally suited for adhesive bonding. Being a subsonic aircraft, it could also take advantage of well-developed, PABST-used BAC-5555 surface treatment and the excellent and well-documented 250°F - cure, FM-73M adhesive film. This would lead to a low cost, highly reliable design.

Substantial improvements in the accuracy and the general applicability of the methods of life prediction are expected when the results of the related roadmap programs ② through ⑧ become available. It is recommended when these results are available, that they be consolidated into a logical engineering procedure and used as appropriate during design, MRB actions, System Deployment/Maintainance Tradeoffs, and in setting up Inspection and Maintenance schedules.

In addition, the following four programs are recommended:

1) Bonded Joints under Tension - Compression Cycling

It is recommended that effects of tension-compression (t-c) cyclic loading, which are experienced in normal aircraft mission profiles, be included in the IM program. To date, only tension-tension (t-t) structural loading has been considered. While intuitively it is expected that fatigue lives would be significantly lower during a t-c loading

cycle, it is possible craze healing in viscoelastic materials may occur as has been recently reported by Wool (Ref. 64), which could directly influence lifetime prediction, especially over long term periods encountered in actual mission profiles.

2) Bonded Joints With Resin Matrix Composite Adherends

In view of the increasing use of resin-matrix composite materials in fabrication of aircraft components, it is recommended that the scope of the IM program be extended to include resin-matrix composite adherend(s). This would expedite the development of the integrated method for composite joints which would be timely in view of the USAF's current commitment for building the composite aircraft in the factory of the future. Accordingly, other specific tasks outlined briefly below, as proposed for the IM follow-on program, reflect the need for incorporating ideas concerning composite adherends.

Such an integrated methodology for lifetime prediction of bonded joints utlizing composite structures must be developed at this time if this technology is to be made available for satisfactory use on predicting long-term (up to twenty years) durability and fatigue life of primary structures using these advanced non-metallic materials.

3) Repair of Composite Split Ends and Delaminations Around Fastener Holes

It is recommended that the extent of splitting of exposed composite panel edges, delaminations around fastener holes and the effect on lifetime of the bonded joint structure be determined. The repair of such split ends by subsequent sealing of the split components with adhesive materials and the change in lifetime so affected should be evaluated. Further spreading of damaged (i.e., split) ends may possibly be avoided by application of an adhesive with subsequent partial compression of the effected parts. In order for this repair procedure to be effective, details will have to be worked out on how to apply the adhesives to get it into the damaged areas effectively before compression. Also, the effect of cure temperature on bonding of metals to composites and composites to composites, addressing the question of possible pyrolization of the composite component (initially at some intermediate state of cure prior to bonding) when bringing the adherends close to the cure temperature of the adhesive during the bonding operation, should be considered.

4) Bonded Joints with Bolt Assist (Ref.: Appendix C)

It is recommended that the question of bolted/bonded joints, and the resulting improvement of bonded joint life, be investigated. Fatigue testing of structural lap joints indicates that the ultimate (fatigue) life of an adhesively bonded joint can be increased by at least a factor of 2 by "tying down" the peel stresses at the overlap edge along the corner singularity with a few bolts strategically positioned at only a small weight penalty to the structure. These experiments were suggested as a result of an existing AFWAL/FDL program at General Dynamics investigating advanced joining techniques (Ref. 65) including adhesive bonding and bolt fastening.

It is recommended that the impact of these findings on joint life prediction as developed in the Integrated Methodology program be evaluated. Considerations should also include the minimum placement of bolts to carry the load between a metal-composite joint and a composite-composite joint.

APPENDIXES

APPENDIX A.

STRESS ANALYSIS VALIDATION

Introduction

It is absolutely essential that some kind of validation of the finite element stress analysis codes be performed, to ensure that the stress analysis model indeed predicts the actual stresses encountered in a bonded joint. This is important particularly in view of the accuracy with which certain fracture parameters need to be determined. Since any stress analysis entails approximations either of a basic nature or for convenience, it is necessary that this validation be done. The basic assumptions need to be checked or their effects need to be estimated. Sometimes this can be accomplished with closed-form analytical asymptotic solutions, but in general this is not possible and it was deemed necessary, therefore, to conduct an experimental program, concurrent with the stress analysis program, to validate the stress analysis procedures used.

A number of different experimental approaches to stress analysis validation were considered in some detail, as described in Reference 67. The technique finally selected is in the area of holographic interferometry, and not by accident considering the success obtained in measuring the time dependence (or lack of it) of FM-73M adhesive material and reported in an archival paper (Ref. 18) during the Fatigue Behavior program (Ref. 4).

A specialized area of holographic interferometry was selected as offering the highest chance of success in a reasonable period of time in this series of life prediction programs. It is that of focused image holography with fictitious fringe-moire', as pioneered and perfected over the last few years by Prof. Sciammarella and his students, albeit on relatively simple, symmetric "thesis environments" (Refs. 68 through 74). A summary of the derivations of the working equations of this technique is briefly given in the following section.

Technical Discussion

Double - exposure holographic interferometry provides surface displacement information along a sensitivity vector given by the angular phase change equation

$$\Delta\phi_0 = (\underline{K}_1 - \underline{K}_2) \cdot \underline{d} = \underline{g} \cdot \underline{d} = n\lambda \quad , \qquad (A1)$$

where $\underline{K}_1$ and $\underline{K}_2$ are the propagation vectors in the illumination and observation directions, respectively; $\underline{d}$ is the displacement of the object point, $\Delta\phi_0$ is the angular phase change, $\underline{g}$ is the sensitivity vector with respect to angular phase change, n is the fringe order, and λ is the laser wavelength.

Ennos (Ref. 75) described a technique to obtain the inplane components of the displacement vector for a two-dimensional surface. The method consists of making simultaneous double exposures of two hologram plates before and after loading the object. If a point of the object is viewed obliquely through these two holograms at equal angles to the surface normal (Figure A1), then the (angular) phase change is

$$\Delta\phi_0 = (\underline{K}_1-\underline{K}_2) \cdot \underline{d} = n\lambda \text{ , for Plate 1} \qquad \text{(A2)}$$

and

$$\Delta\phi_0' = (\underline{K}_1-\underline{K}_2') \cdot \underline{d} = n'\lambda \text{ , for Plate 2.} \qquad \text{(A3)}$$

Subtraction of Equation (A3) from Equation (A2) yields the phase change difference

$$\Delta\phi_0 - \Delta\phi_0' = (\underline{K}'_2-\underline{K}_2) \cdot \underline{d} = (n-n')\lambda \text{ ,} \qquad \text{(A4)}$$

where $(\underline{K}'_2-\underline{K}_2)$ is a vector lying on the surface of the object. Ennos suggested a solution of Equation (A4) by computing the difference n-n' of the orders of the two fringe patterns. Utilizing the fact that the point of observation and point of illumination can be interchanged, the double observation, DO, can be replaced by double illumination, DI, as shown by Butters (Ref. 76) and Boone (Ref. 77) and represented in Figure A2. Accordingly, Equation (A4) can be written as

$$\Delta\phi_0 - \Delta\phi_0' = (\underline{K}_1-\underline{K}_1') \cdot \underline{d} = n_M\lambda \text{ ,} \qquad \text{(A5)}$$

where n_M is the order of the resultant moire' fringe pattern.

In principle, the information can be retrieved in both DO and DI cases by superimposing the two double exposure patterns and observing the resulting moire' pattern. The practical utilization of this idea has been hindered in the

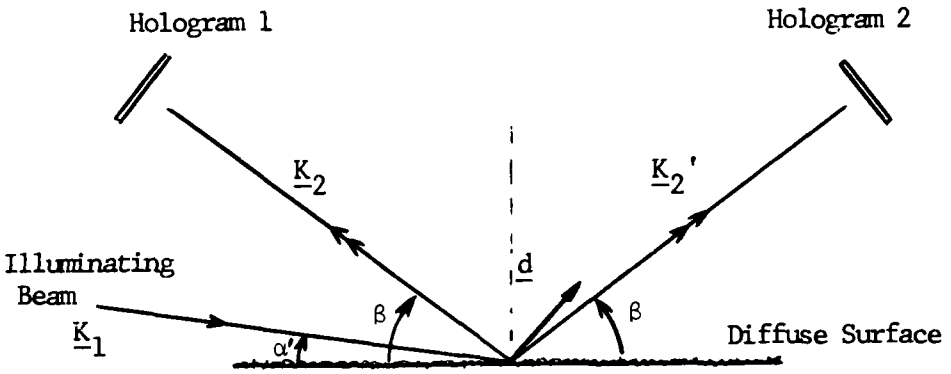

Figure A1 Two-Hologram (Single Illumination Beam) Holographic Interferometry Configuration

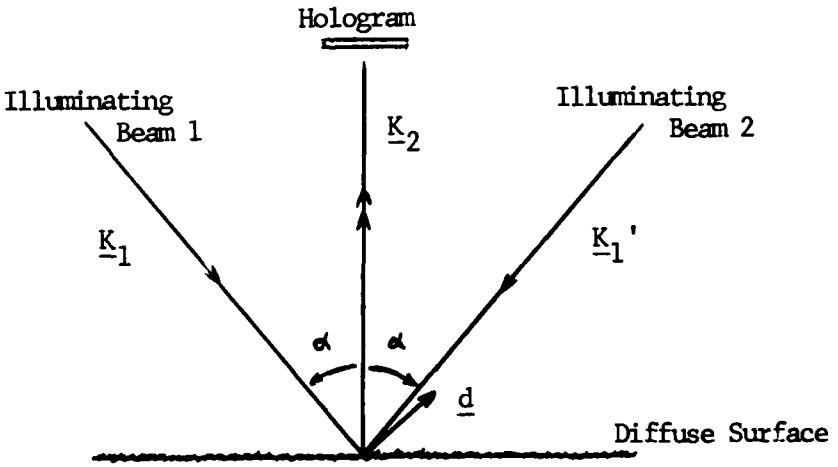

Figure A2 Double-Illumination (Single Hologram) Holographic Interferometry Configuration

past by the poor quality of the resulting moire' patterns encountered in conventional (lensless) holography. There are two improvements which have been found to lead to the generation of good moire' patterns (Ref. 78).

The first improvement is obtained through the use of focused image holography (FIH). Focused image holograms have the unique property that their reconstructions can be carried out using non-coherent light sources, either monochromatic sources (e.g., Na lamp or Hg lamp) or polychromatic sources (e.g., a continuous spectrum or white light source). Use of non-coherent or white light reconstruction eliminates the speckle "noise" characteristic of reconstructed images obtained in conventional holography employing a coherent (laser) reference beam. This makes for sharper fringe patterns with high quality fringe gradients and leads to better visibility and recording of moire' fringes when superimposing two double exposure patterns during optical processing. The reconstructions are sharp even when white light extended sources are used (Ref. 79). In the latter case, as the angle of view changes in the reconstruction, the color changes because of the dispersive nature of the hologram, however, for all colors the image is equally sharp.

Reconstruction of FIH holograms using the conjugate reference beam, rather than the direct reference beam, is an added advantage and convenience in image handling since it permits a larger field of view to be interrogated, either visually or photographically (Ref. 80). Also, use of a telecentric imaging system in FIH with unit magnification eliminates the problem of distortion considering that the lateral magnification is equal to the square of the transverse magnification. Also, the optimum recording parameters for FIH are similar to those of conventional holography, however, since the effect of recording nonlinearities is less noticeable in focused holograms, a 1:1 beam intensity ratio can be utilized which provides for maximum diffraction efficiency. This allows use of . ver power lasers in generating the holograms.

The second improvement leading to the generation of good moire' patterns during optical processing is achieved by having a high initial fringe density in the individual patterns due to each illumination beam. This is obtained by rotating the hologram (plateholder) between exposures simultaneously with the loading of the specimen. For the case of FIH and a plane object (i.e., surface), it has been shown that this rotation of the hologram through an angle about the rotation axis) creates an initial fringe pattern

precisely localized in the hologram plane and parallel to the rotation axis; the fringe spacing, δ, is given by

$$\delta = \lambda \, [\beta'(1-\cos \theta_R)]^{-1} \quad , \tag{A6}$$

where β' is the angle of rotation of the plateholder, and θ_R is the angle between the reference beam and normal to the holographic plate (Ref. 78). Alternatively and equivalently, rotation of the reference beam (i.e., the mirror-M3 in Figure A3 by an amount $\Delta\theta_R$, results in an angle $\Delta\theta$ between the two reconstructed wavefronts in double exposure holography (or between the object wavefront and the reconstructed wavefront in real time holography) given by $\Delta\theta = 2 \cos \theta_R \, \Delta\theta_R$, as shown in Reference 74.

The angular phase of the initial fringe pattern is $f(u) = n\lambda$. When the model is loaded and the plate is tilted, each illumination beam adds a different contribution to the initial phase and two patterns result which are characterized by

$$f(u) + (\underline{K}_1-\underline{K}_2) \cdot \underline{d} = n_1\lambda \text{ for object beam 1} \quad , \tag{A7}$$

and

$$f(u) + (\underline{K}_1'-\underline{K}_2) \cdot \underline{d} = n_2\lambda \text{ for object beam 2} \quad , \tag{A8}$$

where n_1 and n_2 are the fringe order numbers. The equations display additional fringes (as compared with the corresponding equations (A2) and (A3) which are now sufficient to produce diffraction during optical superposition, including spatial filtering. The moire' pattern produced by the optical subtraction of the two patterns given by Equations (A7) and (A8) can be expressed by Equation

$$[f(u)+(\underline{K}_1-\underline{K}_2) \cdot \underline{d}\,]-[\, f(u)+(\underline{K}_1'-\underline{K}_2)\cdot\underline{d}] = (n_1-n_2)\lambda \quad , \tag{A9}$$

or

$$\Delta\phi_0-\Delta\phi_0' = (\underline{K}_1-\underline{K}_1')\cdot\underline{d} = n_R\lambda = \underline{g}\cdot\underline{d} = \underline{d}' \tag{A10}$$

and is effected using the optical processor described later. The corresponding linear phase is given by $d'=n\lambda\,(2\sin\alpha)^{-1}$,

where 2α is the angle between the two illumination beams. The moire' pattern defined by above equations displays the in plane component of the displacement. For collimated illuminations, the sensitivity vector, $\underline{g}$, remains constant over the full field and the displacement is projected into a single plane. Further, the displacement $\underline{d}'$ becomes $\underline{d}_T$ which is normal to the line of sight, or "in-plane".

If achieved fringe densities are sufficiently high, it may even be possible to extract contours of constant strains directly by a moire' pattern on itself and filtering in the optical processing system as described in Reference 78.

Experimental Configuration

A combination focused image holographic interferometer and laser speckle pattern interferometer has been set up to determine whole-field in-plane displacements (and hence strains) of stressed surfaces from double-exposure image-plane holograms and/or specklegrams.

The unique, combination focused-image holographic and speckle pattern interferometer is shown schematically and photographically in Figures A3 and A4, respectively, in the telecentric lens version and was successfully used in two company-sponsored (IRAD) programs studying the general full-field strains around a radial fatigue crack in a tensile specimen of 7075-T6 Al with a notched central hole (Ref. 81), and the study of the crack closure phenomenon in the same specimen after various stages of fatigue (Ref. 82).

In Figure A3, the FIH interferometer consists of the object beams, O1 and O2, and the reference beam, R, which are combined at the photographic plate, PH, after traversing equal path lengths (within the coherence length of the laser) from the first variable beam splitter BS1 to PH. The object is a bonded joint inserted in a specially-designed precision loading apparatus described in Appendix B of Reference 83 and is identical to the one designed and built for Maddux of AFFDL (Ref. 84) for speckle photography studies.

Various adhesively bonded joints, including single lap and double lap up to 18" in length, can be accommodated by the grips of the loading device. Also, illumination and viewing in the bondline thickness-loading plane (i.e., along the edge of the joint) is easily accomplished.

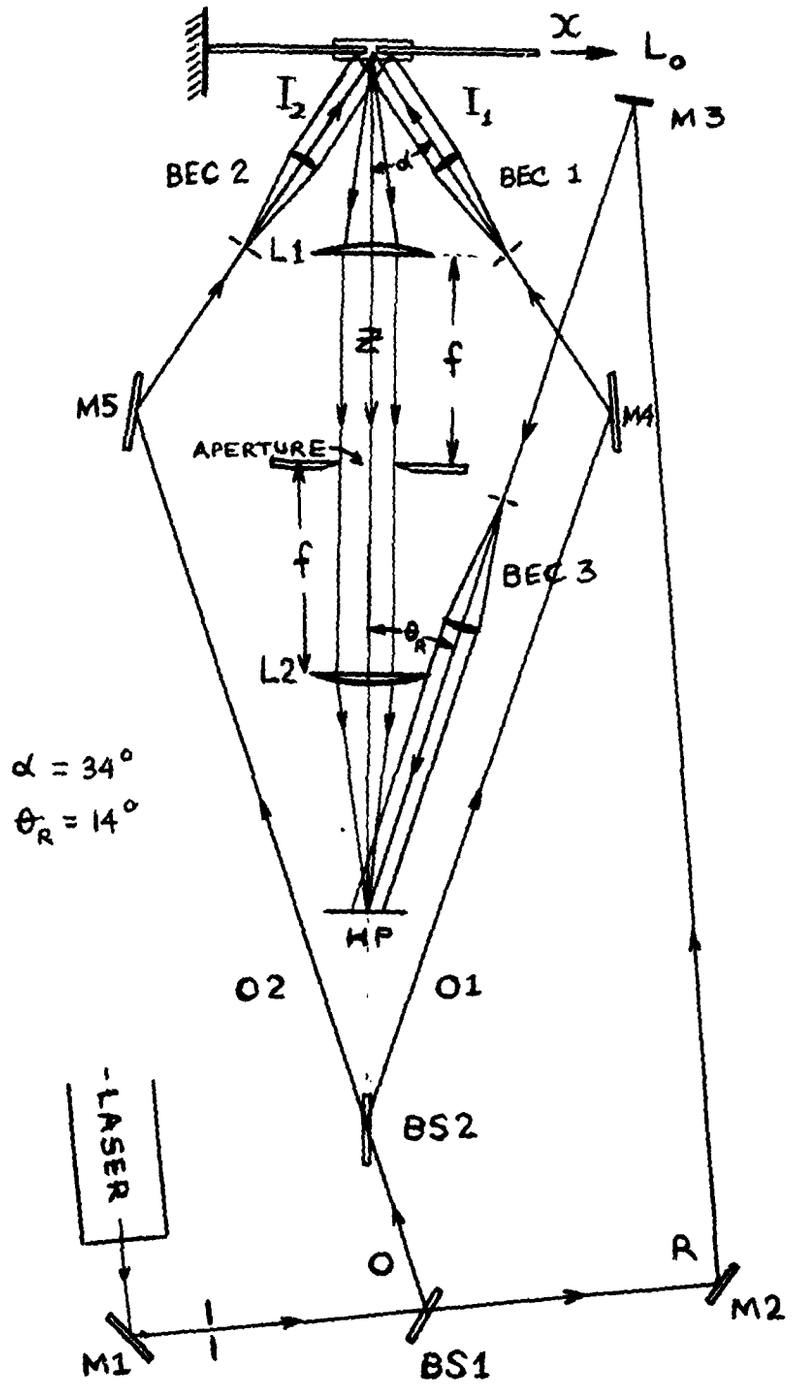

Figure A3 Focused Image Holography/Speckle Interferometer (Schematic)

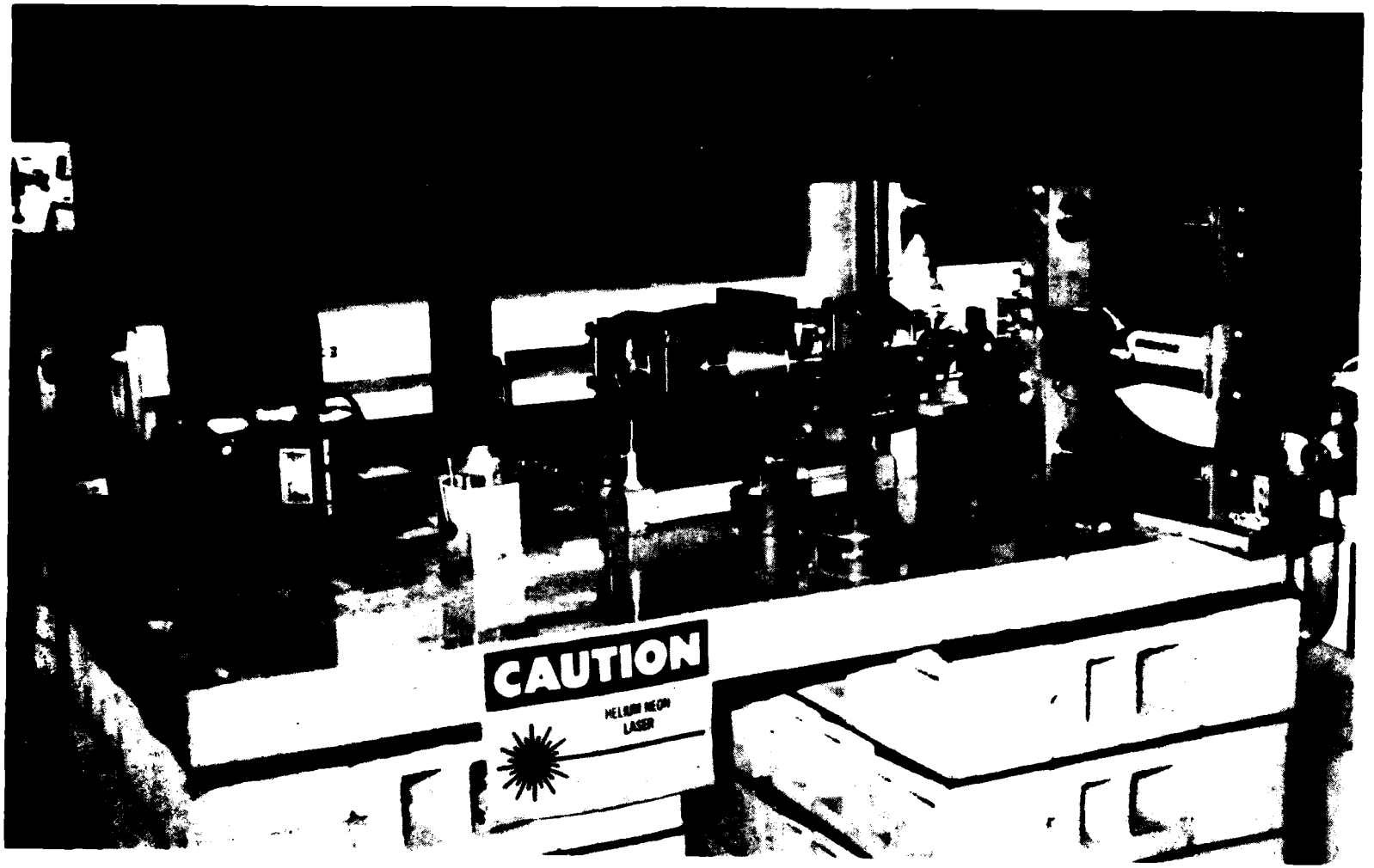

Figure A4 Focused Image Holography/Speckle Interferometer

The bonded joint geometry selected for the stress analysis validation is the double strap joint shown in Figure A5, with Al inner adherends and pyrex glass outer adherends for optical interrogation of the glass-adhesive interface upon differential loading in the loading frame mounted on the holographic table (Figure A4).

With this optical arrangement it is possible to record a double-exposure image-plane hologram which is also a specklegram by suitable choice of reference to object beam intensity ratio utilizing beam splitters BS1 and BS2. Use of a collimated reference beam ensures ease of reconstruction with a (collimated) white light source in the conjugate direction; and use of the telecentric lens system permits <u>in situ</u> white light reconstruction of the double exposure hologram, with the reconstructed image displaying the displacement interference fringes as a real image at the equivalent image plane position, I_2, displayed in Figure A6.

A unit magnification telecentric imaging system (Refs. 85,86) is used consisting of two plano-convex lenses placed two focal lengths apart. An aperture is centrally placed between the two lenses, L1 and L2. This arrangement provides a number of favorable conditions during recording of holograms. First, the image I_2 of object O_1 does not change with small variations in the object distance and for a given object size, the image size ($I_2 = -O_1$) remains constant for all values of a_1 within the depth of field of the telecentric system. The aperture is also used to control the depth of field for sharpest fringe recording. Second, $a_2 = -a_1$, so that the image I_2 is displaced by the same amount as the displacement of the object from its position at the front focal plane of lens L1 and is displaced in the same direction, relative to the lens system, provided the object O_1 is inside the focal plane of L1. If the object O_1 is outside the focal plane of L1 no real image I_2 will be formed.

Finally, the same telecentric system can be used for optical processing without disturbing optical components. This is done by placing the negative in the equivalent object position of the FIH set up at O_1, illuminating it normally with a collimated laser beam, removing the zeroth order beam with an aperture stop at the Fourier transform plane (midway between L1 and L2) and finally allowing only the +1 order to be passed by lens L2 onto the image recording plate at HP.

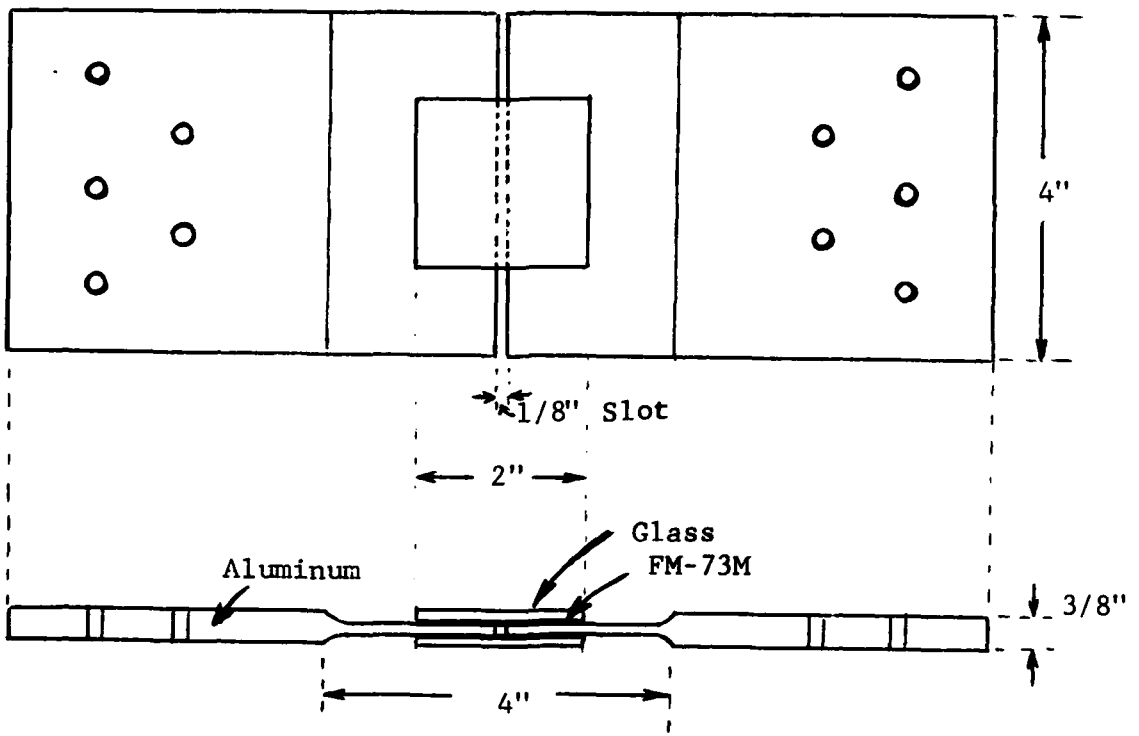

Figure A5 Double-Strap Adhesively Bonded Joint with Glass Outer Adherends

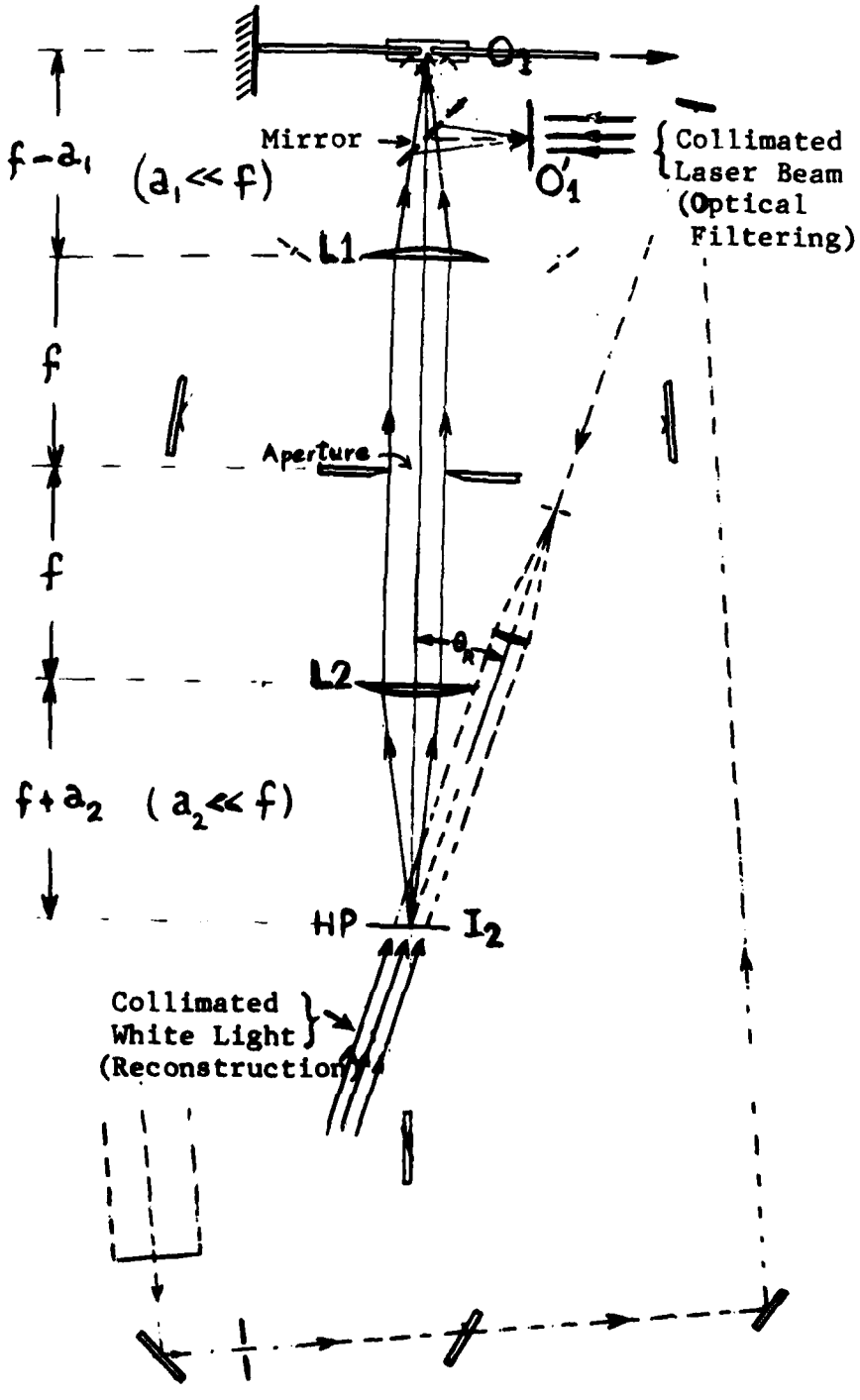

Figure A6 Telecentric Lens System for Focused Image Holography and Optical Filtering

As pointed out in the previous section, rotation of the hologram (plateholder) around an axis contained in its own plane through an angle (β) or equivalently rotation of the collimated reference beam through an angle ($\Delta\theta_R$), generates "carrier" fringes for each of the two illumination beams which greatly increase the visibility and detectivity of the moire' fringes during optical filtering of the double exposure hologram.

Preliminary Results

A number of double exposure holograms of the double strap tensile specimen have been obtained with differential loading and plateholder rotation between exposures, as shown, for example, in Figures A7(a) and A7(b). The latter double exposure was effected with a loading differential of 100 lbs. and a plate (holder) rotation of 2/3° and registers the displacement field superimposed on the "fictitious" fringe system due to the plate rotation. The measured carrier fringe spacing of 1 mm is in agreement with the predicted fringe spacing, however, the fringe density is still not high enough to give good diffraction during optical filtering to display the moire' fringes.

According to Exner and Gilbert (Ref. 87) the desired fringe density in the white light reconstructed real image (plane) should be of the order of 100 lines per inch to achieve good diffraction during optical filtering. This can be achieved by the appropriate selection of both differential loading, ΔL, and holographic plate rotation, β', values. However, achieving the correct ΔL and β' values simultaneously, while trying to maintain fringe localization in the image plane is extremely difficult using the double exposure (dead fringe) technique.

Holographic-Moire' in Real Time

Prof. Sciammarella et al. have very recently solved this problem by using the holographic moire' technique in <u>real time</u> combined with closed circuit TV (Ref. 74). This permits adjusting the aforementioned mutually dependent parameters incrementally while viewing their effects separately and in combination directly on a TV screen at optimum fringe density.

Another important consideration in achieving good moire' fringes is that of contrast, as discussed by Sciammarella et al. The in-plane (x) displacements are given by a moire'

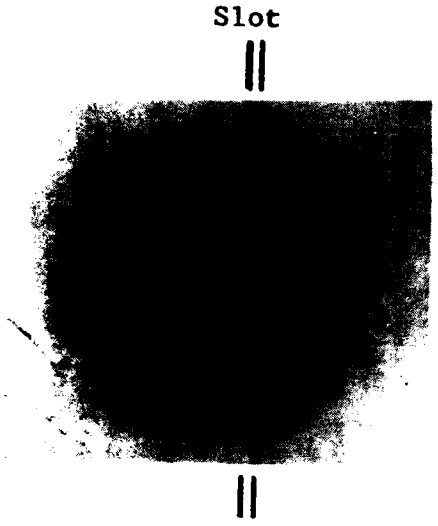

(a) ΔL = 160 lbs.
No Plate Tilt

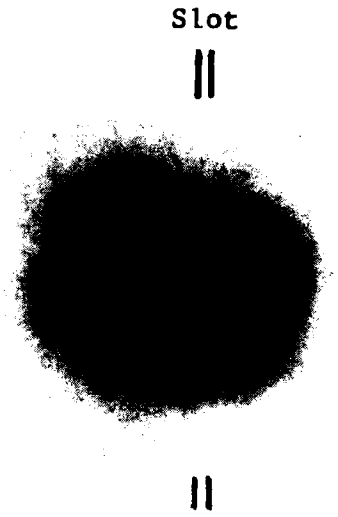

(b) ΔL = 100 lbs.
Plate Tilt = $2/3^{o}$

Figure A7 Double-Exposure Focused-Image Holograms of FM-73M Adhesive of Bonded Joint with Glass Outer Adherends.

pattern that modulates a high frequency signal which depends on displacements perpendicular to the observed plane. The moire' pattern is best observed if the two systems of fringes have an acceptable contrast in the plane of observation and have enough density or form an angle within +30°; this can be facilitated using the real time technique.

As pointed out by Sciammarella, the control of fringe contrast and density is best achieved, i.e., is greatly facilitated, by using the real time technique, instead of the dead fringe (double exposure) method. Recalling also the fact that small leaks in the hydraulic system of our loading device tend to cause fringe wandering, the use of real time observation will greatly facilitate the control of this undesirable feature when recording the desired moire' fringes. Accordingly, a GE closed-circuit TV Model 4T H31 B1, in conjunction with a Panasonic TV camera Model WV-1000 is being set up in the supporting program ④ on Viscoelastic Stress Analysis to conduct holographic-moire' in real time.

The basic arrangement to be used in the holographic moire' in real time will include the experimental arrangement of Figure A3 with the TV camera's axis collinear with that of the telecentric lens system. The camera lens is focussed on the holographic plate which is immersed in an immersion tank mounted on a universal stage. The sequence of events when loading, will be viewed directly on the TV monitor and the evolution of the fringes will be simultaneously recorded on a video tape.

A single exposure will be made of the object in state of rest. The plate will then be either removed from the tank, processed and returned to its original position, or it will be developed in-situ. The controls of the universal stage will make it feasible to eliminate any residual fringes. The carrier fringes will be generated by either rotating the plate holder around an axis contained in its own plane or by rotating the collimated reference beam. The model will be loaded and the rigid-body motions compensated by observing the fringes in the monitor while keeping the visibility as high as possible.

The fringes will be recorded on tape and/or photographed directly from the monitor. For greater accuracy they can be photographed by introducing a beam splitter at 45° to the optic axis of the observation system. When the fringes are photographed, contrast can be improved by optically filtering the carrier as described earlier. The contrast of

the fringes can be directly balanced on the monitor by electronically filtering and by changing the contrast knob.

All that remains in the life prediction series of programs in the area of stress analysis validation is to extend the work of Sciammarella et al. (Ref. 74) in which relatively simple, symmetric "thesis geometries" were used, to apply to our more complex (joint) geometries. This is currently being done in the companion program ④ on Viscoelastic Stress Analysis (Ref. 21) wherein the VISTA finite element stress analyses code will be validated.

It appears also that an extension of this technique, using multiplication of holographic fringes (Ref. 78), will allow smaller regions of surfaces to be interrogated, including strain fields around crack tips and regions of dimensions of the order of the bondline thickness. This is possible because the fringe multiplication technique, in conjunction with the use of image magnifications $\gg 1$, by means of a suitable lens arrangement, will allow moire' displacement patterns to be multiplied at least 10-fold to obtain high fringe density. When this multiplied moire' pattern is shifted on itself, the moire' of moire' so obtained can be filtered in the optical processing (filtering) system to yield a filtered pattern directly representing the loci of constant strain with high sensitivity.

APPENDIX B

Measurement of Crack Initiation and Crack Growth in Cracked Lap Shear Specimens

Appropriate techniques for measuring crack size, a, with time, t, and/or cycle, N, for each specimen geometry were evaluated. These include X-radiography with opaque additive, ultrasonic spectroscopy, acoustic emission (for onset of crack growth or initiation) , optical (visual) with 10X optics and graduated scale, and normal compliance methods. The following summarizes the experiences encountered in each of the above-stated techniques and a rationale for the selection of the technique finally chosen.

X-Radiography With Opaque Additive

Successful application of X-ray technique for monitoring crack growth is contingent upon different X-ray absorption coefficients of the materials of interest and the void. The X-ray attenuation coefficient of FM-73 is not much higher than voids. This small difference in attenuation makes it difficult to identify voids on X-ray records.

A modified X-ray NDE technique which enhances a void's image on the X-ray record has been used at General Dynamics for crack growth monitoring in composite specimens. The opaque additive, diiodobutane (DIB), is introduced to the crack openings. The DIB enters the crack by capillary action. On the X-ray records, the image of the crack is greatly enhanced by the highly attenuating characteristics of the opaque additive.

The radiographic energy source used in this study was a 110-kv Picker portable X-ray unit with a 2.25mm beryllium window and a focal spot of 0.5mm. The X-ray head was located at a distance of 30 inches from the specimen.

X-ray records of a model test joint specimen undergoing cyclic test was made without dismounting the specimen from the fatigue test machine. Visual (20X optics) observations were made of crack growth for comparison with the X-ray negatives.

While the X-ray negatives provided a record of crack growth, their use in crack initiation detection studies were

unsatisfactory. In the vicinity of crack initiation the geometry of the specimens introduced darkened and lightened areas on the negatives which made evaluation difficult. The X-ray technique is inferior to visual observations in the area of crack initiation.

Another area of concern is that opaque additives might contribute to the degradation of the material properties of the bonding material. From visual observations (30X optics) of the failed surfaces, changes in the failure mode were noted when compared with failed specimens with no opaque additive used. As a result of the poor comparison between visual observations and X-ray negatives, this probable altering of material properties was not studied further.

Ultrasonic Spectroscopy

During initial cyclic testing of a notched crack lap shear specimen, ultrasonic spectroscopy was evaluated. Parallel to this ultrasonic evaluation, visual (20X optics) changes in crack length were recorded.

A one-fourth inch Aerotech 25 megahertz transducer and a Sonic Mark IV ultrasonic tester were used with the technique shown in Figure B1. The 25 megahertz signal is introduced normal to the bondline and the presence or absence of the signal reflected from the back surface indicates a bonded or debonded area. Again, visual observations (10X optics) were made and the two methods were compared as to their usefulness as a means of monitoring crack growth.

The comparison between visual and ultrasonic measurements of crack growth were in agreement to within an accuracy of $\pm$ .05 inch.

Acoustic Emission Monitoring (AEM)

Acoustic emissions are pockets of stress waves generated when the materials are undergoing transformations or fracture. AEM technique is increasingly being recognized as an NDE tool.

The primary advantage of AEM is that it can be used to continually monitor damage. The primary disadvantage is it is a measurement of energy released by damage development and cannot be directly associated to material damage state.

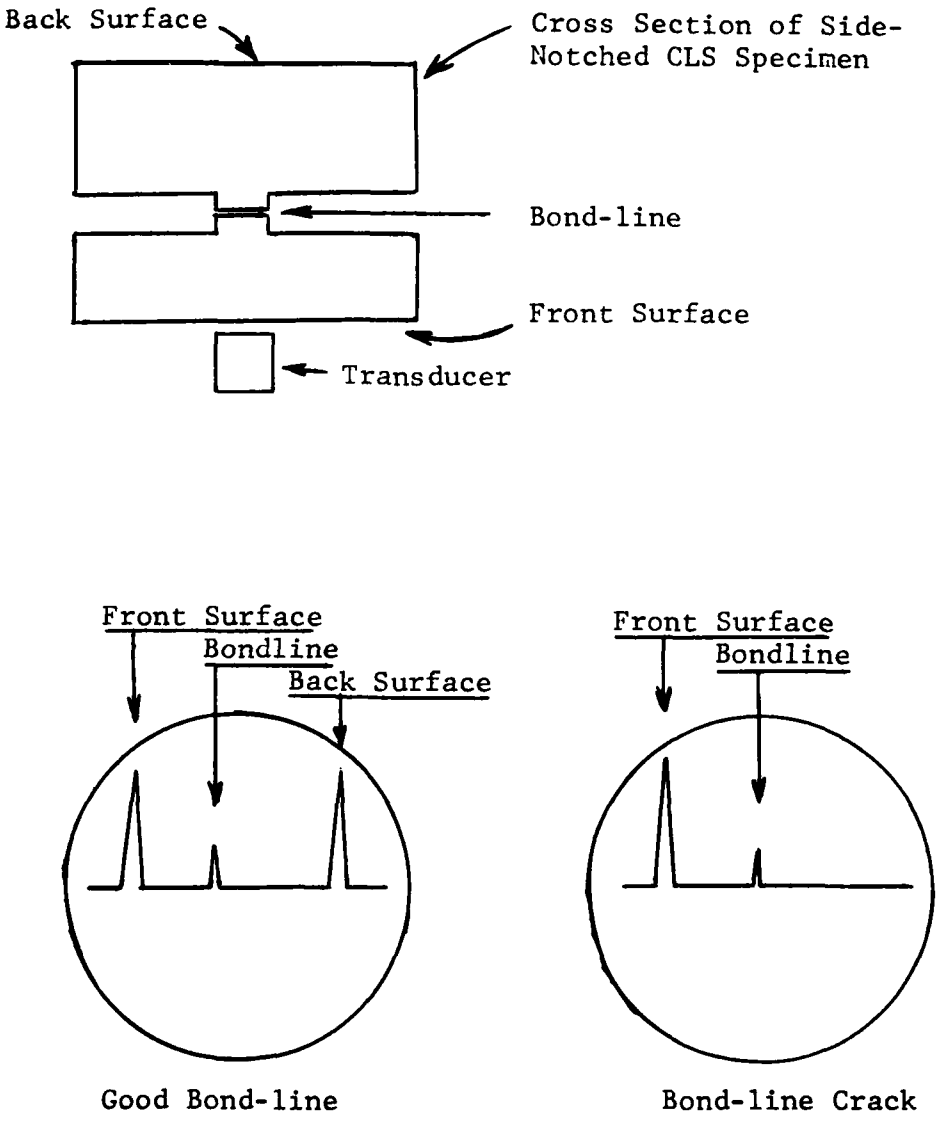

Figure B1 Monitoring Crack Growth in CLS Specimen Using Ultrasonics

A block diagram of AEM instrumentation is shown in Figure B2. Frequencies of acoustic emissions range from audible cracklings to the megahertz region. Signal levels require amplification factors from 1 x 10^3 to 1 x 10^7 depending on the sensitivity desired. AEM differs from other methods in that it is a passive monitoring method and depends entirely on the generation of stress waves within the specimen to provide the excitation function. It provides a means to continuously track the flaw growth and stress redistribution during tests to correlate the damage growth observed by the X-ray technique.

While AEM shows promise for characterizing bonded joint failure, technically, additional work is needed before it becomes a laboratory tool.

Compliance Measurements

A Hewlett Packard X-Y recorder was used with an induction gage to obtain specimen compliance measurements. Results of test and comparison with visual and ultrasonic measurement methods are discussed in Section 2.2.3.7 of Reference 62.

Procedures to Monitor Crack Growth

The results of the above evaluations indicate that a combination of induction gage and ultrasonics technologies can be used to define the crack length. The induction gage can be automated as only readying at minimum and maximum load are required to define the length of the crack. Periodic checking of the crack length with ultrasonics provides a verification of results from induction gage measurements.

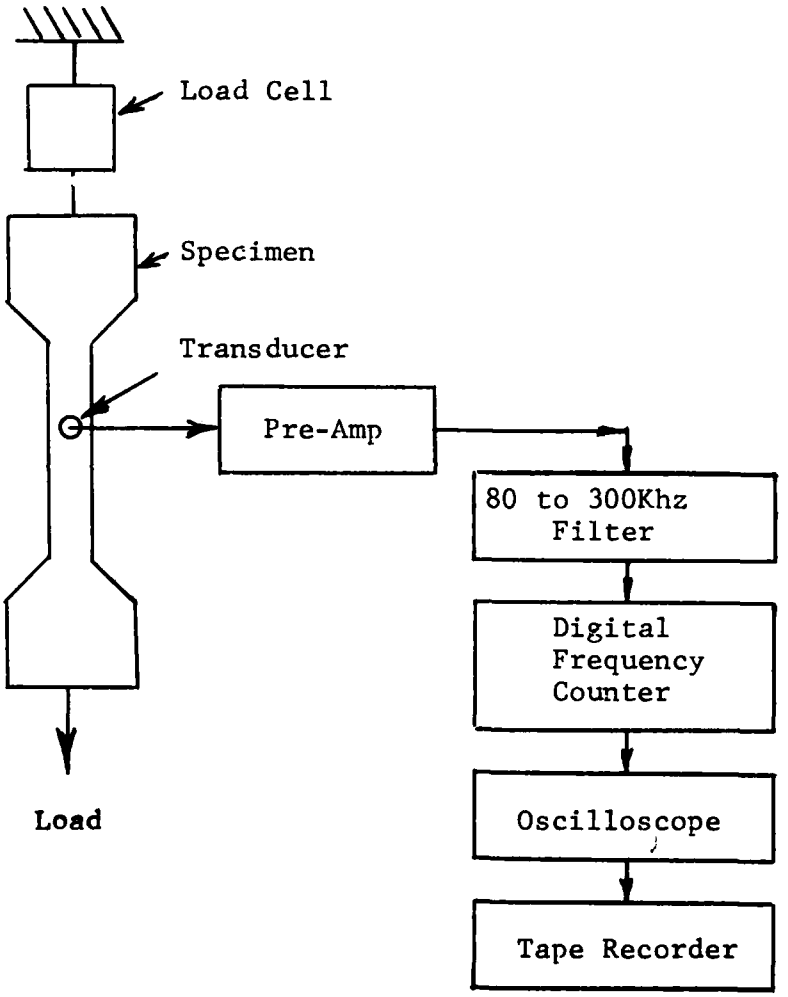

Figure B2 Acoustic Emission Measurement System

APPENDIX C

Fatigue Testing of Bonded/Bolted Structural Lap Joints

Six SLJ specimens with bolt assist were fatigue tested to determine the effects of the fasteners on crack propagation and on fatigue life. For these tests, only the thick adherends (0.375 in.) were used. The two different fastener geometries used are shown in Figures C1 and C2, respectively. For fastener hole patterns #1 and #2, NAS-1154-14 fasteners were used, consisting of 0.250" diameter, 100° countersink, flush head steel fasteners, heat treated to the 160-180 Ksi strength level. A third type of specimen with the fastener hole pattern #2, but without the adhesive interlayer, served as the "control". In order to have adequate shear strength in the fasteners for this bolted only design, it was necessary to use NAS1581-A6-16 fasteners. These are 0.375-inch diameter, 100° countersink, flush head steel fasteners, heat treated to the 160-180 Ksi strength level. All specimens containing fasteners were tested at maximum load levels of 20,000 and 25,000 pounds only. For both fastener hole pattern specimens, the ultrasonic technique of monitoring the crack front was used. Table C1 summarizes the test results. Figure C3 shows typical failure patterns in the SLJ bonded/bolted specimens and the change in the crack growth in the adhesive bond introduced by the bolts.

All normal SLJ bonded specimens tested without fasteners failed by fatigue propagation in the adhesive interlayer, as described earlier. All the bonded/bolted specimens finally failed through the load transfer member, (i.e., at the bolt). It appeared that once the fatigue crack in the adhesive interlayer reached and/or passed the fastener, fatigue cracks initiated and propagated from the fastener hole and failure occurred through the load transfer member. On the two specimens tested without the adhesive interlayer, failure occurred shortly after a fatigue crack started propagating from one of the holes in the fastener pattern. As on Specimen number 16, the first failure occurred by fatigue when a small section about one inch long broke out at the lower fastener hole in the load transfer member. Within 60 cycles, both fasteners at the center of the specimen failed by bearing in the aluminum load introduction member.

Table C2 summarizes the fatigue life of the bonded only and bonded/bolted SLJ specimens. Note that with only a few fasteners, the lifetime of the SLJ bonded joint is increased

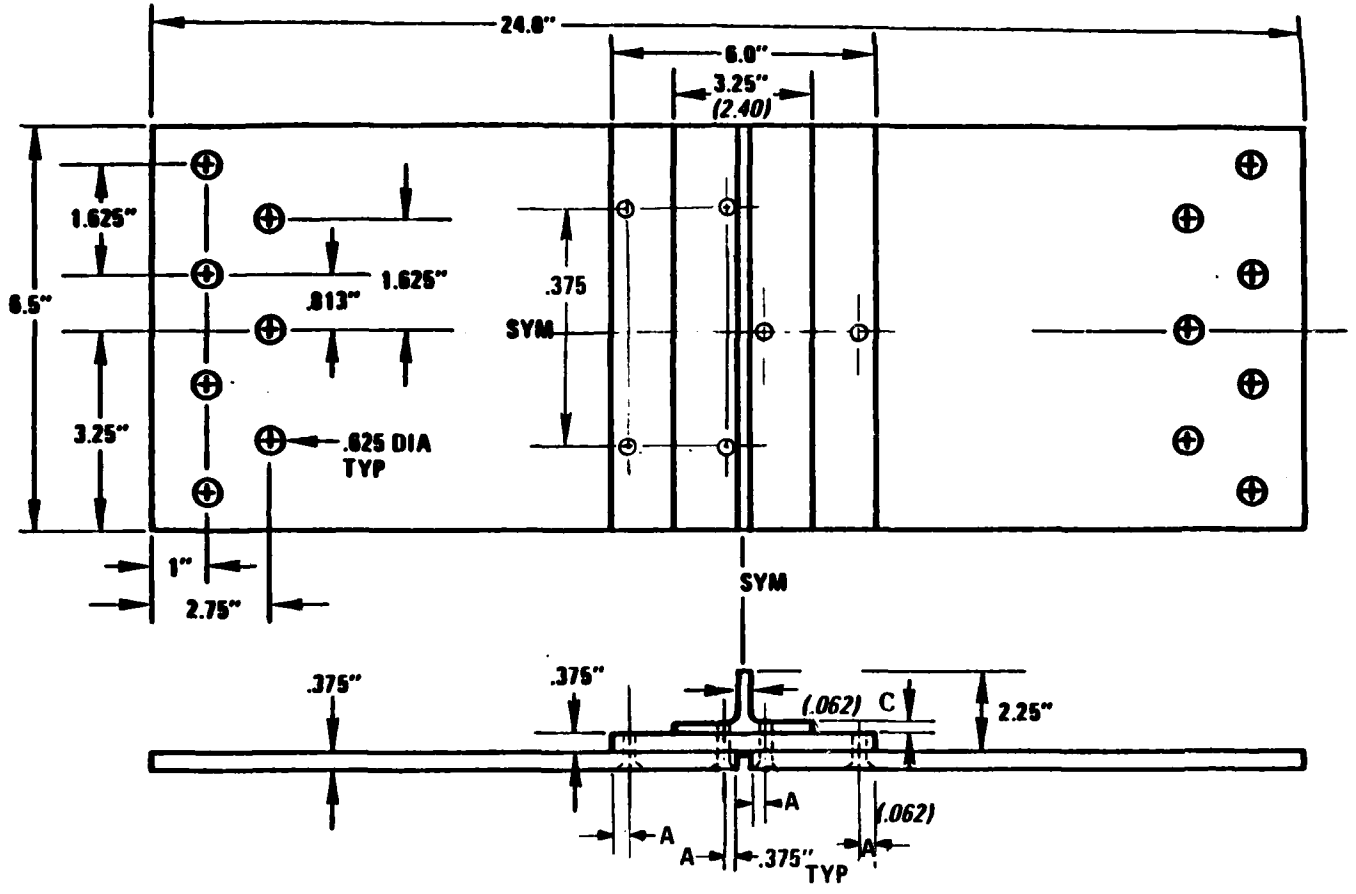

Figure C1 Fastener Hole Pattern #1 For Thick Adherend SLJ.

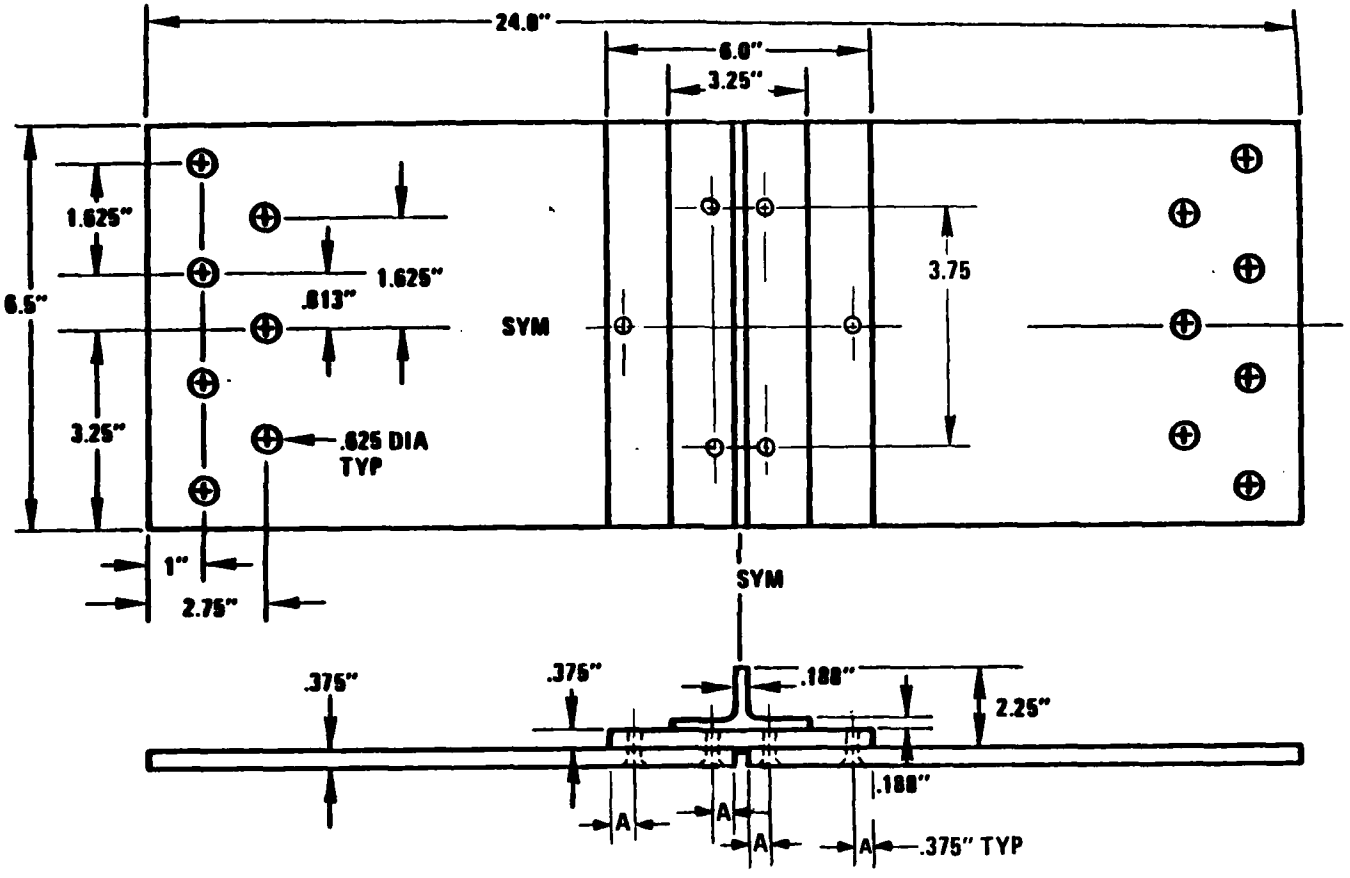

Figure C2 Fastener Hole Pattern #2 For Thick Adherend SLJ.

Table C1 Test Results For SLJ Bonded/Bolted Joints

SPECIMEN NC.	MAX TEST STRESS KSI	ADHEREND THICKNESS	FASTENER HOLE PATTERN	CYCLES TO FAILURE
11	20	.375"	#1	30,199 M
12	25	.375"	#1	10,752 M
14	20	.375"	#2	30,572 M
15	25	.375"	#2	14,831 M
16*	20	.375"	#3	15,849 M
17*	25	.375"	#3	5,581 M

Notes:

M = Failure Through Metal

Fastener hole patterns #1 and #2 - NAS 1154-14 fasteners

Fastener hole pattern #3 - NAS 1581-A6-16 fasteners

* = Bolted Only

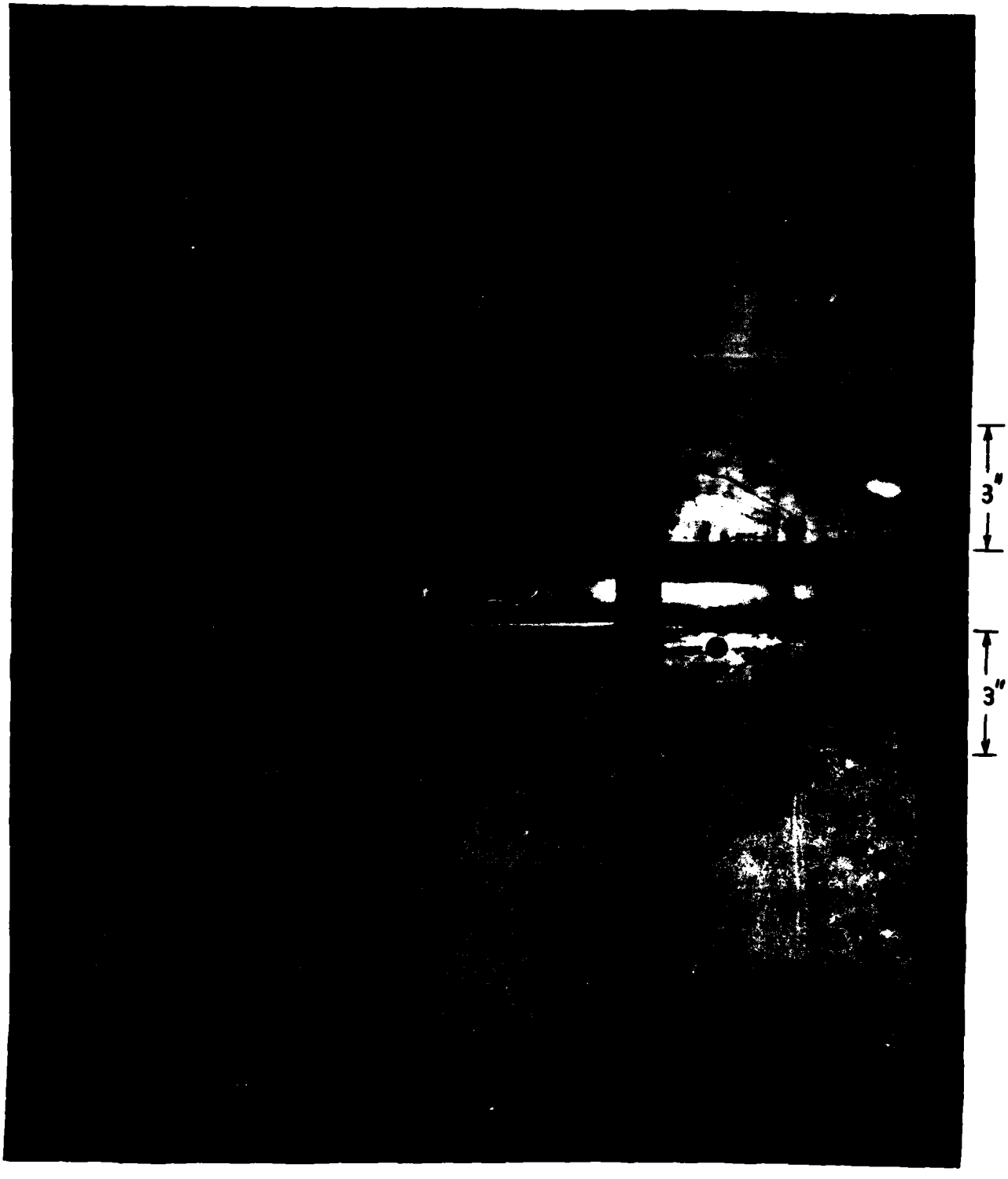

Figure C3 Failed Thick Adherend, Bonded/Bolted SLJ With Measured Crack Fronts.

by at least a factor of two. This increase in lifetime can probably be attributed to containment of the high peel stresses along the overlap end by the fasteners.

Table C2 Comparison Of Cycles-To-Failure Data For Bonded Only And Bonded/Bolted SLJ's

MAXIMUM LOAD, LBS	1/8 IN. ADHEREND	3/8 IN. ADHEREND		
	BONDED ONLY		BONDED/BOLTED	
			PATTERN #1	PATTERN #2
	NO. OF CYCLES AT FAILURE			
15K	203,786*	377,579		
20K	36,479	14,258	30,199	30,572
25K	7,957	1,744	10,752	14,831

* Failure In Metal Plate

APPENDIX D

LOCUS OF FAILURE IN FM-73U MODEL JOINT

It was observed in the Fatique Behavior program (Ref. 19) that failed surfaces of FM-73M (matte Dacron scrimmed) model joints, both dry and those conditioned for approximately 9 months at 140°F and condensing humidity, showed two quite similar general features of failure, but with some important differences.

One general feature consists of an apparent primarily adhesive failure zone (interface debond) emanating from the (calculated) high-stress region of the overlap, the so-called load-transfer edge. This "adhesively failed" region is variously referred to as the "slow-crack-growth" region or the "fatigue-failed" zone and constitutes the fingernail feature described by Marceau et al. (Ref. 88). These symmetric slow-failed regions are labelled A and A', respectively, in Figure D1 .

The second general feature of the failed joint surfaces consists of the primarily cohesive failure zone between the aforementioned two symmetric slow-failed regions. This "cohesively failed" zone is also referred to as the "fast crack" zone or the "statically failed" region and generally occurs along the scrim plane parallel to and midway between the two adherend adhesive interface planes, labelled C and C' in Figure D1.

These two distinct features of the failed surfaces are much more pronounced in the dry joint. In the wet joints, the "slow growth" zone, although still recognizable, is smaller in extent, and generally appears interspersed with small cohesive failure nodules.

The second main feature of the wet failed joint surface, viz., the fast growth cohesive zone, extends over a correspondingly larger area of the overlap than for the dry joint. Some small adhesive failure regions are found to dot the primarily cohesive failure region. This same topography is evident in the dry joints fatigued at low frequency (0-17 Hz) and at high temperature (140°F).

Optical study of the fracture surfaces reveals that, as the stress is reduced, the size of the adhesive interface delamination region increases. Correspondingly, the number

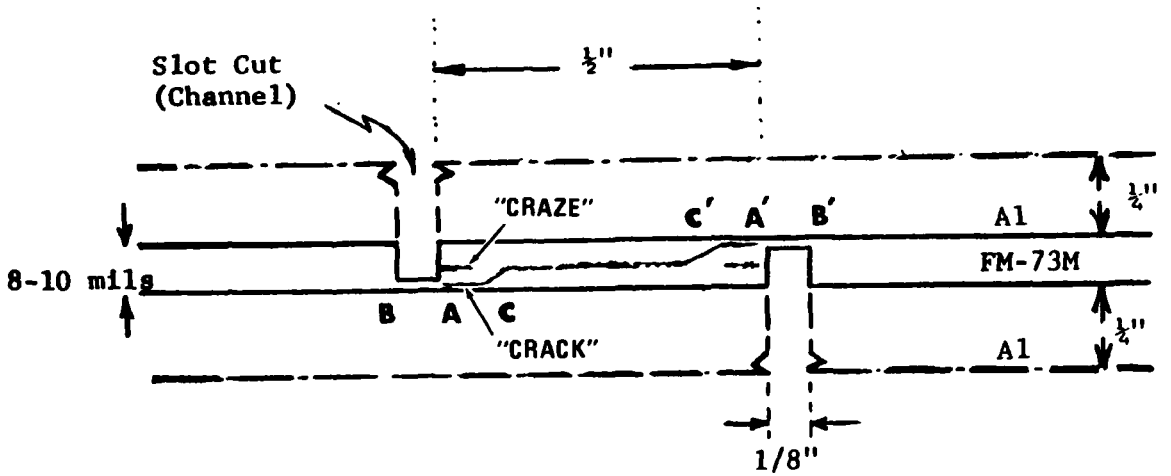

Figure D1 Crack and Craze Loci in FM-73M
Model Joint Interlayer

of cycles to failure increases with decreasing load, as expected.

The above-described dependence on cyclic frequency of the slow and fast crack growth regions in model joints with scrimmed adhesives has also been observed by Marceau et al. (Ref. 88). They observed both features in the fast cycle (30 Hz) specimens, but saw no evidence of the zone of slow crack propagation for the slow cycle (1 cycle per hour) specimens and the sustained load specimens. This observation indicates again that the time at load is an important factor in the joint failure process.

In the current Integrated Methodology program, it was desirable to determine the precise role of the scrim material in the locus of failure of the model joint, and in bonded joints of general geometry so as to be able to prescribe failure criteria for the different cases. Accordingly, model joints with unscrimmed adhesive were fabricated as follows.

Failed model joints obtained from the Fatigue Behavior program were prepared by removing the old adhesive from the adherends using nitric acid. The bare adherends were then anodized (BAC5555) and primed (BR127A). The two layers of FM-73U were placed on the bonding area of one adherend and then brought to 121°C and outgassed in a vacuum oven. The second adherend was then placed in contact with the adhesive, the assembled joint held in an alignment jig and the whole assembly placed in a press at 121°C for one hour.

Three such joints were tested at 1 Hz, and a maximum load of 8.89 kN (2000 lbs) with an R factor R=0.1. Final failure occurred in the aluminum adherends after an average of 100,000 cycles. Figure D2(a) shows a schematic of the crack growth sequence in two of the joints which contained considerable spew. In these joints, a crack initiated at the 90° corner of the top adherend. It then grew down towards the bottom adherend as well as up towards the free surface of the spew. Once the spew crack growth reached the bottom adherend, it grew as an interfacial debond for about 0.254mm (0.010 in.) before branching into the bottom adherend for a period of slow fatigue crack growth which was terminated by a fast ductile failure. Figure D2(b) shows a photograph of crack growth initiating at the free surface of the spew which was not as extensive in the third joint.

The model joints which were made of FM-73M and tested under similar conditions in the Fatigue Behavior program (Ref. 19) had fatigue lifetimes which never exceeded 30,000

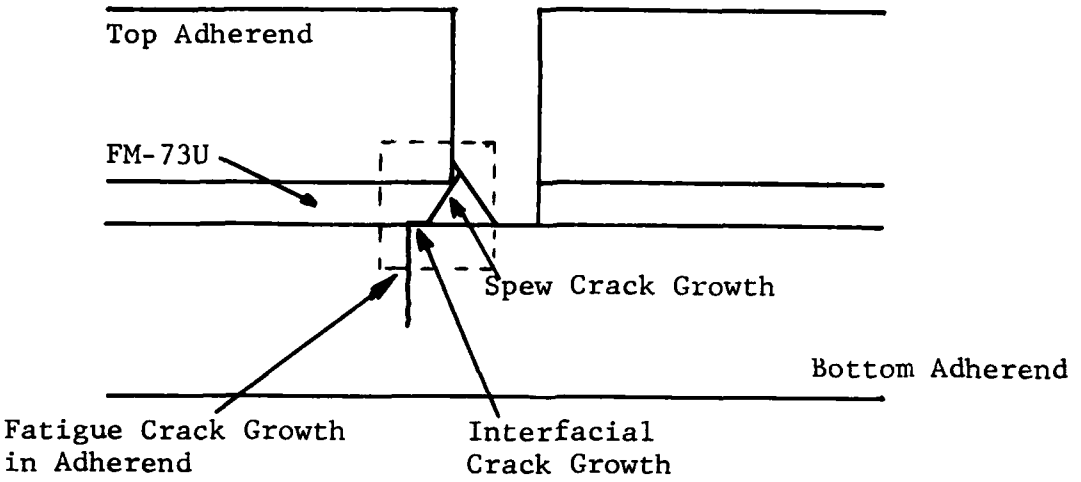

(a) Schematic

(b) Photograph, 40X

Figure D2 Crack Growth Sequence in Model Joint with FM-73U Adhesive

cycles. The scrim material clearly reduces the fatigue strength of the adhesive by providing sources of microcracking at the matrix/scrim interface. In proposing the fatigue testing of joints made of FM-73U, it was thought that the extent of slow interfacial debonding prior to catastrophic failure would be increased because the cohesive fracture energy of the adhesive would be increased. The fact that the interfacial debond was much shorter in the unscrimmed joints and also that it branched into the adherend indicates that, not only does the scrim decrease the cohesive fracture energy but also that it decreases the adhesive fracture energy.

In conclusion, an examination of the shear stresses in the scrim plane has indicated that long interfacial debonds will result in scrim plane shear stresses that are greater than the shear strength of the adhesive. Furthermore, it has been determined that the scrim fibers reduce the fatigue strength of the adhesive. The predictive model for damage growth in a model joint therefore consists of a period of slow interfacial debond growth governed by the variation of J-integral with debond length and the adhesive fracture properties of the FM-73M until the shear strength of the adhesive in the scrim plane is exceeded.

APPENDIX E

PUBLICATIONS

The following presentations, technical reports, and publications cover work carried out under this contract. They were either prepared or appeared publicly during the reporting period:

Romanko, John, "Surface Analysis of Aircraft Adhesive Materials," 4th Southwest Electron Spectroscopy Users' Conference, Rice University, Houston, TX, June 6, 1980.

Romanko, John and Jones, W. B., Jr., "Fatigue Mechanisms in Adhesively bonded Joints," International Conference on Adhesion and Adhesives, Durham, England, Sept. 3-5, 1980. Also Intnl. Conf. Adhesion and Adhesives: Service Technology and Applications, The Plastics and Rubber Institute, Publ., pps. 11.1-11.7, 1980.

Romanko, John, "XPS (ESCA) Studies of Surfaces of Adhesively Bonded Joints," Physics Colloquium, University of Texas, Arlington, TX, October 8, 1980.

Romanko, John, "Applications of Lasers and Holographic and Speckle Interferometry in the Aircraft Industry," Optical Society of America, Texas Section, Dallas, TX, November 12, 1980.

Romanko, John, "Integration/Test Plan for Adhesive Bonded Joint Life Predictions," and Liechti, K. M., "Viscoelastic Stress Analysis," both at Coord. Mtg. on Service Life Prediction on Adhesively Bonded Joints, Austin, TX, Dec. 18, 19, 1980.

Romanko, John, "Surface Analysis of Adhesively Bonded Joints," 5th Southwest Electron Spectroscopy Users' Conference, Univ. of Texas, Austin, TX, 5 June 1981.

Romanko, John, "Stress Analysis Validation," and Liechti, K. M., "Viscoelastic Stress Analysis," both at Coord. Mtg. on Service Predictions for Adhesively Bonded Joints, Fort Worth, TX, July 22,23 1981.

Romanko, John and Knauss, W. G., "Fatigue Mechanisms in Adhesive Joints," Chapter 5, Developments in Adhesives - 2, edited by A. J. Kinloch, Applied Science Publ., pps. 173-205, 1981.

Liechti, K. M., and Knauss, W. G., "The Use of Crack Profile Measurements to Determine Mode Interactions of Propagating Cracks at Material Interfaces," ASME Winter Annual Meeting, Washington, D.C., Nov. 15-20, 1981; also in 1981 - Advances in Aerospace Structures and Materials, ASME Publication AD-01, pps. 51-60, 1981.

Jones, Jr., W. B., and Romanko, J., "Fatigue Behavior of Adhesively Bonded Joints," American Society of Mechanical Engineers ASME Annual Fall Meeting, Washington, D.C., Nov. 15-20, 1981; Also in: 1981 Advances in Aerospace Structures and Materials, ASME Publication AD-01, pps. 61-65, 1981.

Romanko, John, "Fatigue Behavior Program Results," and "Integrated Methodology for Adhesive Bonded Joint Life Predictions," Liechti, K. M., "Viscoelastic Stress Analysis," both at Coord. Mtg. on Service Life Predictions for Adhesively Bonded Joints, United Technologies, Chemical Systems Division, Dec. 21-22, 1981.

Romanko, John, "Fatigue Behavior and Life Predictions of Bonded Joints," American Institute for Aeronautics and Astronautics, North Texas Section, Univ. Texas (Arlington), Feb. 20, 1982.

Romanko, John, "Methodology for Life Predictions of Bonded Joints," ASTM E24.04.09 Task Group on Crack Growth in Adhesive Joints, Meeting at ASTM Headquarters, Philadelphia, PA, Apr. 27, 1982.

Jones, Jr., W. B., "A Systems Approach to Adhesively Bonded Structural Joints;" Romanko, John, Liechti, K. M., and Knauss, W. G., "Life Prediction Methodology for Adhesively Bonded Joints;" Knauss, W. G., and Liechti, K. M., "Interfacial Crack Growth and its Relation to Crack Front Profiles;" All 3 papers at ACS/International Symposium on Adhesive Joints: Their Formation, Characteristics and Testing, Kansas City, MO, Sept. 12-17, 1982.

Liechti, K. M., "Viscoelastic Stress Analysis Including Moisture Diffusion for Adhesively Bonded Joints;" Knauss, W. G., "Non-Linear Mechanics and the Fracture of Adhesive Joints;" Romanko, John, "Integrated Methodology for Adhesive Bonded Joint Life Predictions;" All three papers at Second NASA/DOD Workshop on Adhesives and Adhesion, Hyannis, MA, Oct. 20-21, 1982.

REFERENCES

1. Contract F33615-75-C-5178, "Laminated Wing Structures," sponsored by USAF AFML/FIBC, Wright-Patterson AFB, OH 45433, and conducted by General Dynamics, Fort Worth Division, "Fort Worth, TX, June 1975-June 1980.

2. Contract F33615-76-C-3138, "Advanced Technology Wing Structure," sponsored by USAF AFML/FIBC Wright-Patterson AFB, OH 45433, and conducted by Vought Corporation, Dallas, TX, November 1976 - March 1980.

3. Contract F33615-76-C-5205, "Structural Properties of Adhesives," sponsored by USAF AFML/MBC Wright-Patterson AFB, OH 45433, and conducted by Vought Corporation, Advanced Technology Center, Inc., Dallas, Texas, May 1976 - May 1978.

4. Contract F33615-76-C-5220, "Fatigue Behavior of Adhesively Bonded Joints," sponsored by USAF AFML/MBC Wright-Patterson AFB, Ohio 45433, and conducted by General Dynamics, Fort Worth Division, Fort Worth, Texas, July 1976 - March 1980.

5. Contract F33615-75-C-5224, "Fracture Mechanics for Structural Adhesive Bonds," sponsored by USAF AFML/MBC Wright-Patterson AFB, OH 45433, and conducted by Lockheed Corp., Burbank, CA, 1 July 1977 - 30 June 1978.

6. Goland, M., and Reissner, E., "The Stresses in Cemented Joints," J. Appl. Mech. 11, 1944, A17-A27.

7. Hart-Smith, L. J., Adhesive-Bonded Single-Lap Joints, NASA, CR-11236, January 1973.

8. Contract F33615-75-C-3016, "Primary Adhesively Bonded Structure Technology (PABST)", sponsored by USAF AFFDL/Wright-Patterson AFB, Ohio 45433, and conducted by Douglas Aircraft Co., McDonnell Douglas Corp., Long Beach, California, March 1975 - December 1978.

9. Schliekelmann, Rob. J., "Operational Experience with Adhesive bonded Structures," AGARD Lecture Series No. 102, Bonded Joints and Preparation for Bonding, AGARD-LS-102, pps. 1.1 - 1.30, March, 1979.

10. Knauss, W. G., "Delayed Failure - The Griffith Problem for Linearly Viscoelastic Materials," International Journal of Fracture Mechanics, 6, March 1970, pp. 7-20.

11. Knauss, W. G., "Stable and Unstable Crack Growth in Viscoelastic Media," Transaction of the Society of Rheology, 13, 1969, pp. 291-313.

12. Knauss, W. G., "The Mechanics of Polymer Fracture," Applied Mechanics Review, 26, June 1973, pp. 1-17.

13. Schapery, R. A., "A Theory of Crack Initiation and Growth in Viscoelastic Media: I - Theoretical Development," International Journal of Fracture, 11, Feb. 1975, pp. 141-159.

14. Schapery, R. A., A Theory of Crack Growth in Viscoelastic Media, Texas A&M University, College Station, Texas, Report MM 2764-73-1, 1973.

15. Christiansen, R. M., "A Rate-Dependent Criterion for Crack Growth," Int. J. Fracture, 15, 3-21, 1979.

16. McCartney, L. N., "Crack Growth Laws for a Variety of Viscoelastic Solids Using Energy and COD Fracture Criteria," Int. J. Fracture, 15, 31-40, 1979.

17. Barenblatt, G. I., "The Mathematical Theory of Equilibrium Cracks in Brittle Fracture," Adv. Appl. Mechs. 7, 55-129, Academic Press, New York, 1962.

18. Romanko, John and Knauss, W. G., "On the Time-Dependence of Poisson's Ratio of a Commercial Adhesive," J. Adhesion, 10, 1980, pp. 269-277.

19. Romanko, John and Knauss, W. G., Fatigue Behavior of Adhesively Bonded Joints, Vols. I & II, AFWAL-TR-80-4037 (Final Report for Period July 1976 to December 1979) April, 1980.

20. Contract F33615-80-C-5093, "Basis for Accelerated Testing of Adhesively Bonded Joints," sponsored by AFWAL/MLBC Wright-Patterson AFB, OH 45433 and conducted by Texas Research Institute Inc., Austin, Texas.

21. Contract F33615-80-C-5167, "Viscoelastic Stress Analysis Including Moisture Diffusion for Adhesively Bonded Joints," sponsored by AFWAL/MLBC Wright-Patterson AFB, OH 45433 and conducted by General Dynamics, Fort Worth Division.

22. Knauss, W. G. and Emri, I. J., "Nonlinear Viscoelasticity Based on Free Volume Considerations," Computers and Structures, 13, (1981) pp. 123-128.

23. Schapery, R. A., "On the Application of a Thermodynamic Constitutive Equation to Various Nonlinear Materials," Purdue Univ. Publ. AA & ES 68-4, June 1968.

24. Contract F33615-79-C-5117, "Residual Stresses in Adhesive Joints," sponsored by AFWAL/MLBC Wright-Patterson AFB, OH 45433 and conducted by Texas A&M University, Mechanics and Materials Center, College Station, Texas.

25. Findley, W. N., Cho, U. W., and Ding, J. L., "Creep of Metals and Plastics Under Combined Stresses, A Review," ASME Journal of Engineering Materials and Technology, 101, 1979.

26. Kanuss, W. G., "A Study of the Time Dependence in Fracture Processes Relating to Service Life Prediction of Adhesive Joints and Advanced Composites," Tech. Final Report AFOSR-TR-81-0590, by Cal Inst. Tech., Graduate Aeronautical Laboratories, Pasadena, CA, 30 April 1981.

27. Hopkins, I. L., and Hammings, R. W., "On Creep and Relaxation," J. Appl. Physics 28, #8, 1957, pp. 906-909.

28. Heymans, L. J., Ph.D. Thesis 1982, California Institute of Technology.

29. Brinson, H. F., Griffith, W. I., and Morris, D. H., "Creep Rupture of Polymer Matrix Composites," Experimental Mechanics, Sept. 1981, pp. 329-335.

30. Schapery, R. A., "Nonlinear Fracture Analysis of Viscoelastic Composite Materials Based on a Generalized J-Integral Theory," Proc. Jap. U.S. Conf. on Composite Materials, Tokyo, Jan. 1981.

31. Quarterly Progress Report No. 8 (1 June 1981 to 31 August 1981) "Integrated Methodology for Adhesive Bonded Joint Life Predictions," Fort Worth Division Technical Report FZM-6990, September, 1981.

32. Quarterly Progress Report No. 9 (1 Sept. 1981 to 31 December 1981) "Integrated Methodology for Adhesive Bonded Joint Life Predictions," Fort Worth Division Technical Report FZM-7010, December, 1981.

33. Contract F33615-81-C-5114, "Time Dependent Fracture," sponsored by AFWAL/MLBC Wright-Patterson AFB, OH 45433 and conducted by Chemical Systems Branch, United Technology Inc., Sunnyvale, CA.

34. Douglas Aircraft Co., "Primary Adhesively Bonded Structure Technology (PABST) Full-Scale Test Report," Tech. Report AFWAL-TR-80-3112, Wright-Patterson AFB, OH 45433, November 1980.

35. Quarterly Progress Report No. 2 (1 December 1979 to 29 February 1980) "Integrated Methodology for Adhesive Bonded Joint Life Predictions," Fort Worth Division Technical Report FZM-6892, March 1980.

36. Quarterly Progress Report No. 3 (1 March to 31 May 1980) "Integrated Methodology for Adhesive Bonded Joint Life Predictions," Fort Worth Division Technical Report, FZM-6891, June 1980.

37. Quarterly Progress Report No. 4 (1 June to 31 August 1980) "Integrated Methodology for Adhesive bonded Joint Life Predictions," Fort Worth Division Technical Report, FZM-6931, Sept. 1980.

38. Weitsman, Y., "Optimal Cool-Down on Linear Viscoelasticity," J. of Applied Mechanics, 47, #1 (1980), pp. 35-39.

39. Weitsman, Y., "Stresses on Adhesive Joints Due to Moisture and Temperature," J. Composite Materials, 11, (Oct. 1977), pp. 378-394.

40. Weitsman, Y., "Interfacial Stresses in Viscoelastic Adhesive Layers Due to Moisture Sorption," Int. J. Solids Structures, 15, (1979), pp. 701-713.

41. Jen, M. H. R., and Weitsman, Y., 1981 Advances in Aerospace Structures and Materials, Presented at the Winter Annual Meeting of the American Society of Mechanical Engineers, Washington, D.C., Nov. 15-20, 1981.

42. Williams, M. L., "Stress Singularities Resulting From Various Boundary Conditions in Angular Corners of Plates in Extension," J. Appl. Mech., 19, 526-528, Dec. 1952.

43. Williams, M. L., "The Structural Analysis of Viscoelastic Materials," AIAA Journal, 2, 5 May 1964, 785-809.

44. Williams, M. L., and Kelley, F. N., "The Interaction Between Polymeric Structure, Deformation, and Fracture," Polymer Networks: Structural and Mechanical Properties, edited by A. J. Chompff, Plenum Press, 1971.

45. England, A. H., Complex Variable Methods in Elasticity, p. 64, Wiley-Interscience, (1971).

46. Malyshev, B. M., and Salganik, R. L., "The Strength of Adhesive Joints Using the Theory of Fracture," Int. J. Fracture Mech., Vol. 1, 1965, pp. 114-128.

47. Comninou, M., "The Interface Crack," J. Appl. Mech., Vol. 44, 1977, pp. 631-636.

48. Achenbach, J. D., Keer, L. M., Khetan, T. P., and Chen, S. H., "Loss of Adhesion at the Tip of an Interface Crack," to be published in Journal of Elasticity.

49. Comninou, M., and Dundurs, J., "A Closed Crack Tip Terminating at an Interface," Paper No. 78-WA/APM-28, presented at Winter Meeting of ASME, San Francisco, California, December 10-15, 1978.

50. Westmann, R. A., "Crack Emanating From An Open Notch," Journal of Elasticity, Vol. 4 (1974), pp. 173.

51. Knauss, W. G., "On the Steady Propagation of a Crack in a Viscoelastic Sheet: Experiments and Analysis," Deformation and Fracture of High Polymers, Plenum Press, 1973.

52. Heer, E., and Chen, J. C., "Finite Element Formulation for Linear Thermoviscoelastic Materials," JPL Technical Report 32-1381, June 1, 1969.

53. MARC Viscoelasticity Documentation, MARC Prony Series Modification, MARC Analysis Research Corp., Palo Alto, CA 94306.

54. Liechti, K. M., "The Application of Optical Interferometry to Time Dependent Unbonding," Ph.D. Thesis 1980, California Institute of Technology, Pasadena, California 91125.

55. Smelser, R. E., "Evaluation of Stress Intensity Factors for Bi-Material Bodies Using Numerical Crack Flank Displacement Data," Int. J. of Fracture, 15, (1979) pp. 135-143.

56. Smelser, R. E. and Curtin, M. E., "On the J-Integral for Bi-Material Bodies," Int. J. of Fracture, 13, (1977), pp. 382-384.

57. Quarterly Progress Report No. 5 (1 September to 30 November 1980) "Integrated Methodology for Adhesive Bonded Joint Life Predictions," Fort Worth Division Technical Report FZM-6952, December, 1980.

58. Kelley, F. N. and Trout, J. L., "Elements of Solid Rocket Service Life Predictions," AIAA Paper No. 72-1085, AIAA/SAE 8th Joint Propulsion Specialist Conference, New Orleans, LA, Nov. 29-Dec. 1, 1972.

59. "Materials Properties Handbook, FM-73 Adhesive," General Dynamics Fort Worth Division Tech. Report, FZM-7055, July 1980.

60. "PABST General Material Property Data," AFFDL-TR-77-107, prepared for AFFDL, W-P AFB, by Douglas Aircraft Co., Long Beach, CA, September 1978.

61. Francis, E. C., Hufferd, W. L., Lemini, D. G., Thompson, R. E., and Briggs, W. E., "Time Dependent Fracture in Adhesive Bonded Joints," United Technology, Chemical System Division Tech. Report CSD 2769-1R-01, May 1982.

62. Quarterly Progress Report No. 7 (1 March to 31 May 1981) "Integrated Methodology for Adhesive bonded Joint Life Predictions," Fort Worth Technical Report FZM-6975, June 1981.

63. Douglas Aircraft Co., "Primary Adhesively Bonded Structure Technology (PABST), Phase Ib: Preliminary Design," Tech. Report AFFDL-TR-76-141, Wright-Patterson AFB, OH 45433, December 1976.

64. Wool, R. P. and O'Connor, K. M., "Craze Healing in Polymer Glasses," Polymer Engineering and Science, 21 (No. 14) 970-977 (1981).

65. Contract F33615-80-C-3226, "Initial Quality of Advanced Joining Concepts," sponsored by USAF AFFDL Wright-Patterson AFB, OH 45433 and conducted by General Dynamics, Fort Worth Division, Fort Worth, TX September 1980 - July 1983.

66. Dattaguru, B., Everett, R. A., Jr., Whitcomb, J. D., and Johnson, W. S., Geometrically-Nonlinear Analysis of Adhesively Bonded Joints, presented at the 23rd AIAA/ASME/ASCE/AHS Structures, Structural Dynamics, and Materials Conference, New Orleans, LA, May 1982. Also NASA/LaRC Tech. Memo #84562, September 1982.

67. Quarterly Progress Report No. 6 (1 December 1980 to 28 February 1981) "Integrated Methodology for Adhesive Bonded Joint Life Predictions," Fort Worth Division Technical Report FZM-6961, pps. 22-28, March 1981.

68. Sciammarella, C. A. and Gilbert, J. A., "A Holographic Moire' Technique to Obtain Separate Patterns for Components of Displacements," Experimental Mechanics, 16 (6), 215-220,1976.

69. Sciammarella, C. A. and Chawla, S. K., "Multiplication of Holographic Franges, Its Application to Crack Detection," Proc. of 6th Int. Conf. of Exp. Stress Analysis, W. Germany (Sept. 1958).

70. Gilbert, J. A., Sciammarella, C. A., and Chawla, S. K., "Expension to Three Dimensions of Holographic-Moire' Technique to Separate Patterns Corresponding to Components of Displacement," Experimental Mechanics, 18 (9), 321-327,1978.

71. Sciammarella, C. A. and Chawla, S. K., "Holographic Moire Technique to Obtain Displacement Components and Derivatives," Mech. Res. Comm., 4, 5 (1977).

72. Sciammarella, C. A. and Chawla, S. K., "A Lens Holographic-moire' Technique to Obtain Components of Displacements and Derivatives," Experimental Mechanics, 18 (10), 373-381,1978.

73. Chawla, S. K. and Sciammarella, C. A., "Localization of Fringes Produced by Rotation of the Recording Plate in Focused-image Holography," Experimental Mechanics, 20 (7), 240-244,1980.

74. Sciammarella, C. A., Rastogi, P. K., Jacquot, P., and Narayanan, R., "Holographic Moire' in Real Time," Experimental Mechanics, 82 (2), 52-63, 1982.

75. Ennos, A. E., "Measurement of In-plane Surface Strain by Hologram Interferometry, J. Phys. E., J. Sci. Enstrum. Ser. 21, 1968, 731.

76. Butters, J. N., Application of Holography to Instrument Diaphragm Deformations and Associated Topics, The Engineering Uses of Holography, Cambridge University Press, London, New York, 1970.

77. Boone, P. M., Holographic Determination of In-Plane Deformations, Opt. Technol., 2, 1970.

78. Chawla, S. K., "Displacement and Strain Measurement Using Focused Image Holography," Ph.D. Thesis, 1978, Illinois Institute of Technology, Chicago, Illinois.

79. Brandt, G. B., "Image Plane Holography," Appl. Opt. 8, 1421-1429, (1969).

80. Klimenko, I. S., and Skrotskii, G. V., "Focused-Image Holography," Sov. Phys. Usp., 16, 88-98, (1973).

81. Romanko, John, "Techniques in Holographic Interferometry," General Dynamics Fort Worth Division, ERR-FW-1329 (29 December 1972).

82. Hagemeyer, J. W., "Fatigue Crack Closure Studies," General Dynamics Fort Worth Division ERR-FW-1596 (31 December 1974).

83. Romanko, John, "Measurement of Surface Strains and Fatigue Crack Detection by Laser Speckle Pattern Techniques," General Dynamic Fort Worth Division, ERR-FW-1582 (30 December 1973).

84. Adams, F. D., and Maddux, G. E., "On Speckle Diffraction Interferometry for Measuring Whole Field Displacements and Strains," W-P AFB Tech. Report AFFDL-TR-73-123, Dec. (1973).

85. Axelrad, D. R. and Kalousek, J., Stress Holographic Interometry, McGill University, Montreal, Canada.

86. Van Ligten, R. F. and Osterberg, H., "Holographic Microscopy," Nature, 211, 282-283, (July 1966).

87. Exner, G. A., and Gilbert, J. A., "Displacement Analysis Using Image-Plane Holography," 1977 SESA Spring Meeting, Dallas, TX, May 15-20, 1977.

88. Marceau, J. A., McMillan, J. C., and Scardino, W. M., "Cyclic Testing of Adhesive Bonds," 22nd National SAMPE Symposium, San Diego, CA, April 26-28, 1977.

89. Hein, V. L., and Erdogan, F., "Stress Singularities in a Two Material Wedge," Int. J. Fracture, 7, (1971), pp. 317-330.

* U.S. GOVERNMENT PRINTING OFFICE 1980-659-062/709

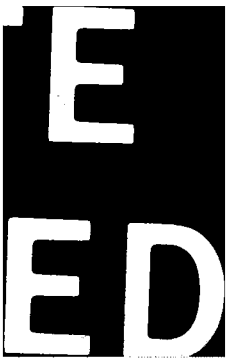
E
ED